[redacted]

(NASA-CR-150279) ANALYSIS OF H-ALPHA FLARE SPECTRA Final Report (Lockheed Missiles and Space Co.) 89 p HC A05/MF A01 CSCL 03B

N77-26054

Unclas

G3/92 30412

LOCKHEED

MISSILES & SPACE COMPANY, INC. • SUNNYVALE, CALIFORNIA

A SUBSIDIARY OF LOCKHEED AIRCRAFT CORPORATION

LMSC-D558824

Final Report
January 1977

ANALYSIS OF H-α FLARE SPECTRA

J. L. Kulander

Submitted to
MARSHALL SPACE FLIGHT CENTER
Alabama 35812

Contract NAS8-31777

ELECTRO-OPTICS LABORATORY
LOCKHEED PALO ALTO RESEARCH LABORATORY
LOCKHEED MISSILES & SPACE COMPANY, INC
A SUBSIDIARY OF LOCKHEED AIRCRAFT CORPORATION

TABLE OF CONTENTS

ABSTRACT

H-alpha spectra taken at 15 second intervals from the event of 5 Sept. 1973 have been interpreted by comparison with synthetic profiles. These spectra were taken with the multislit spectrograph at the Lockheed Solar Observatory. A sequence of 27 high resolution H-alpha profiles was obtained from the second brightest flare kernel. The profiles were generally self reversed with a maximum peak intensity of 1.16 x continuum and a maximum central intensity of .91 x continuum. The line characteristics such as red and violet peak intensities and positions, center shifts and intensities and wing intensities were tabulated.

Synthetic H-alpha profiles were generated from a finite layer assuming simple parametric forms for the source function and velocity field. The velocity chosen always decreased with optical depth and had the same sign. For absorption profiles, bisector shifts were calculated for a variety of velocities.

The velocity field and source function were derived as a function of optical depth and time. The depth variation of these quantities is not as large as predicted by flare theories nor is the predicted velocity usually outward. The velocity observed was initially outward lasting for about 5 minutes after which it changed to a downward direction. The surface velocity rose rapidly to about 12 km/sec decaying slowly to 0 after about 5 minutes. The velocity decreased with increasing optical depth falling roughly by a factor of two at a line center optical depth of 10.

The line center optical thickness of the flare remained essentially between 60 and 300. The Doppler half width varied between .36 and .52 Å. The local electron temperature required to give the correct intensities seemed to be 7000 - 10000 ^{o}K. The temperatures derived from the Doppler widths on the other hand were 16000 - 33000 ^{o}K indicating perhaps turbulent velocities of 15 - 20 km/sec. The shifting of the line centers and peaks indicate that the actual velocity may change sign at some depth in the flare and future work should include other velocity models.

A paper desrribing this work is being submitted to Solar Physics.

Analysis of Time Dependent H-alpha Flare Spectra

I. INTRODUCTION

The basic objective of this study is to obtain the gross velocity field as a function of time from a study of H-alpha flare profiles at one flare position along with specifying the approximate behavior of the source function.

Research into solar flare mechanisms has been very active in recent years. This work has been mainly theoretical although numerous patrol and specific observations have been made. With the advent of satellite and ATM observations we are able to use other UV and x-ray lines to extend the models. These space observations have not however really provided good sets of high resolution spectra over the flare region throughout the entire time development of the flare. Such a set of extensive H-alpha profiles with resolution of about 0.05 Å has been obtained at the Lockheed Solar Observatory. These data have been obtained with the new unique multislit spectrograph.

With support from NASA and components provided by Lockheed, the multislit spectrograph was built and tested in 1970 and 1971. It was in nearly continuous operation between 1972 and 1974. The most important unique feature of this H-alpha spectrograph is the 30 entrance slits spaced evenly every 22 arc seconds across an active region. This allows a very complete spatial picture of the active region to be composed. The length of the slit is about 30 arc seconds and H-alpha profiles can be obtained at as many positions along the slit as desired.

Spectra were taken at 15 second intervals encompassing the flash phase of hundreds of flares. The profiles obtained show a wide variation from absorption to emission, some showing self-reversals others not. The red to violet emission peak intensity changes rapidly with time and position as does the asymmetry of the line. Some regions show broad emission features with no self reversal.

As discussed in section II we have chosen a region of high intensity in the flare event of 5 September 1973 for analysis. It was determined that this event would probably have the greatest interest in terms of Skylab and other observations. The 5 September 1973 flare was a large complex flare with several emission regions and an associated large erupting filament. A surge later developed near the filament which was observed to slow and change back to inflowing matter. We have chosen one location at the flare center and obtained smoothed line profiles as shown in section II. A sequence of 26 profiles observed at 15 second intervals was chosen.

In section III we describe the theoretical calculation of line profiles for a flare layer and illustrate the effect of different source function and velocity parameters on the line profiles. We also show in section III the wavelength shift of the bisector of an H-alpha absorption line for various velocity fields. The comparison of these shifts with those observed is one of the methods used to infer the velocities in section IV.

Section IV describes the comparison of observed and calculated H-alpha profiles and the inferrence of the atmospheric velocities. Each observed profile is carefully matched to the best source function and velocity as a function of optical depth. We find that neither the observed profile shifts nor self reversed peak intensities are as great as those predicted by most theories (Hyder, 1968; Nakagawa, 1970; Nakagawa, 1973; Canfield, 1974; Kostyuk, 1976). Thus, the flare region studied here does not exhibit the large velocities nor the large variation in source function predicted.

A paper describing this work will be submitted to Solar Physics.

We would like to acknowledge many helpful discussions with Sara Smith and Steve Schoolman.

II. DATA REDUCTION

In the time interval between April 1972 and April 1974 over 300 flares were observed in H-alpha with the multislit spectrograph at the Lockheed Rye Canyon Solar Observatory. We have compared the flares observed at Lockheed with those observed by various Skylab experimenters, particularily NRL.

A flare of particular interest with a great deal of overlapping coverage is that of 5 September 1973. The NRL S082A spectrograph took 8 frames of this event. The multislit spectrograph obtained spectra at over 60 locations within the flare at 15 second intervals before and after the flash phase. A photograph of the flare in H-alpha is shown in Figure II.1. Slits were positioned almost directly across the centers of two of the brightest flare emission kernels. The line profiles in the brightest flare segment show little self reversal while those in the second brightest segment (designated B) retain a degree of self absorption. The H-alpha time history of segment B is illustrated in Figure II.2 by a series of microdensitometer tracings at one second spacings within the flare. Each series of tracings represent a different time in the development of the flare. One series is shown expanded in Fig. II.3.

Individual line profiles have been obtained at various

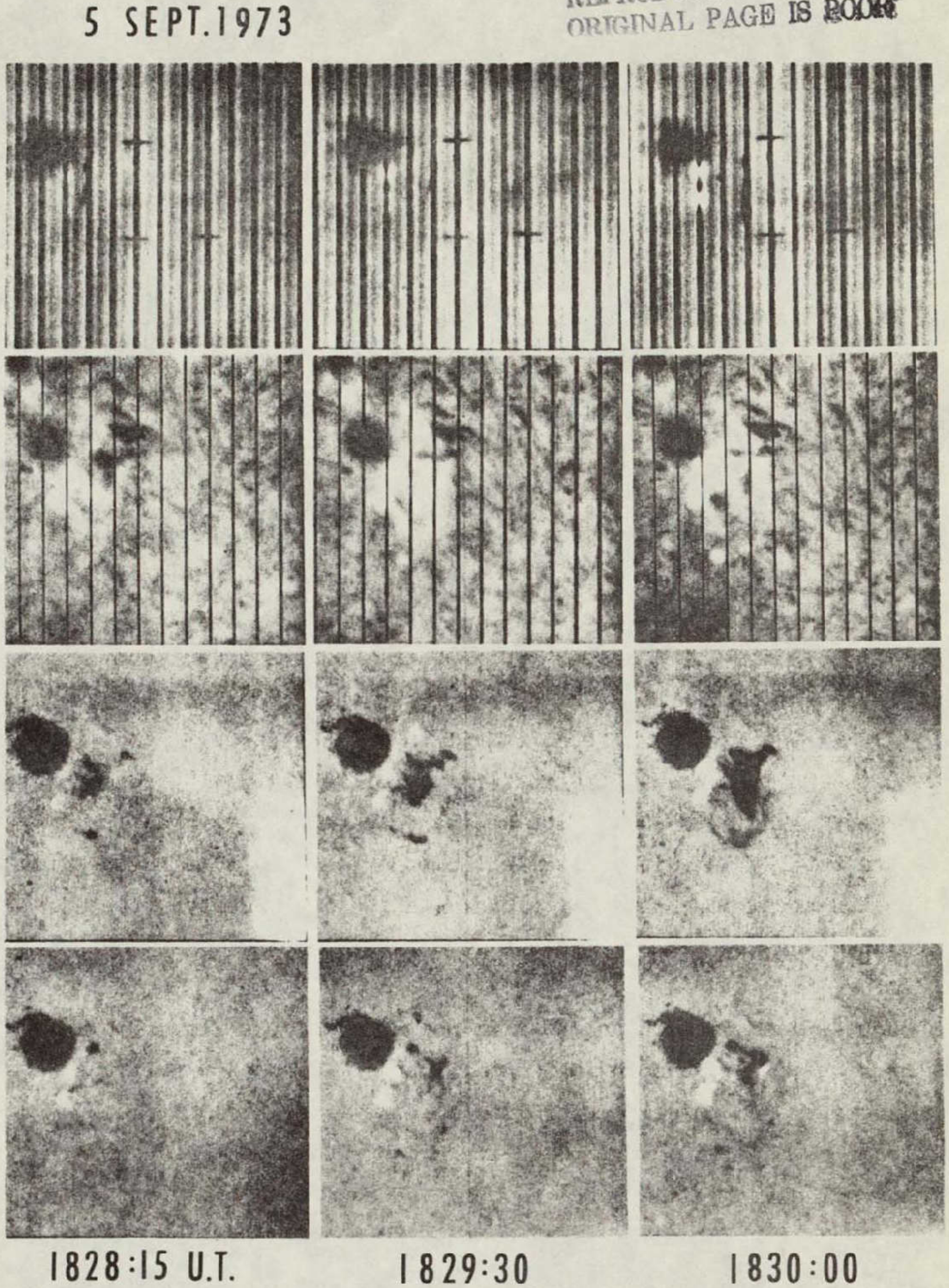

Figure II.1 Start of flare with the eruption of a filament already underway. In the top row, the dark parallel lines are an array of Hα spectra formed by the slits shown on the Hα photographs in the second row. The third and fourth rows are Hα filtergrams at Hα -1.2Å and Hα +1.2Å. The violet wings are on the left.

5 SEP 73

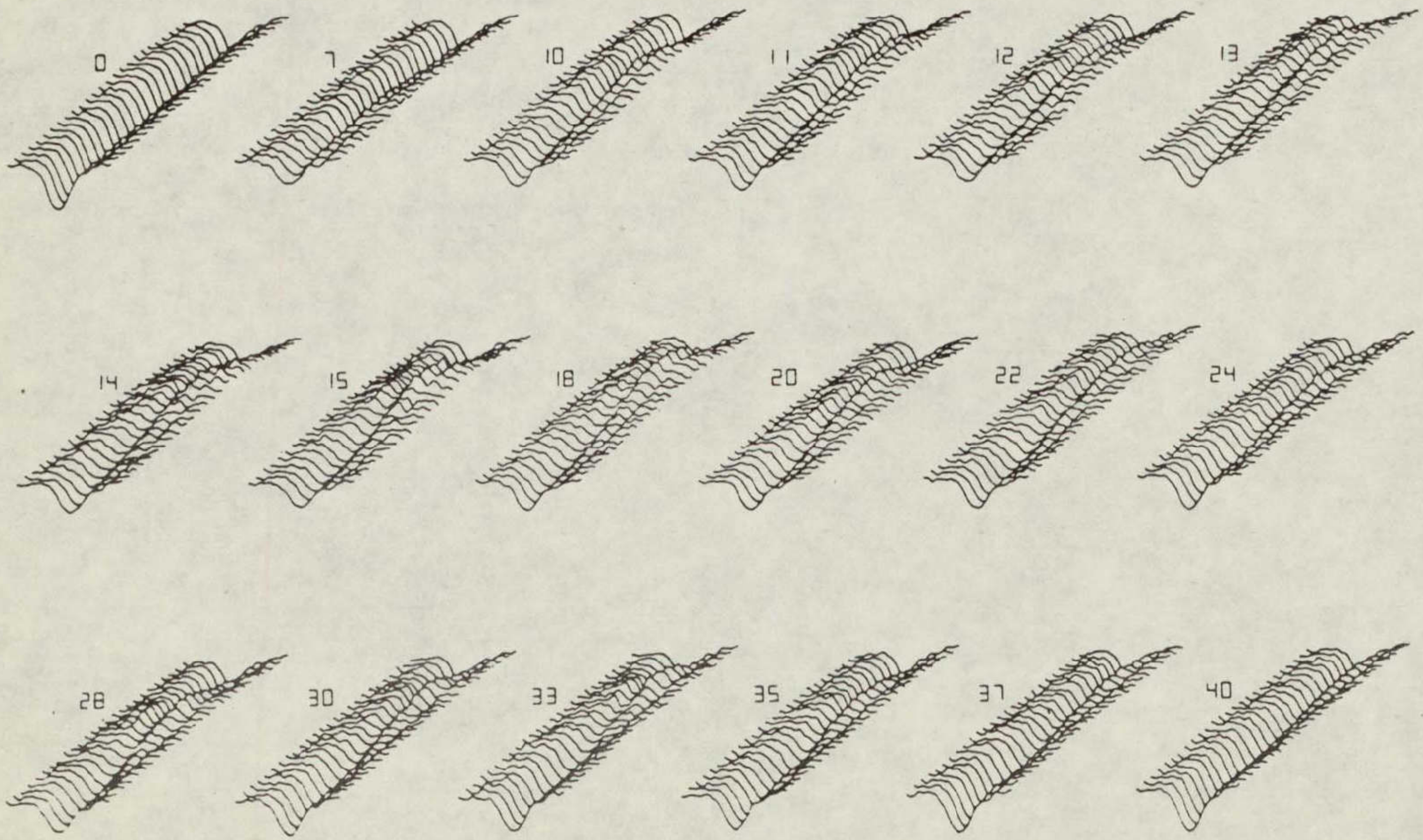

B

Figure II.2 Topographic display of the second brightest flare element as shown in the violet wing of Figure II.1 The segment of the flare shows a pronounced degree of self-absorption throughout its lifetime.

Figure II.3

Topographic display at one location in point B of the 5 Sept. 1973 flare.

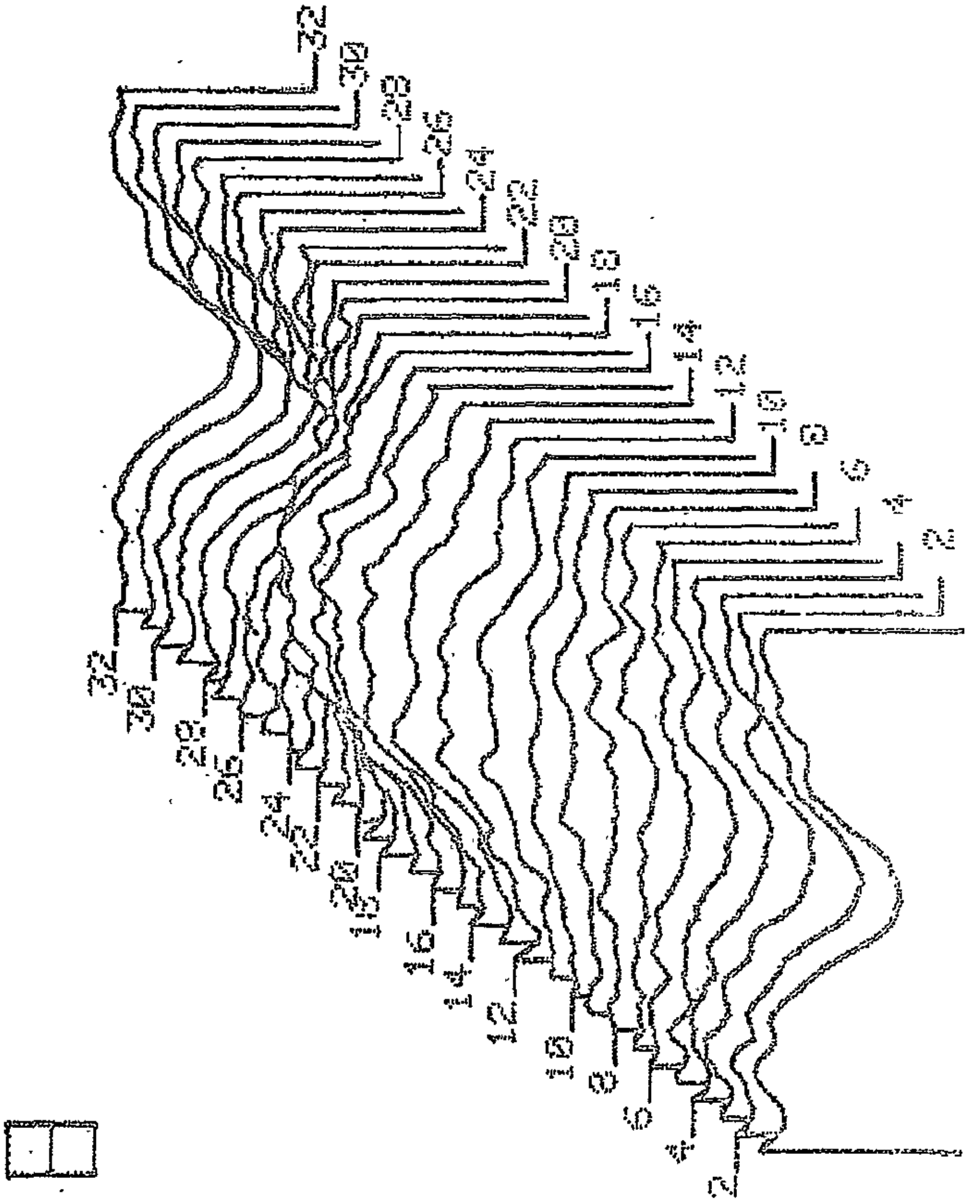

NEXT FRAME

locations within the flare as a function of time. Profiles are illustrated in Figure II.4 for a typical flare position in segment B. The dotted curves represent the quiet sun H-alpha profile.

Expanded smoothed H-alpha profiles were obtained for another typical position within flare segment B. These profiles are shown in Figures II.5-32. The first profile was taken considerably before the flare and represents the quiet sun profile. The other profiles are taken at 15 second intervals. The intensity scale was determined by comparison of the quiet sun profile with that observed by White (1962, 1964) showing a central intensity of .154 x continuum.

Qualitatively we see that red and violet emission peaks develop after about one minute and remain throughout the sequence. The red peak intensity is always greater than the violet except for four times near the end of the sequence. The red wing always has a greater intensity than the violet wing.

The following parameters for each profile are listed in Table II.1: central intensity, center wavelength shift, red and violet peak intensities and wavelength positions and red and violet wing intensities (at $\pm$ 3 Å). The subscripts c, V and R refer to center, violet and red respectively. I_V is the violet peak intensity, I_R the red peak intensity. IW_V and IW_R are the violet and red wing intensities. All

Table II.1

CHARACTERISTICS OF H-α PROFILES

Frame	I_C	$\Delta\lambda_C$	I_V	$\Delta\lambda_V$	I_R	$\Delta\lambda_R$	IW_V	IW_R
0	.154						.818	.832
1	.476	-.087 Å					.867	.867
2	.542	-.116					.846	.867
3	.570	-.087			.951	.896	.853	.923
4	.559	+.029	.909	-.954	.944	1.012	.825	.867
5	.710	-.087	.937	-.809	1.017	.896	.825	.916
6	.678	-.145	.867	-.780	.979	.867	.762	.832
7	.797	-.087	.916	-.578	.965	1.012	.804	.895
8	.839	-.087	.983	-.722	1.077	.809	.853	.874
9	.552	-.116	.804	-.722	.909	.809	.706	.776
10	.909	-.202	1.035	-.925	1.168	.751	.867	.909
11	.832	-.145	.902	-.636	1.077	.694	.769	.874
12	.490	-.087	.783	-.896	.881	.780	.706	.769
13	.668	-.145	.755	-.722	.948	.636	.741	.776
14	.695	+.058	.853	-.694	.944	.751	.727	.804
15	.643	-.029	.885	-.809	.916	.809	.755	.853
16	.671	-.058	.790	-.607	.825	.694	.790	.825
17	.538	-.116	.783	-.838	.818	.780	.727	.769
18	.441	-.087	.748	-1.098	.769	.809	.699	.755
19	.615	-.087	.797	-.694	.825	.578	.797	.825
20	.727	0	.860	-.694	.881	.780	.783	.839
21	.664	-.058	.867	-.722	.874	.549	.776	.874
22	.657	-.116	.832	-.694	.846	.520	.776	.846
23	.629	+.058	.860	-.780	.818	.694	.825	.874
24	.685	+.029	.871	-.809	.839	.838	.804	.860
25	.615	-.029	.832	-.954	.832	.751	.825	.867
26	.535	0	.797	-1.098	.755	.722	.804	.839
27	.517	0	.818	-.867	.776	.780	.790	.874

Δλ in Å
I in continuum units

Table II.2

CHARACTERISTICS OF H-ALPHA PROFILES

Frame #	I_R/I_V	I_V/I_c	V_c	V_V	V_R
0					
1			-.25		
2			-.33		
3			-.25		2.56
4	1.039	1.626	.083	-2.73	2.89
5	1.095	1.320	-.25	-2.31	2.56
6	1.129	1.279	-.41	-2.23	2.48
7	1.053	1.149	-.25	-1.65	2.89
8	1.096	1.172	-.25	-2.06	2.31
9	1.131	1.457	-.33	-2.06	2.31
10	1.129	1.139	-.58	-2.64	2.15
11	1.194	1.084	-.41	-1.82	1.98
12	1.125	1.598	-.25	-2.56	2.23
13	1.140	1.241	-.50	-2.06	1.82
14	1.107	1.227	.17	-1.98	2.15
15	1.035	1.376	-.083	-2.31	2.89
16	1.044	1.177	-.17	-1.73	1.98
17	1.045	1.455	-.33	-2.39	2.23
18	1.028	1.696	-.25	-3.14	2.89
19	1.035	1.296	-.25	-1.98	1.65
20	1.024	1.183	0	-1.98	2.23
21	1.008	1.306	-.17	-2.06	1.57
22	1.016	1.266	-.33	-1.98	1.49
23	.951	1.367	.17	-2.23	1.98
24	.963	1.272	.083	-2.31	2.39
25	1.000	1.353	-.083	-2.73	2.15
26	.947	1.490	0	-3.14	2.06
27	.949	1.582	0	-2.48	2.23

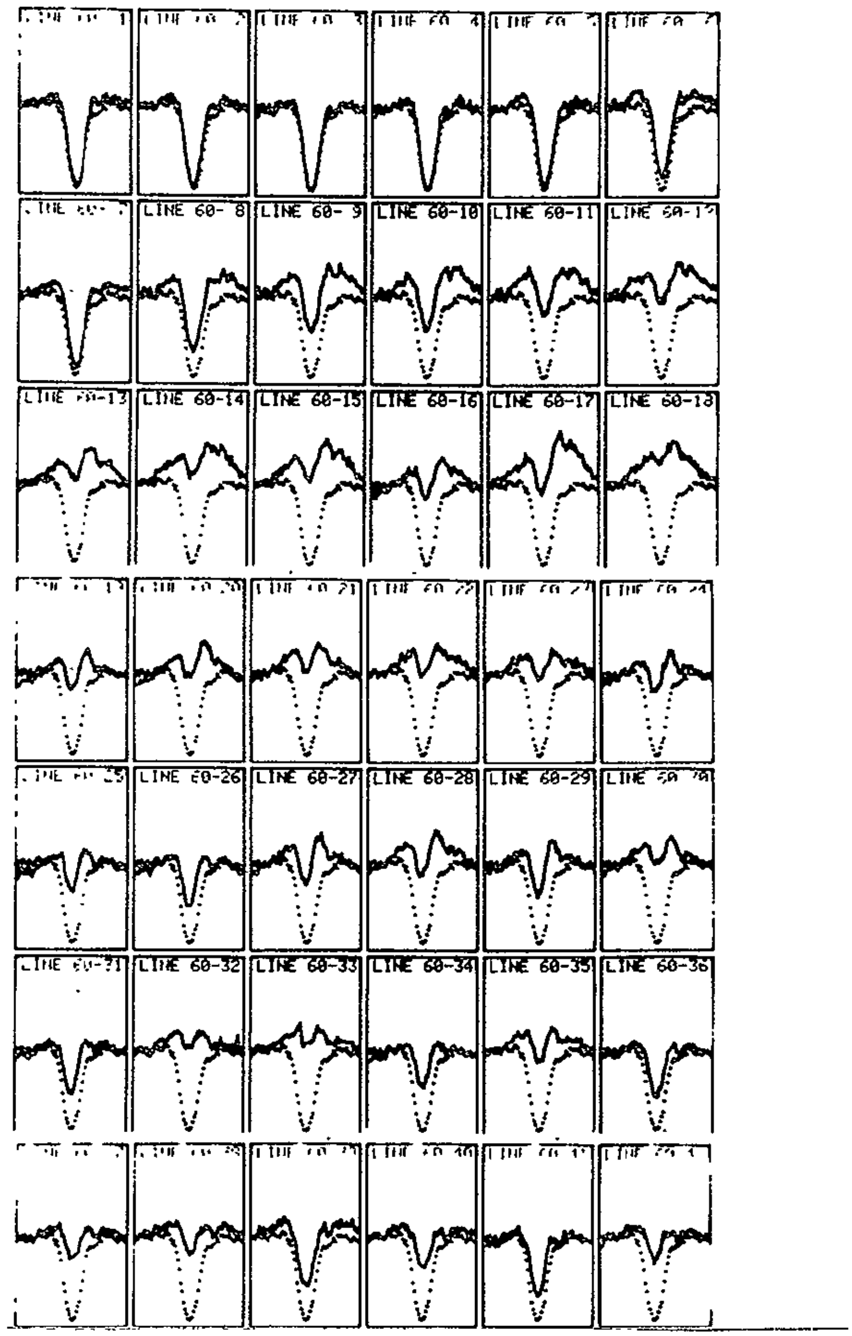

Figure II.4 H-alpha Profiles for Various Times.

Fig. II-5. H-alpha Profile - Pre-Flare

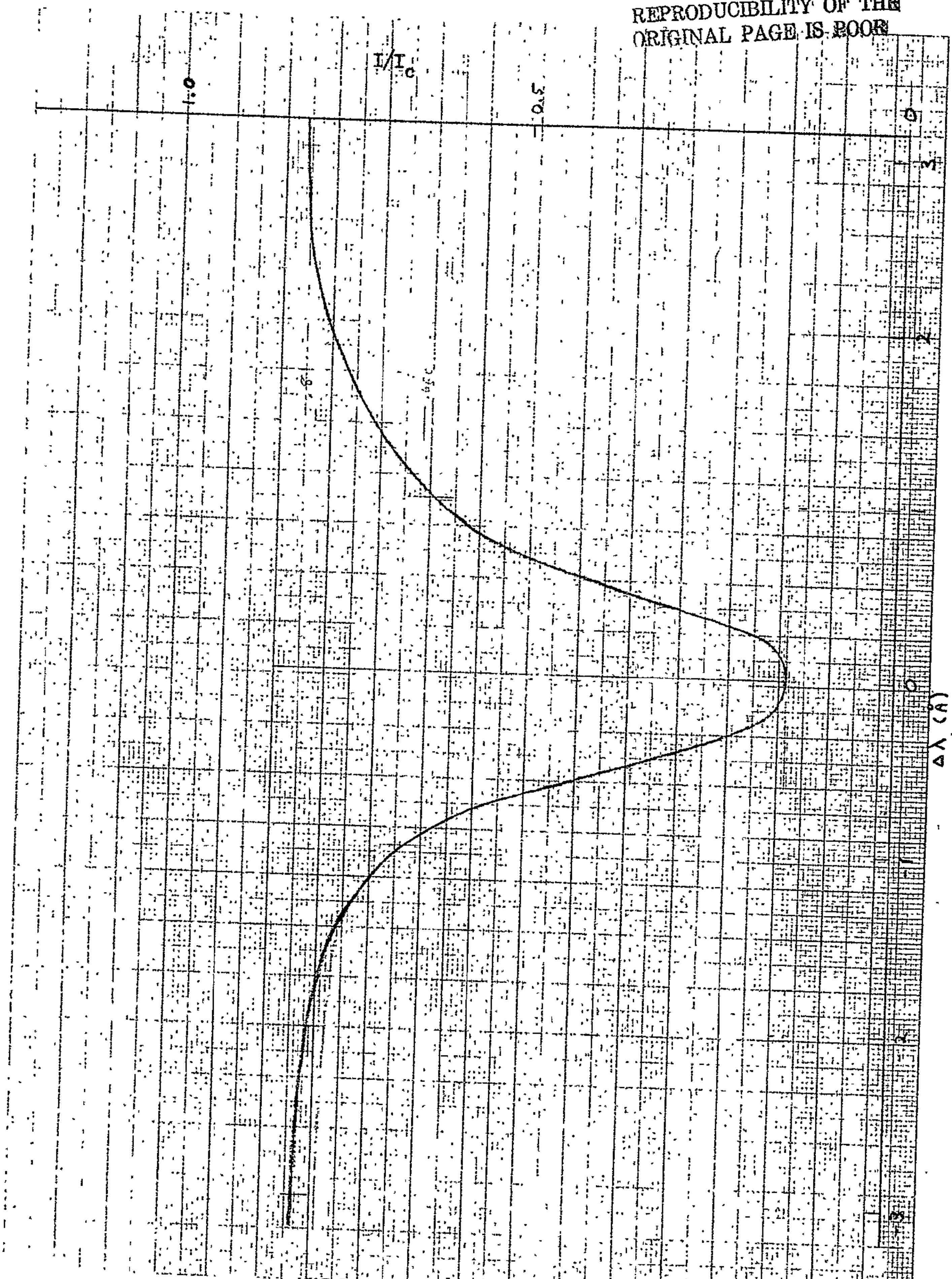

Fig. II-6. H-alpha profile. Frame 1

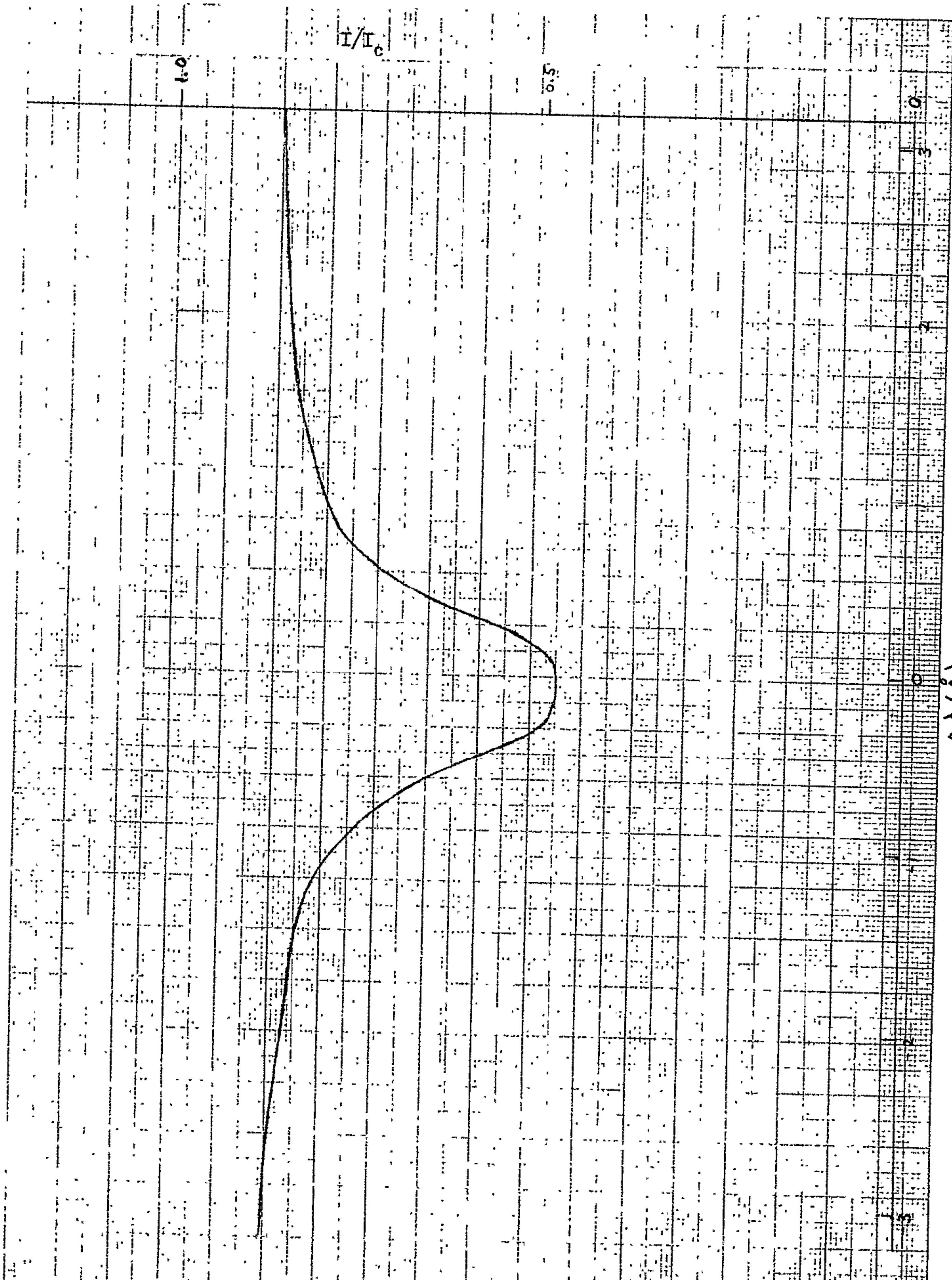

Fig. II-7. H-alpha profile. Frame 2

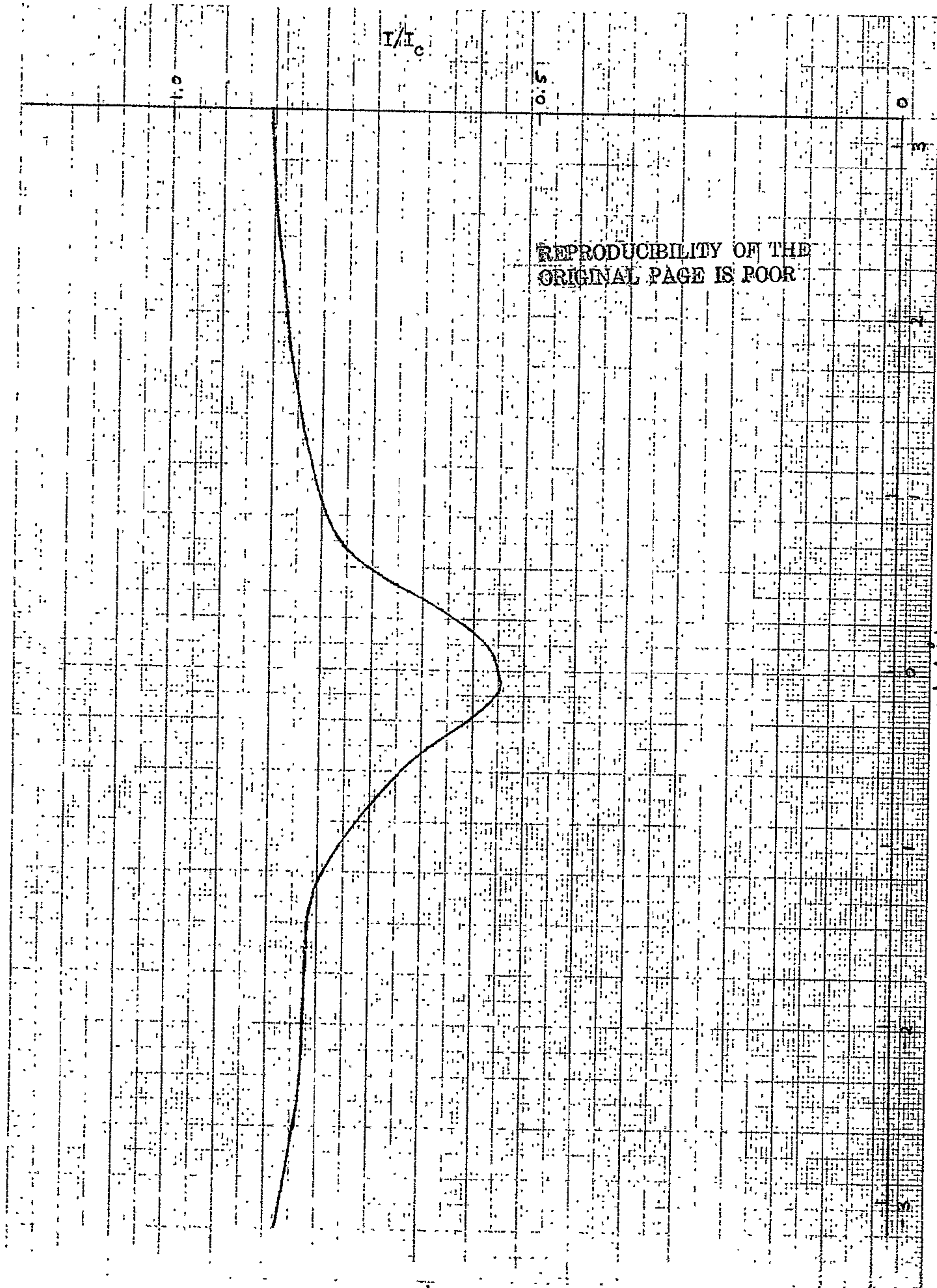

Fig. II-8. H-alpha profile. Frame 3

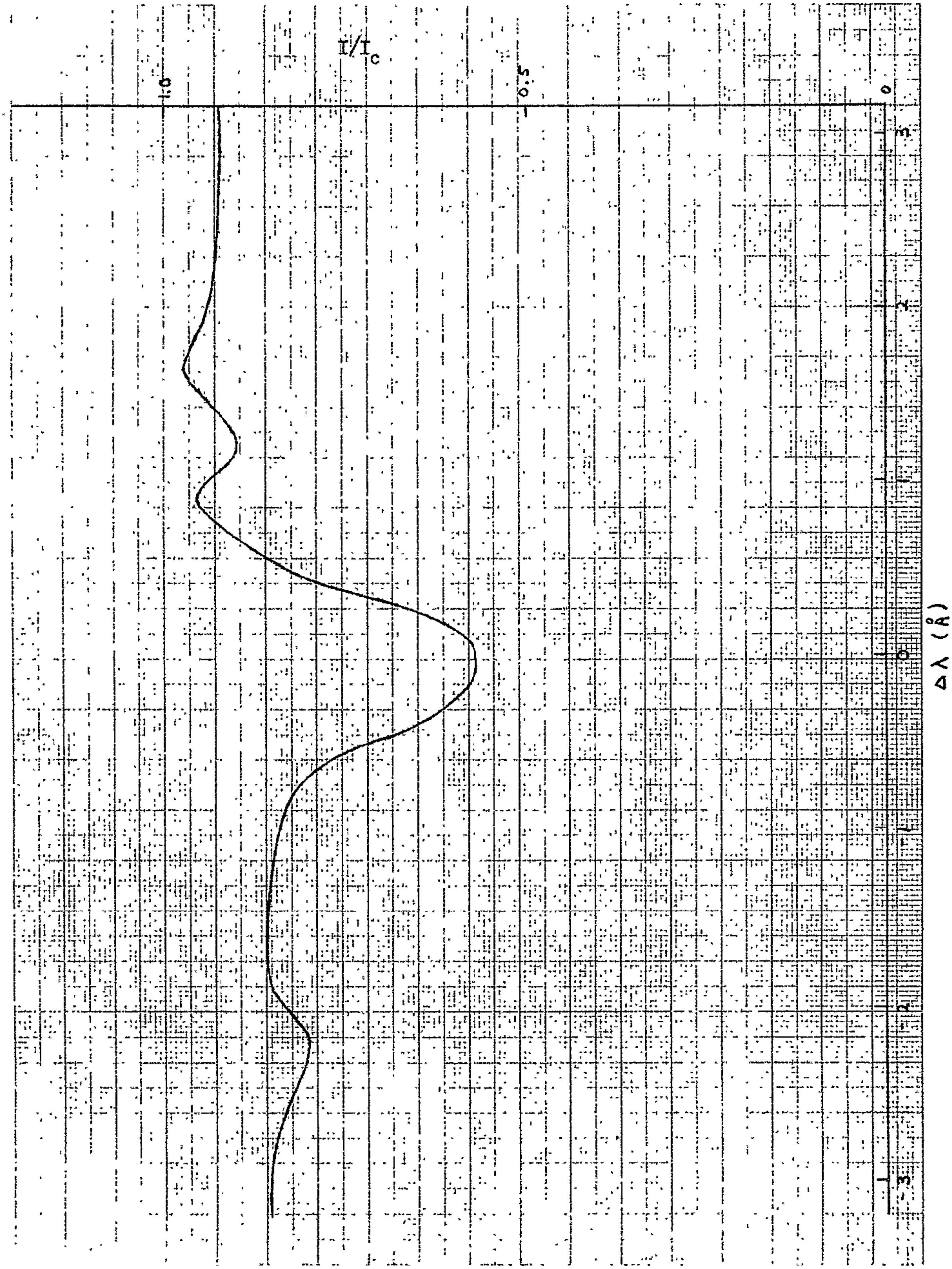

Fig. II-9. H-alpha profile. Frame 4

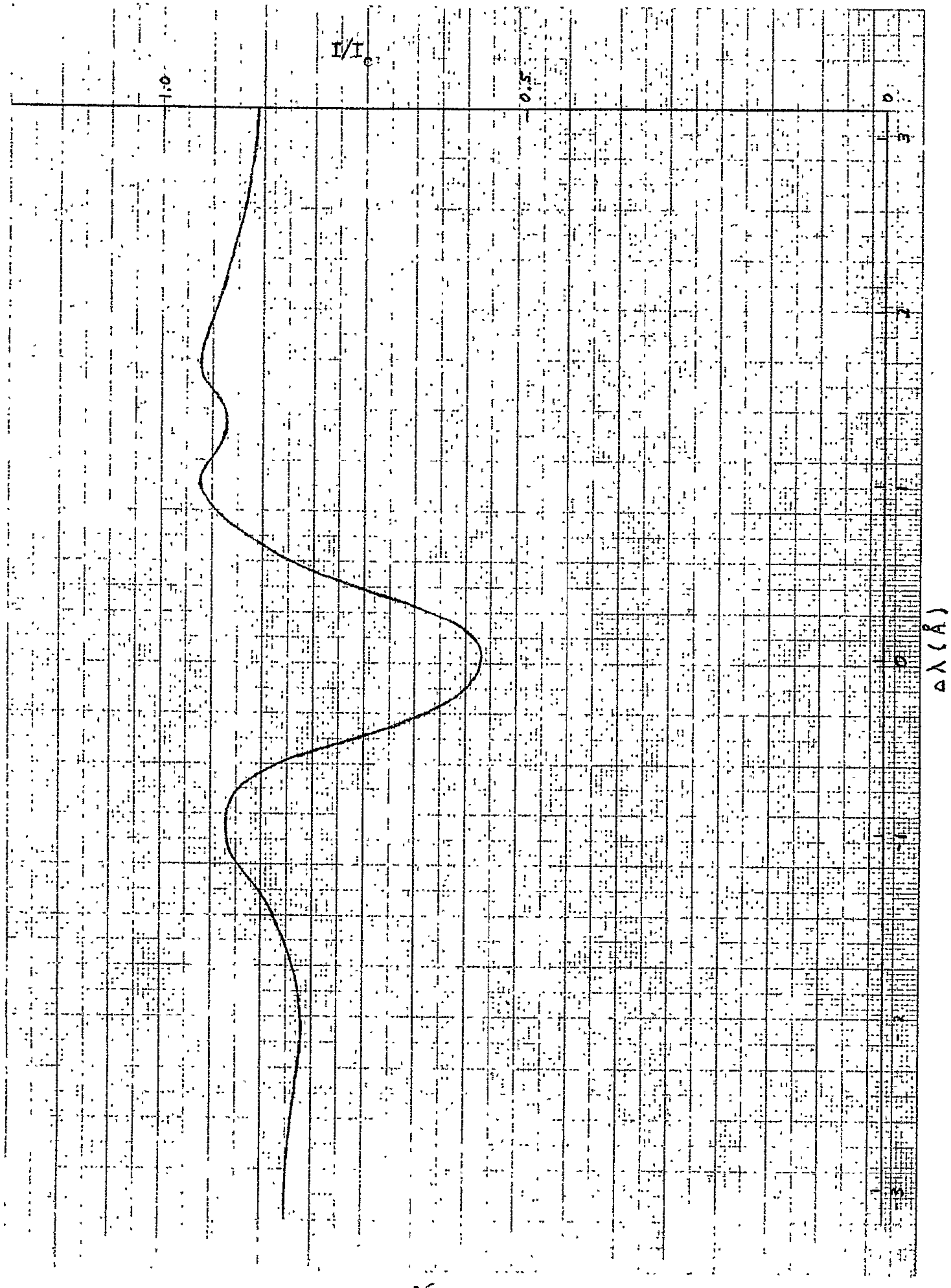

Fig. II-10. H-alpha profile. Frame 5

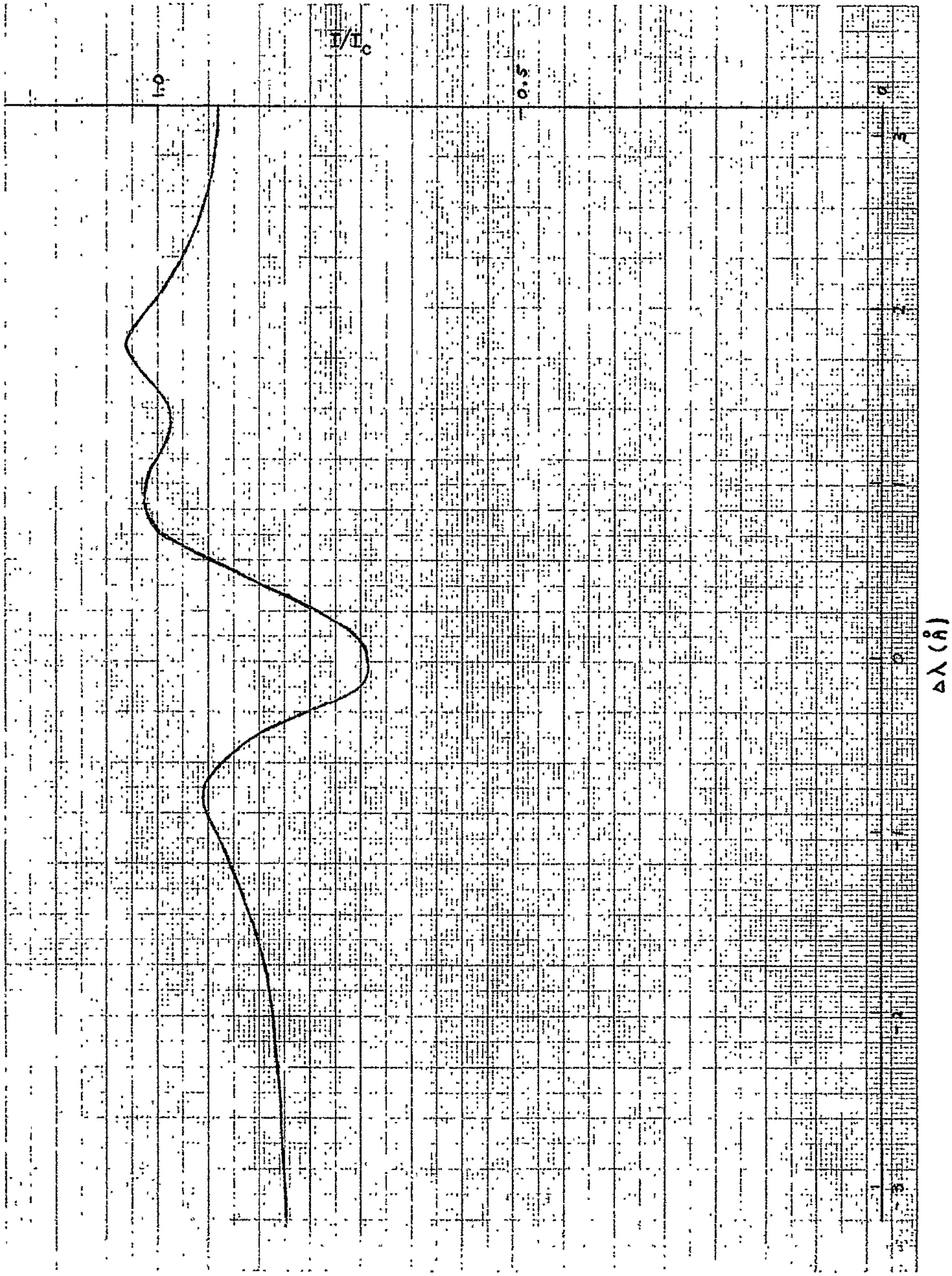

Fig. II-11. H-alpha profile. Frame 6

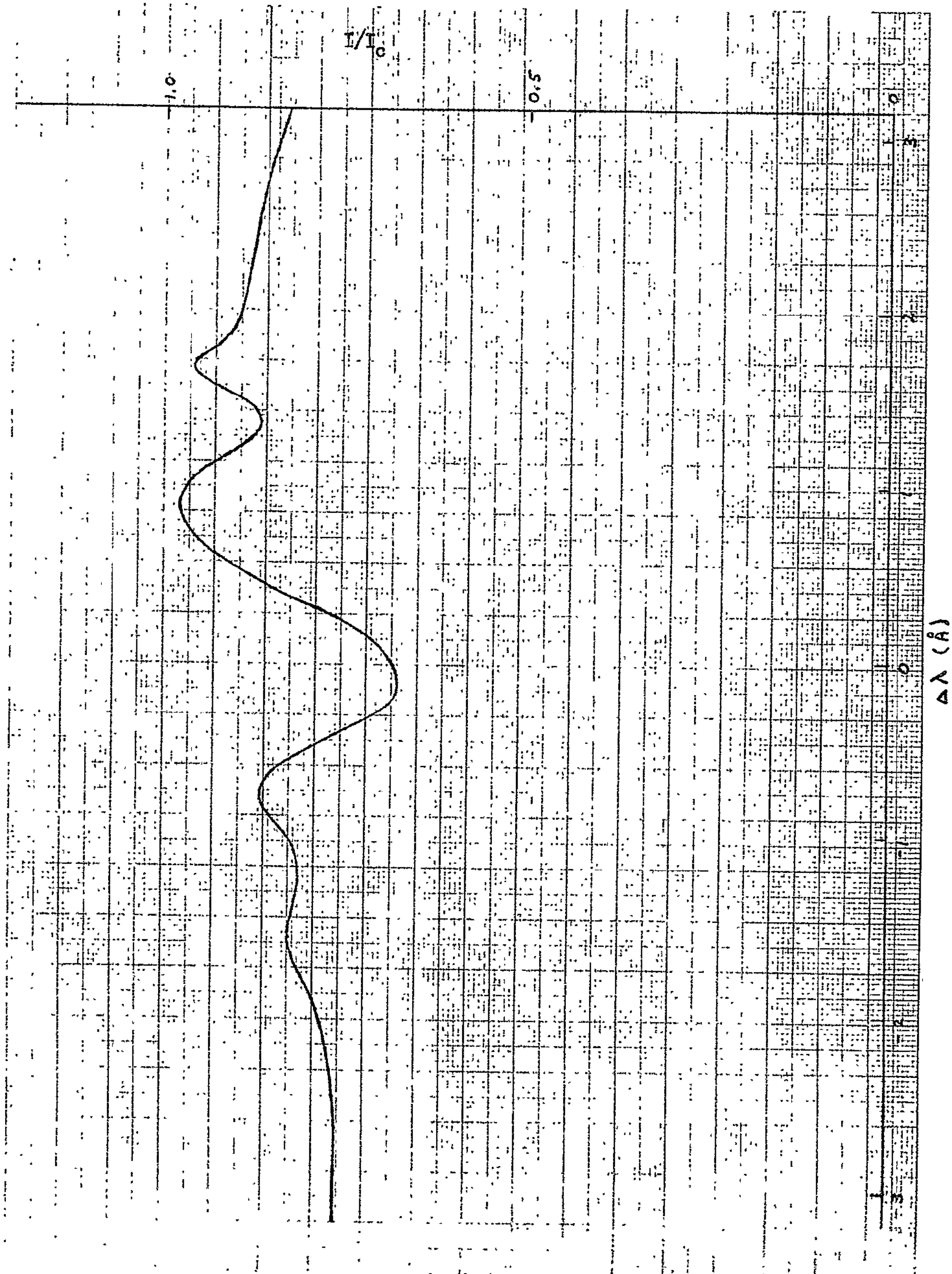

Fig. II-12. H-alpha profile. Frame 7

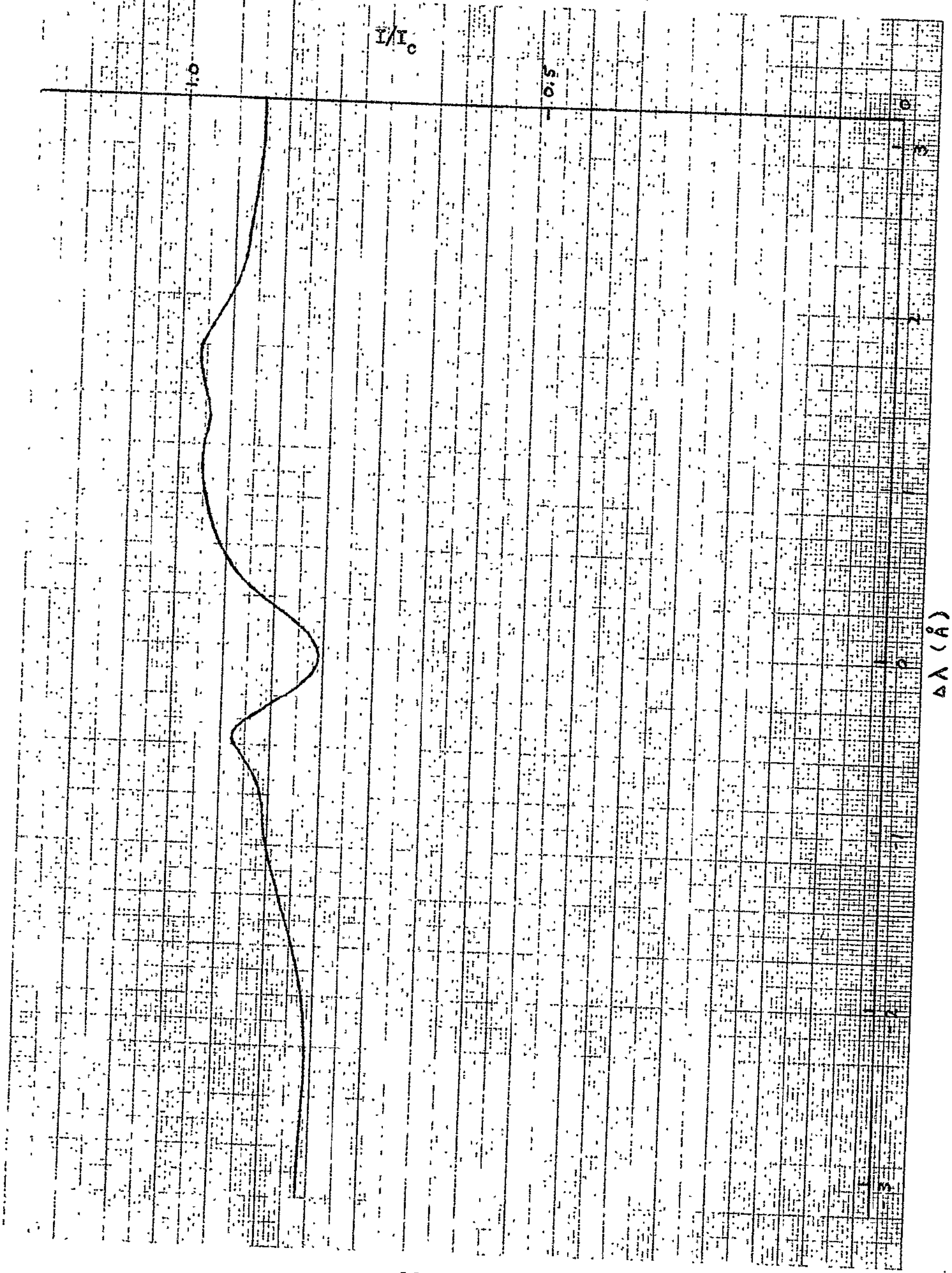

Fig. II-13. H-alpha profile. Frame 8

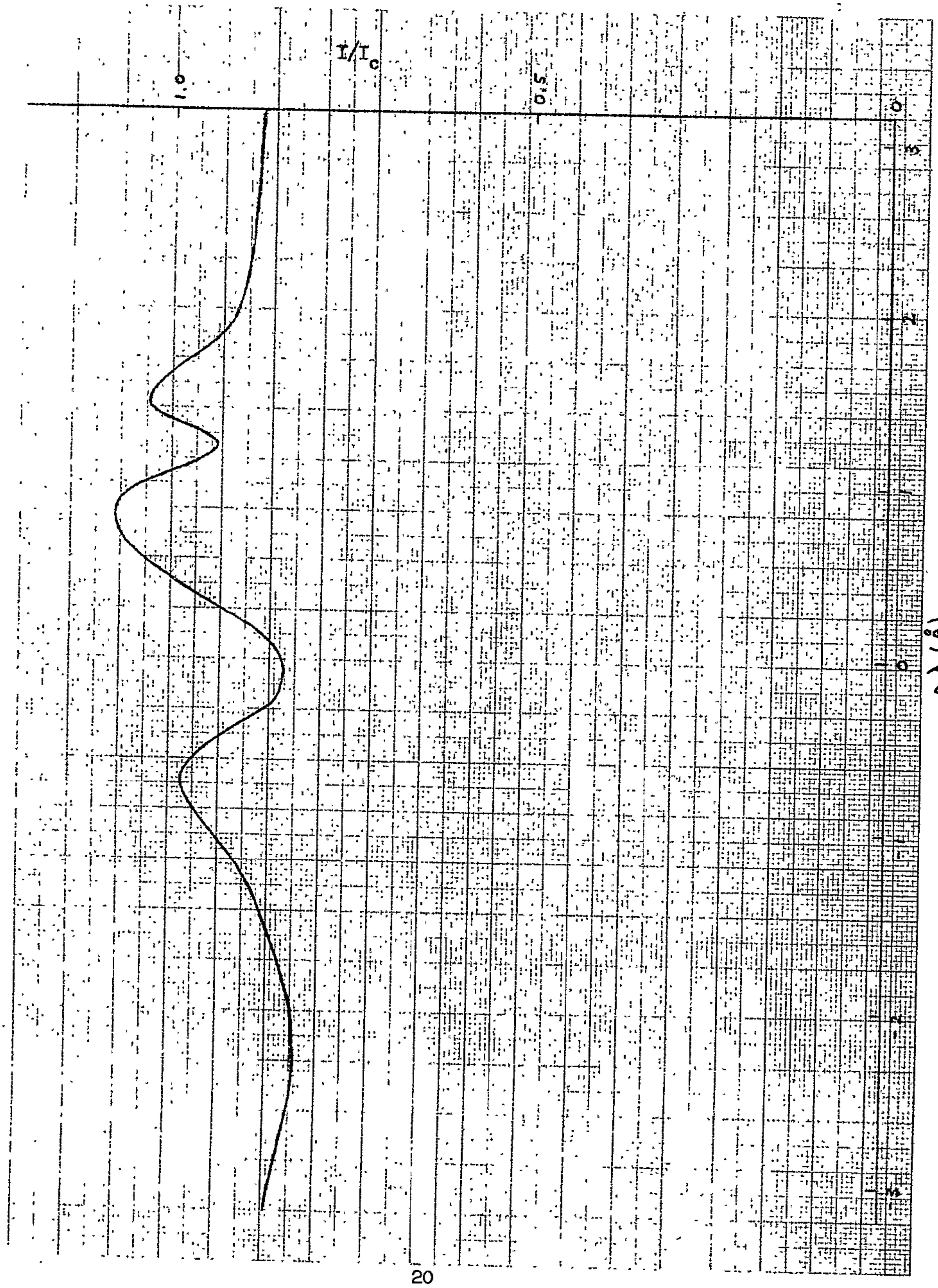

Fig. II-14. H-alpha profile. Frame 9

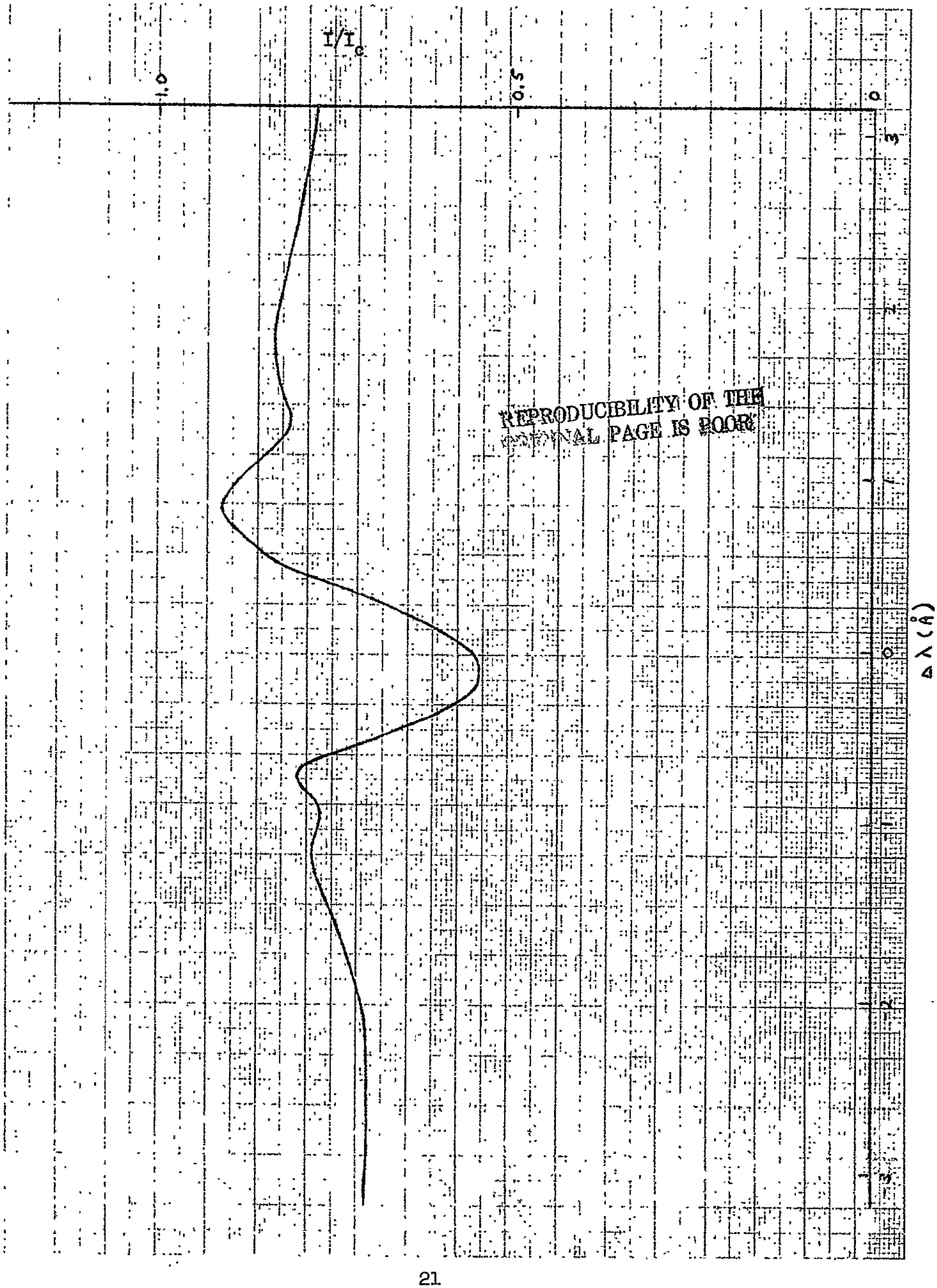

Fig. II-15. H-alpha profile. Frame 10

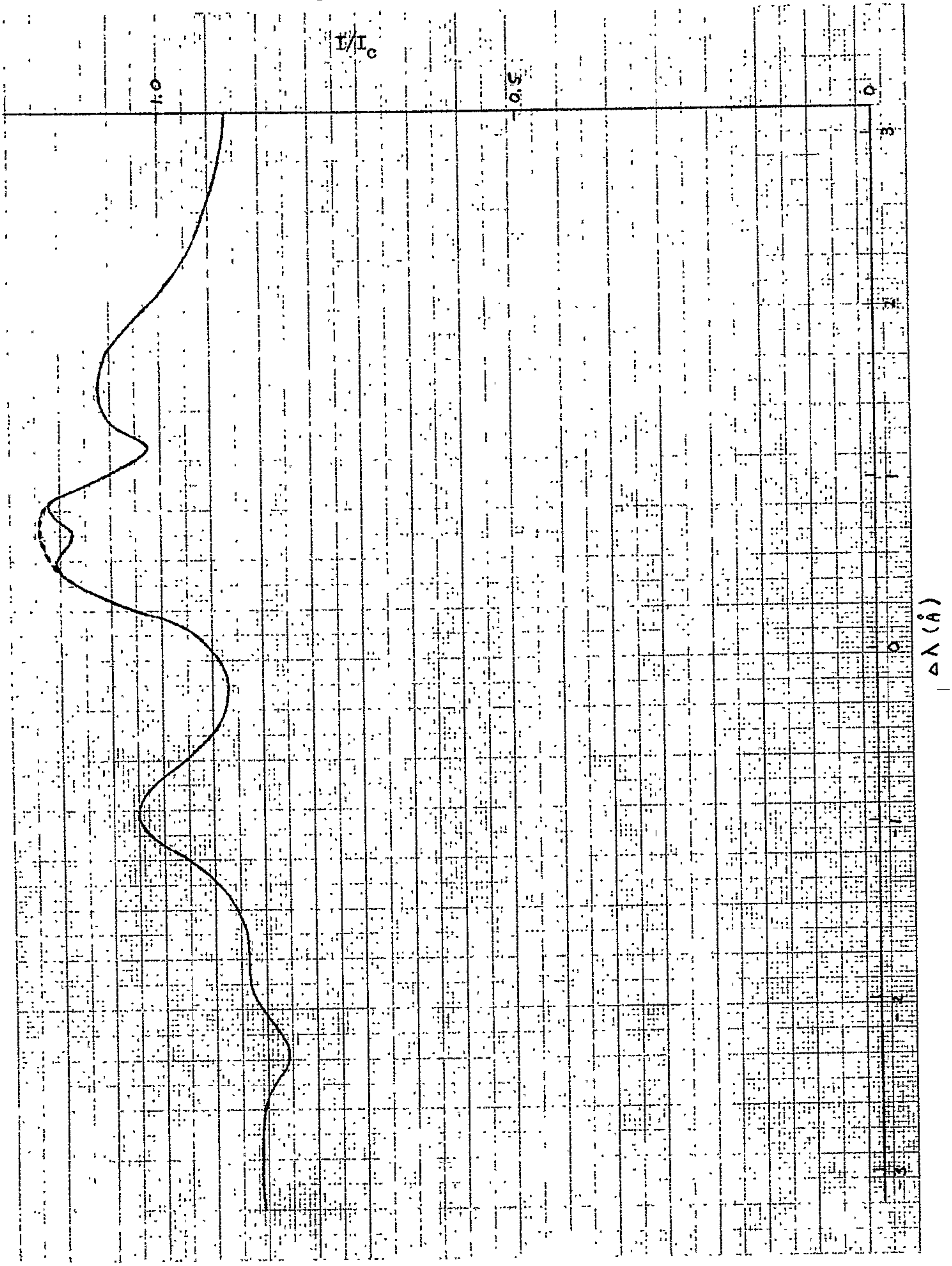

Fig. II-16. H-alpha profile. Frame 11

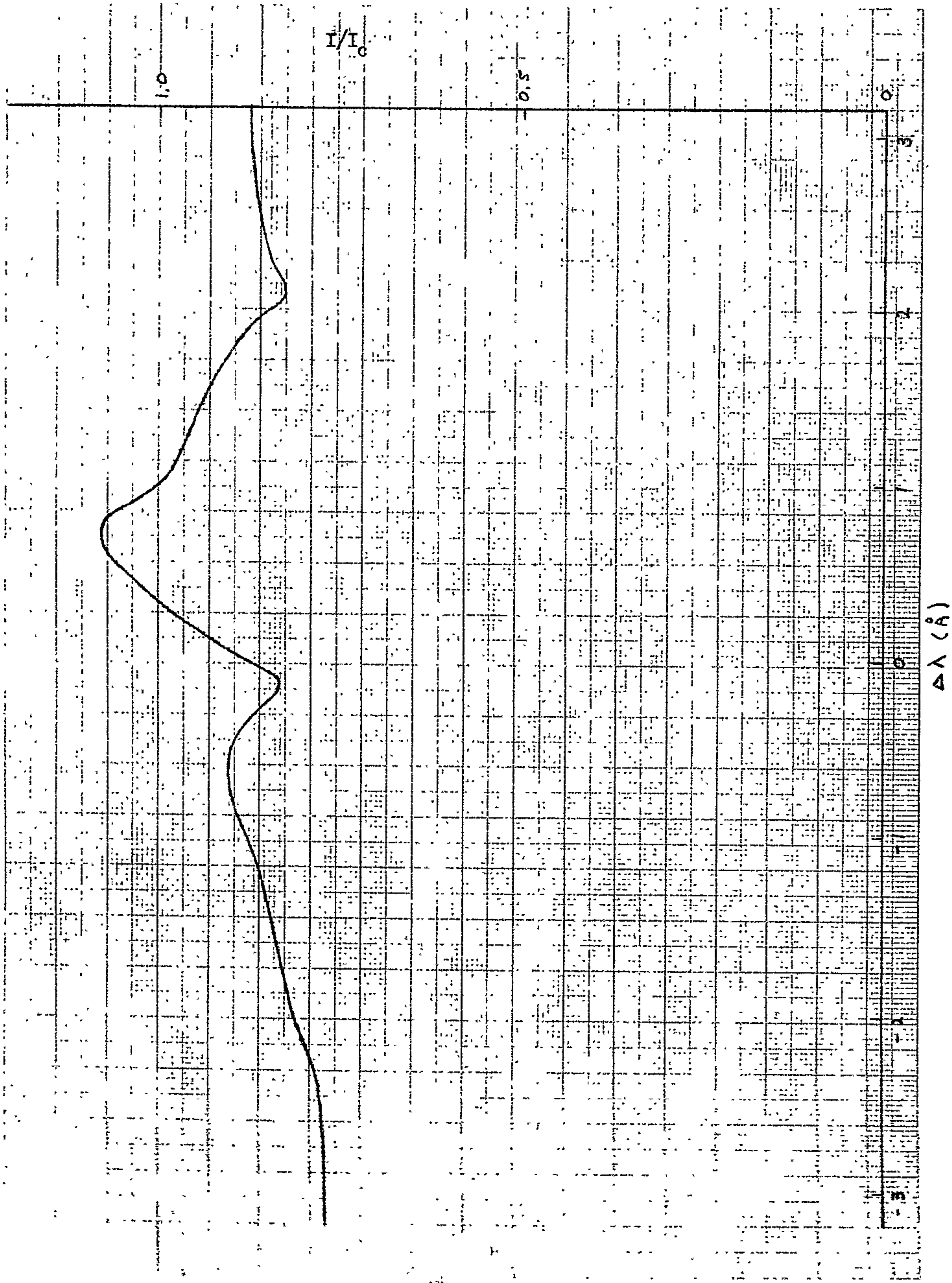

Fig. II-17. H-alpha profile. Frame 12

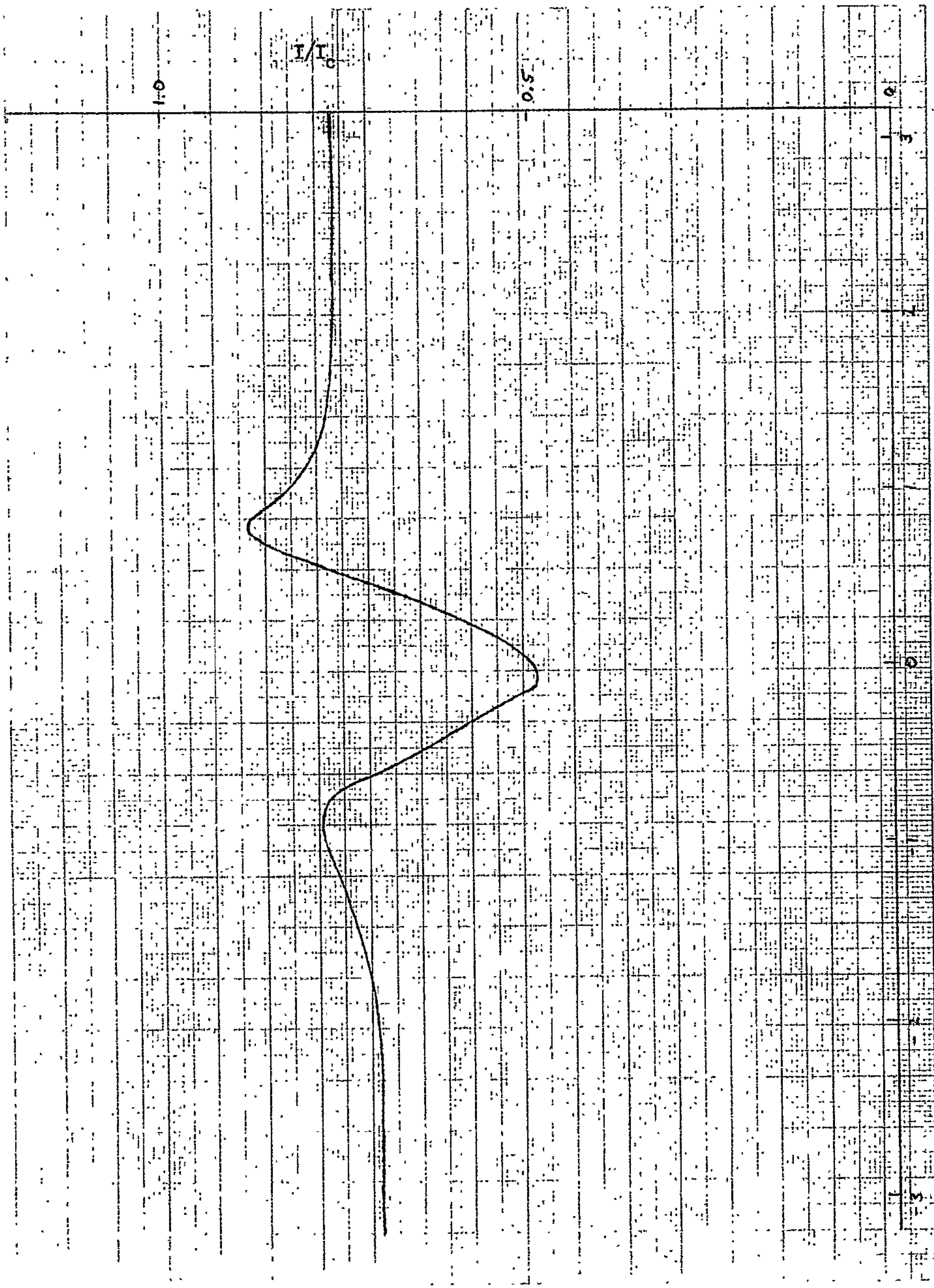

Fig. II-18. H-alpha profile. Frame 13

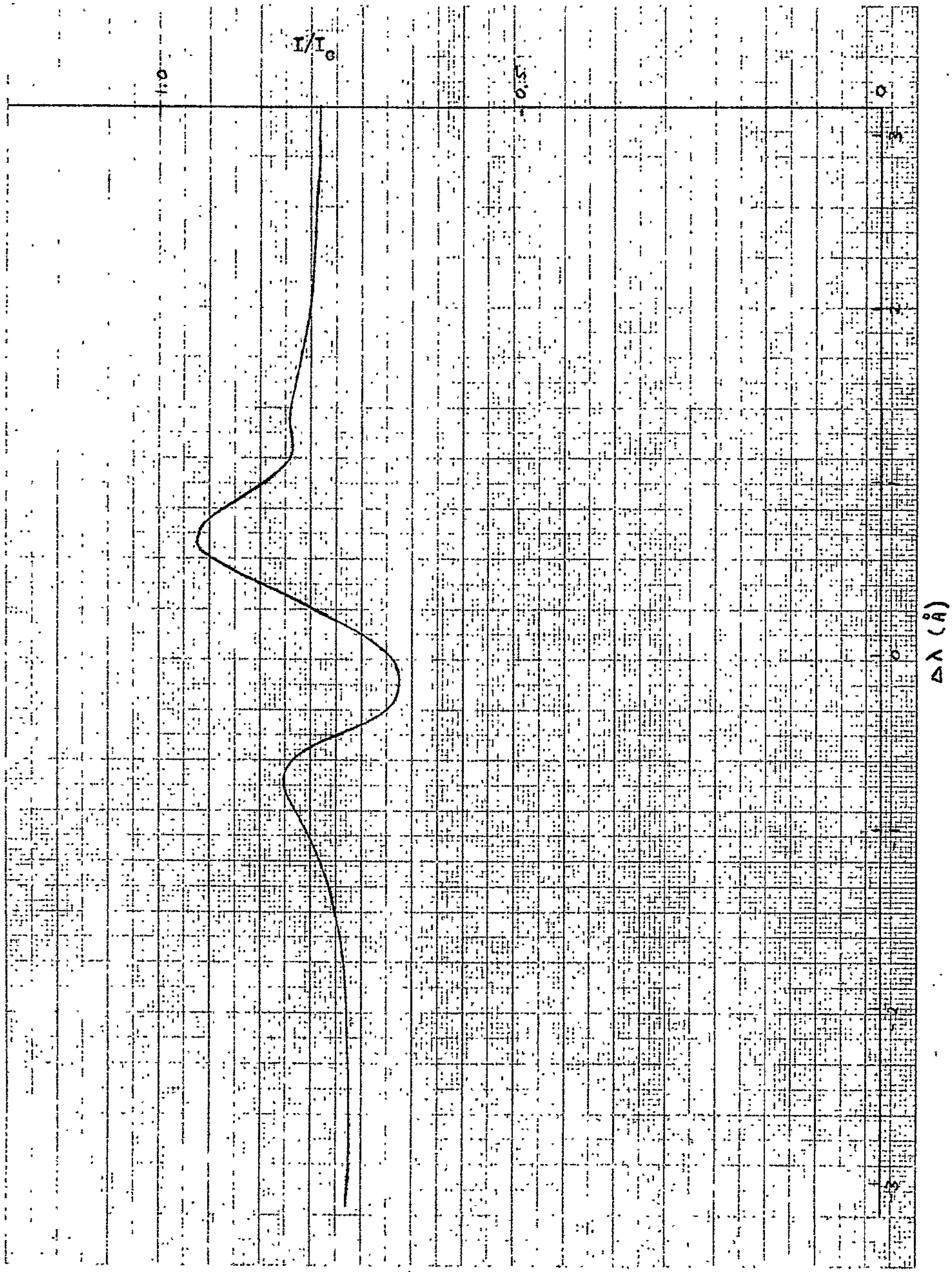

Fig. II-19. H-alpha profile. Frame 14

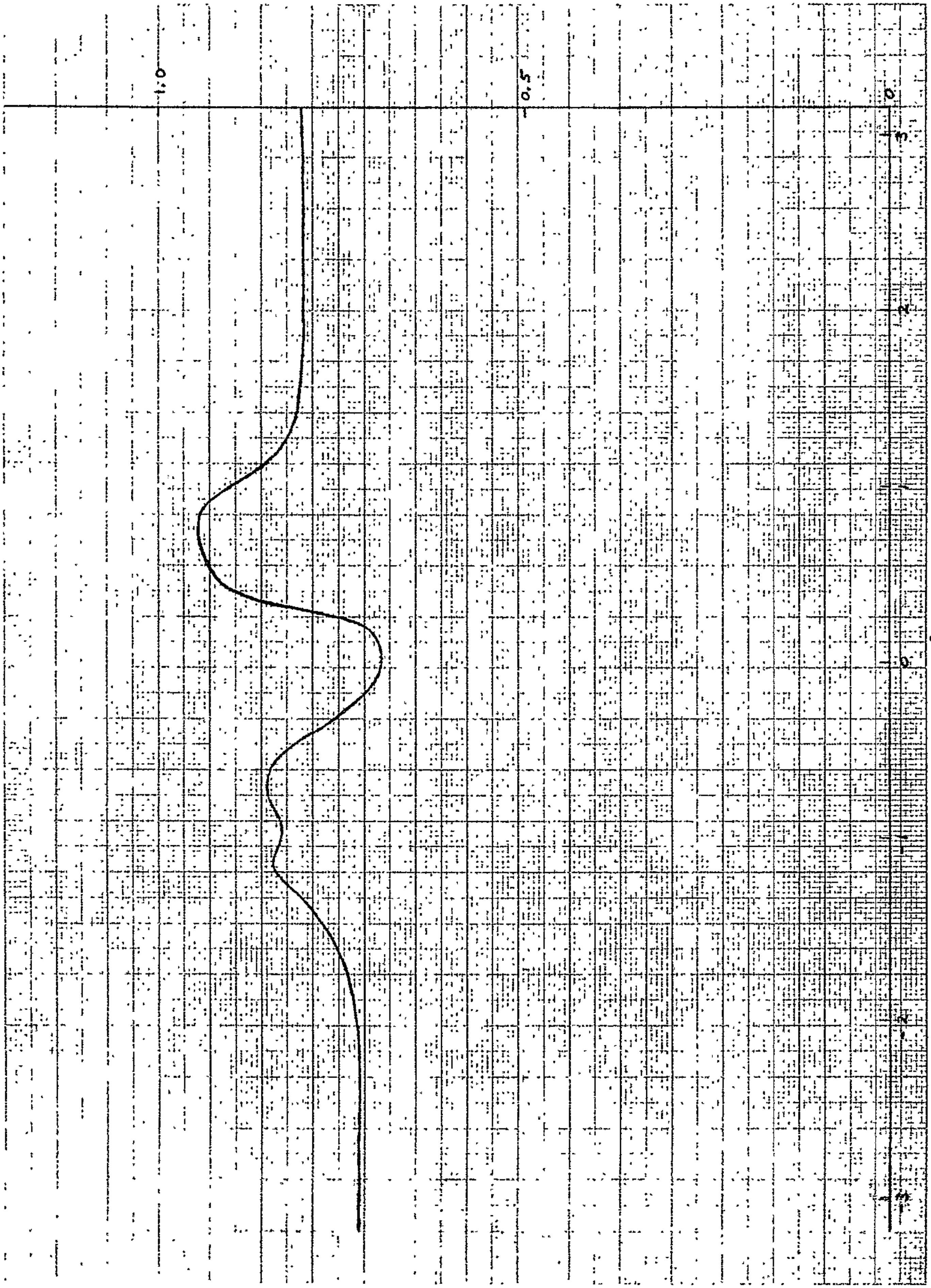

Fig. II-20. H-alpha profile. Frame 15

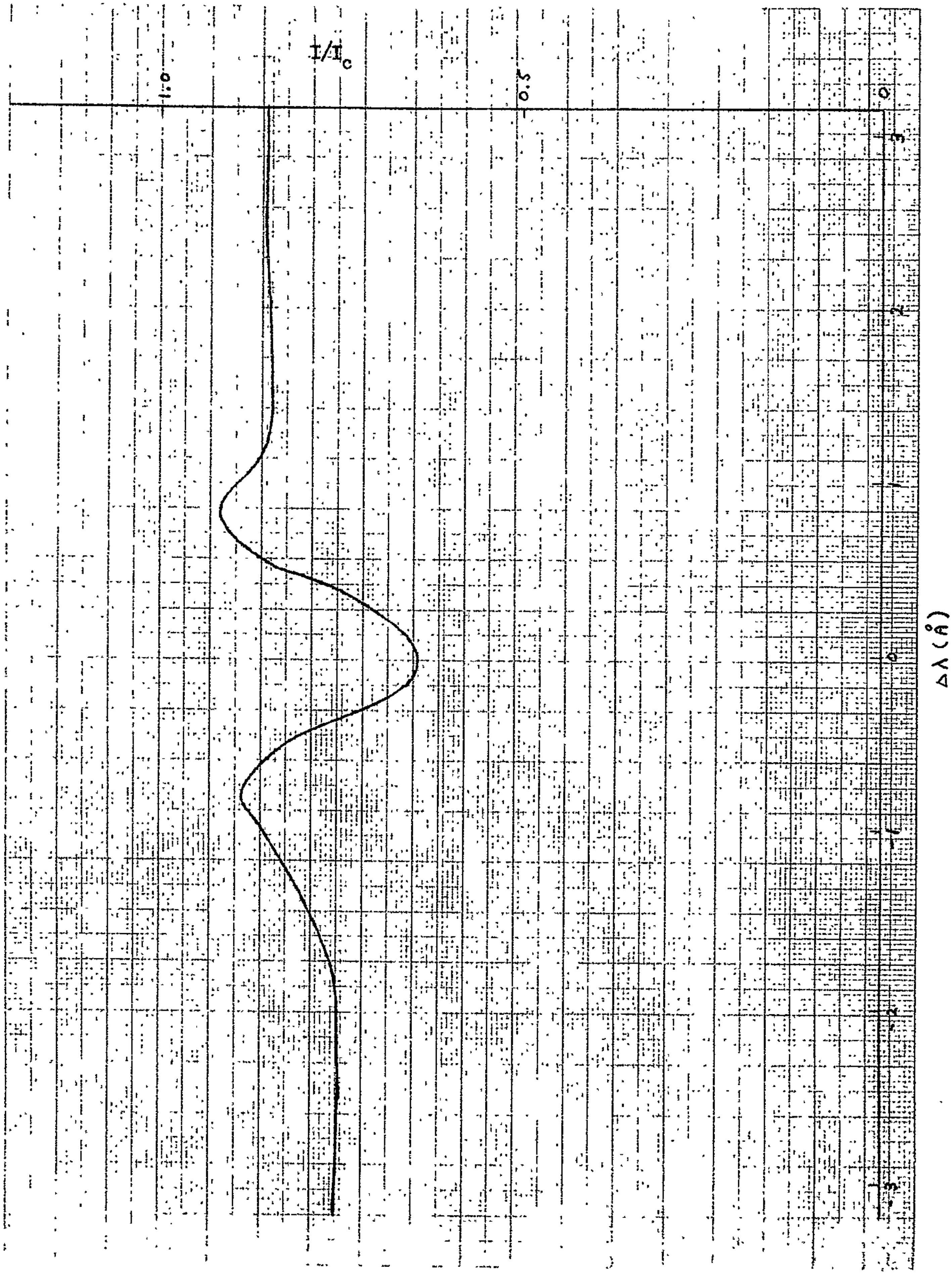

Fig. II-21. H-alpha profile. Frame 16

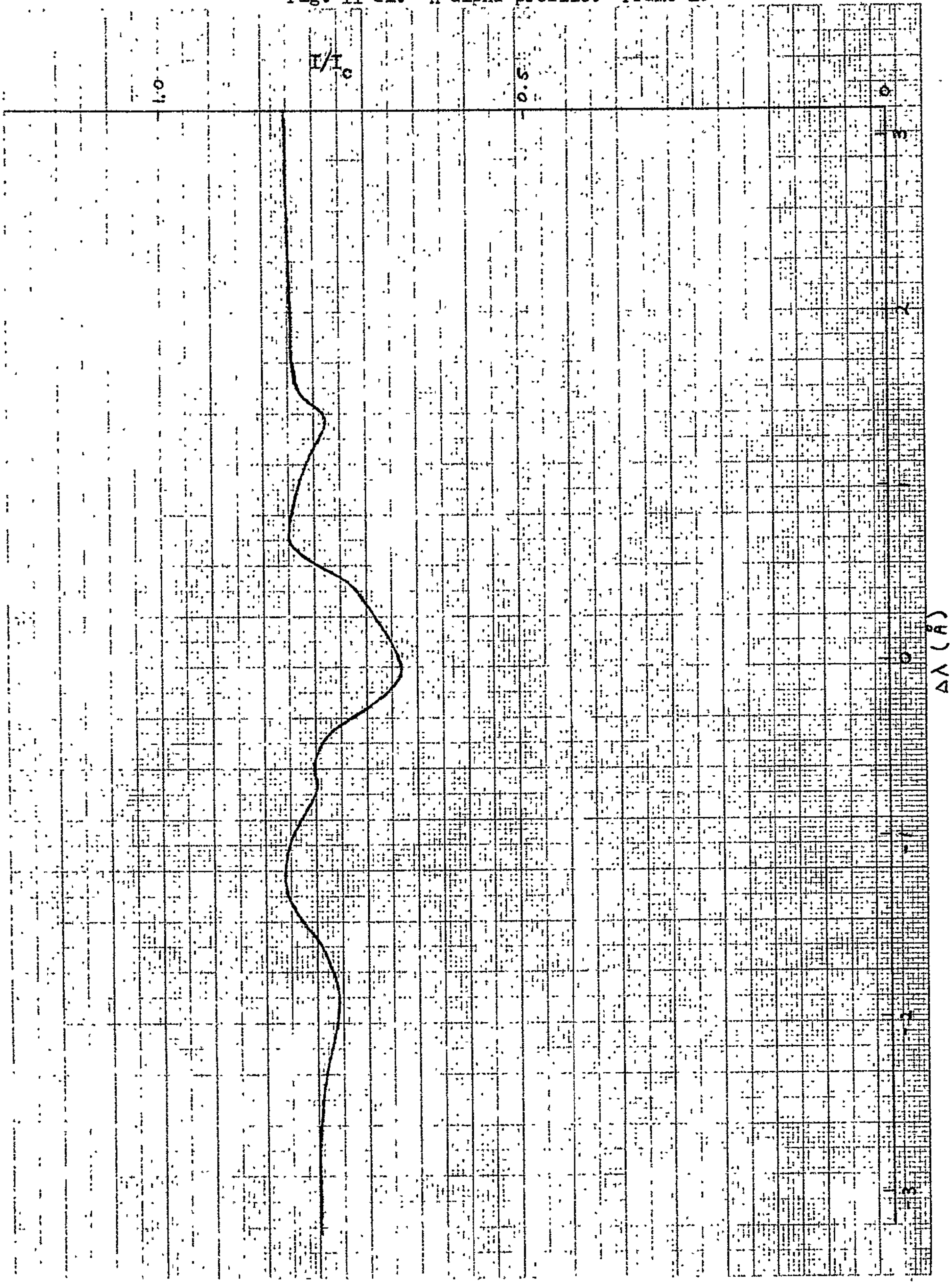

Fig. II-22. H-alpha profile. Frame 17

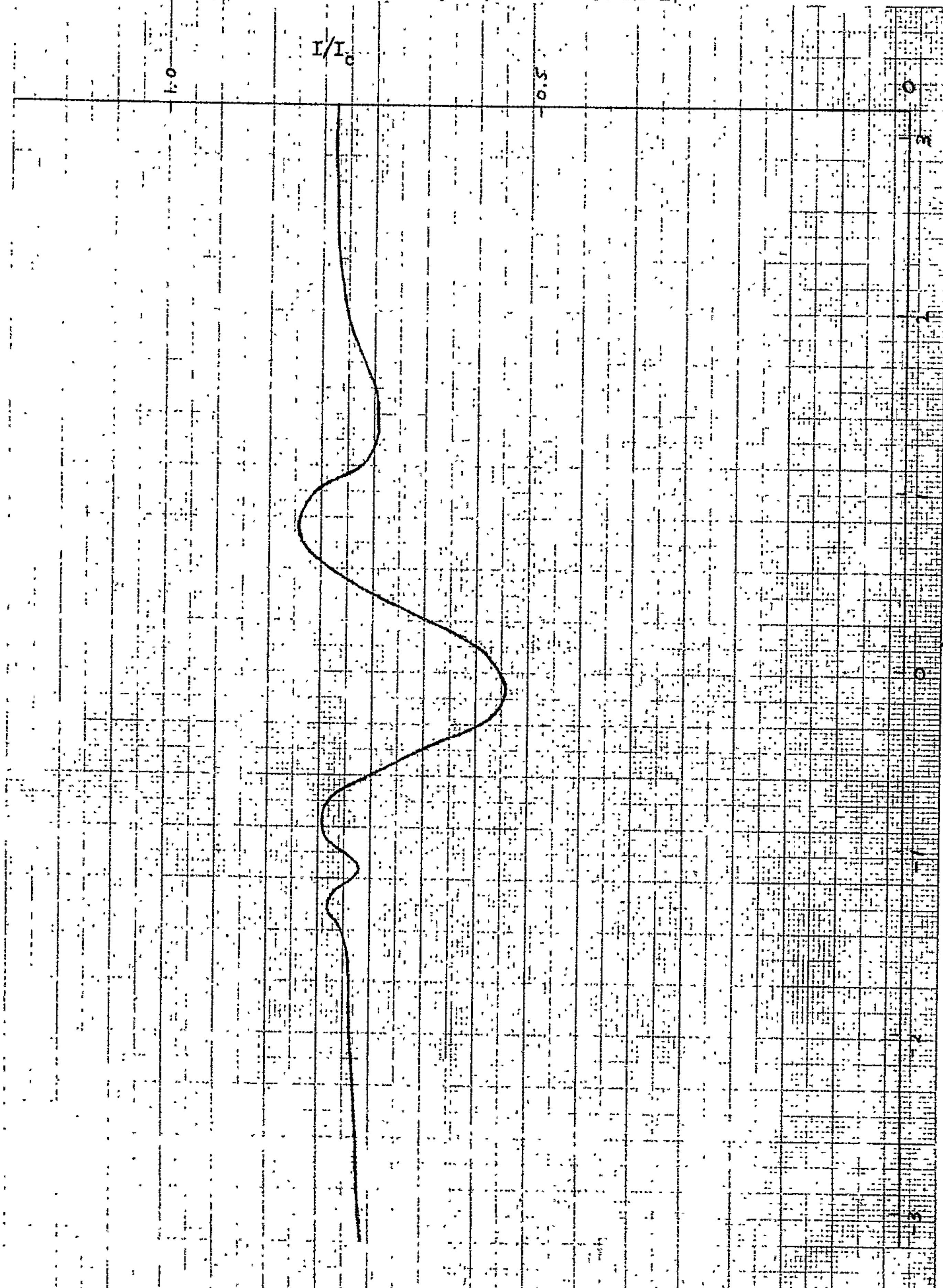

Fig. II-23. H-alpha profile. Frame 18

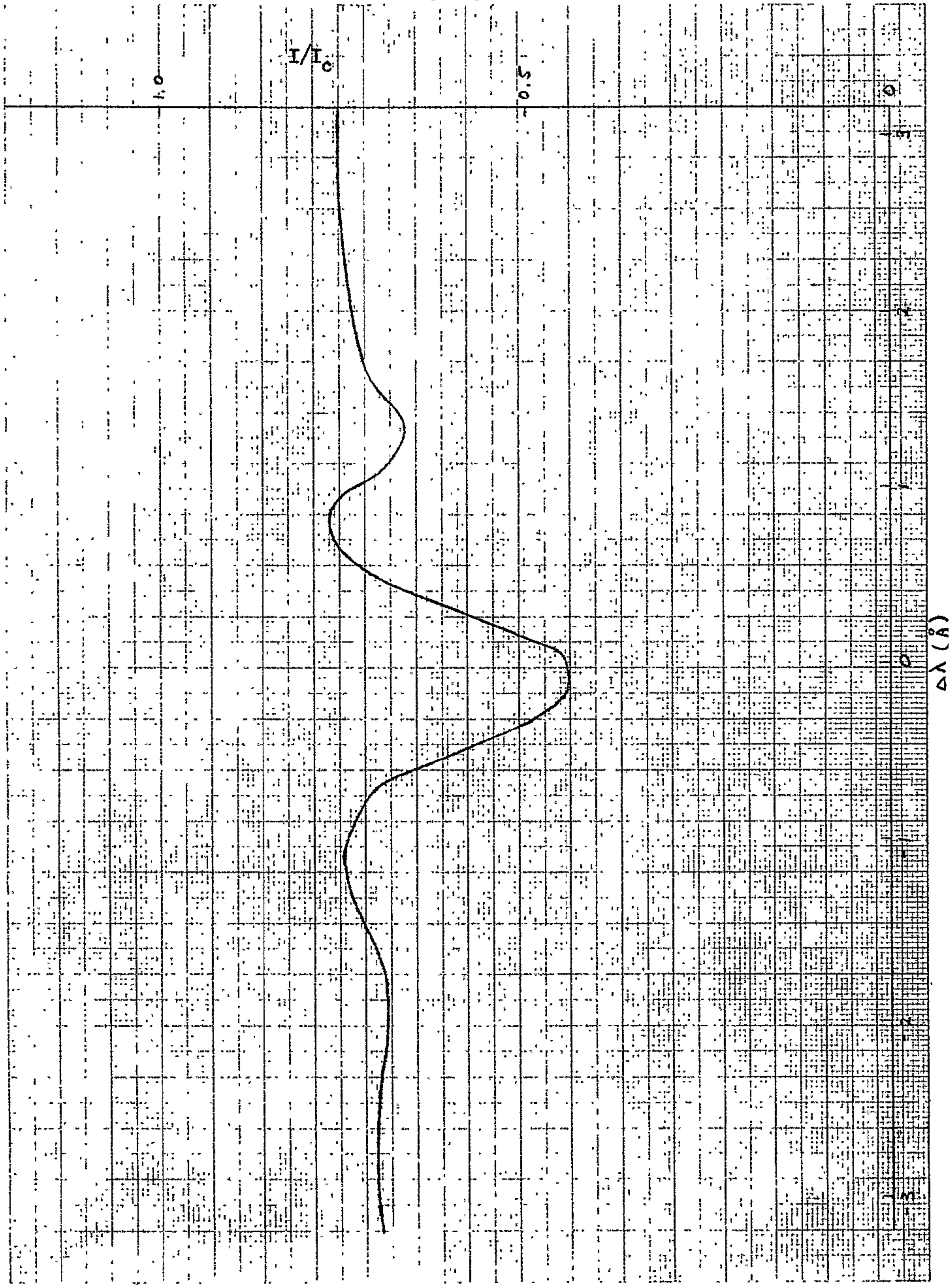

Fig. II-24. H-alpha profile. Frame 19

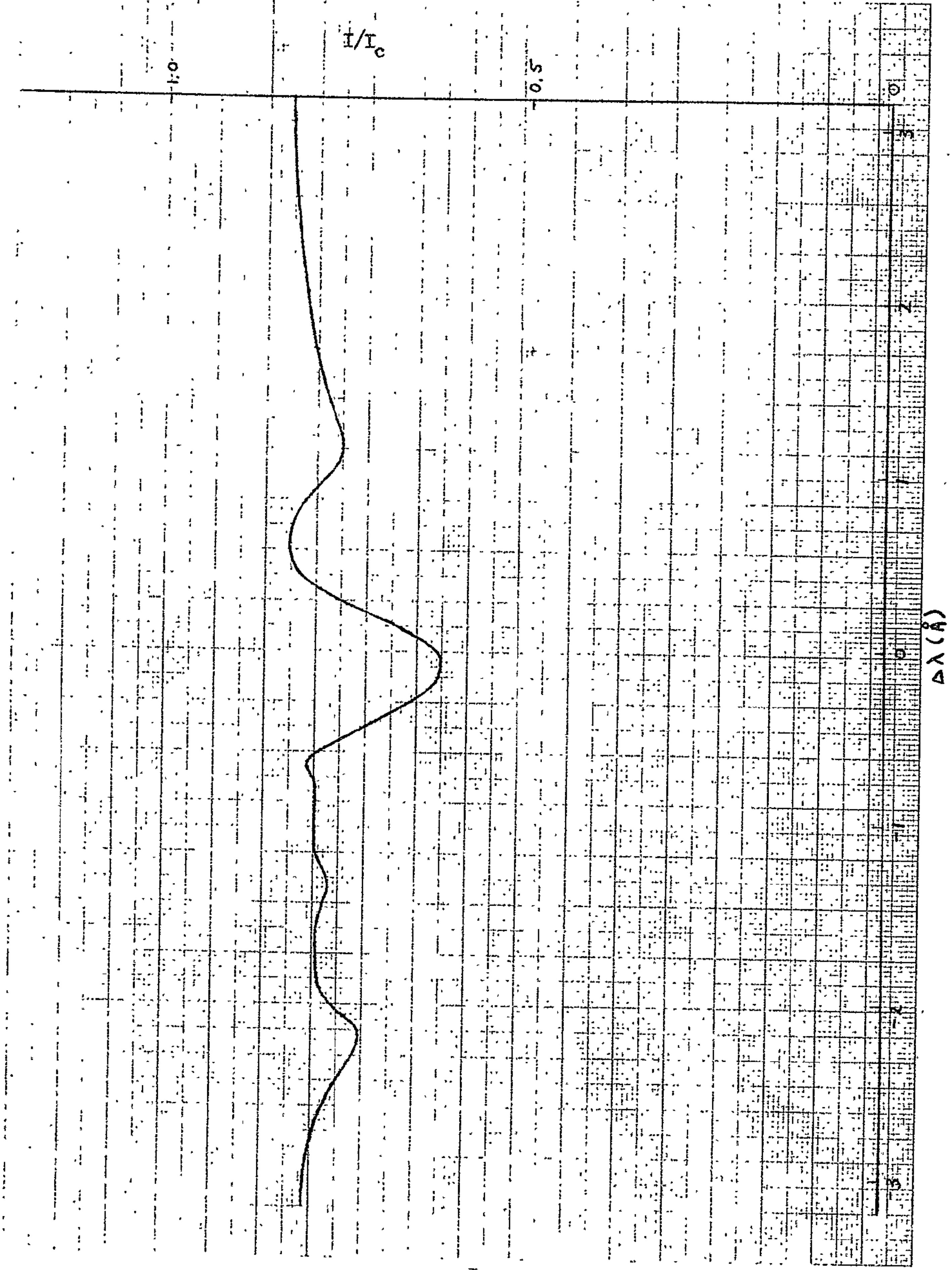

Fig. II-25. H-alpha profile. Frame 20

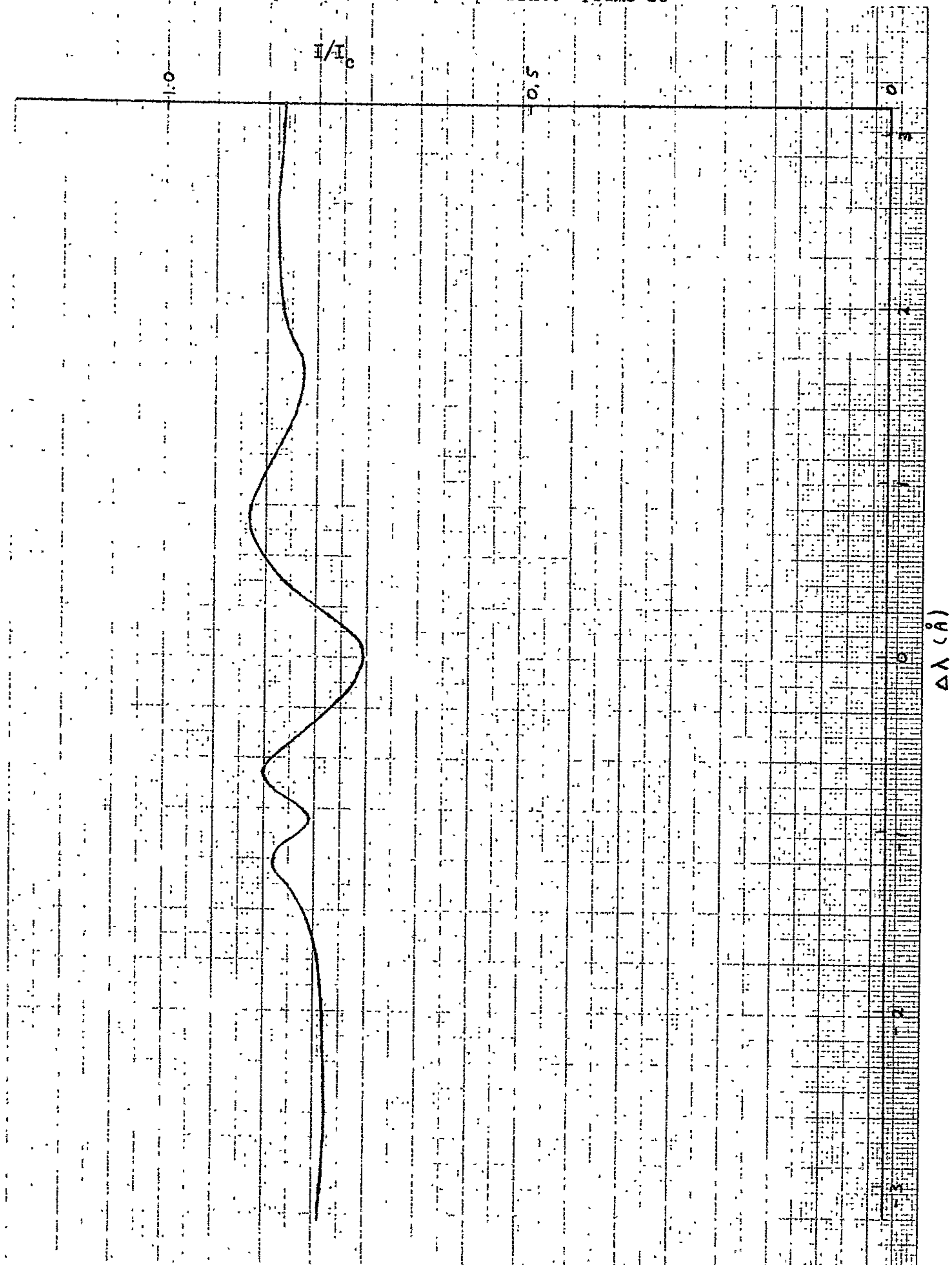

Fig. II-26. H-alpha profile. Frame 21

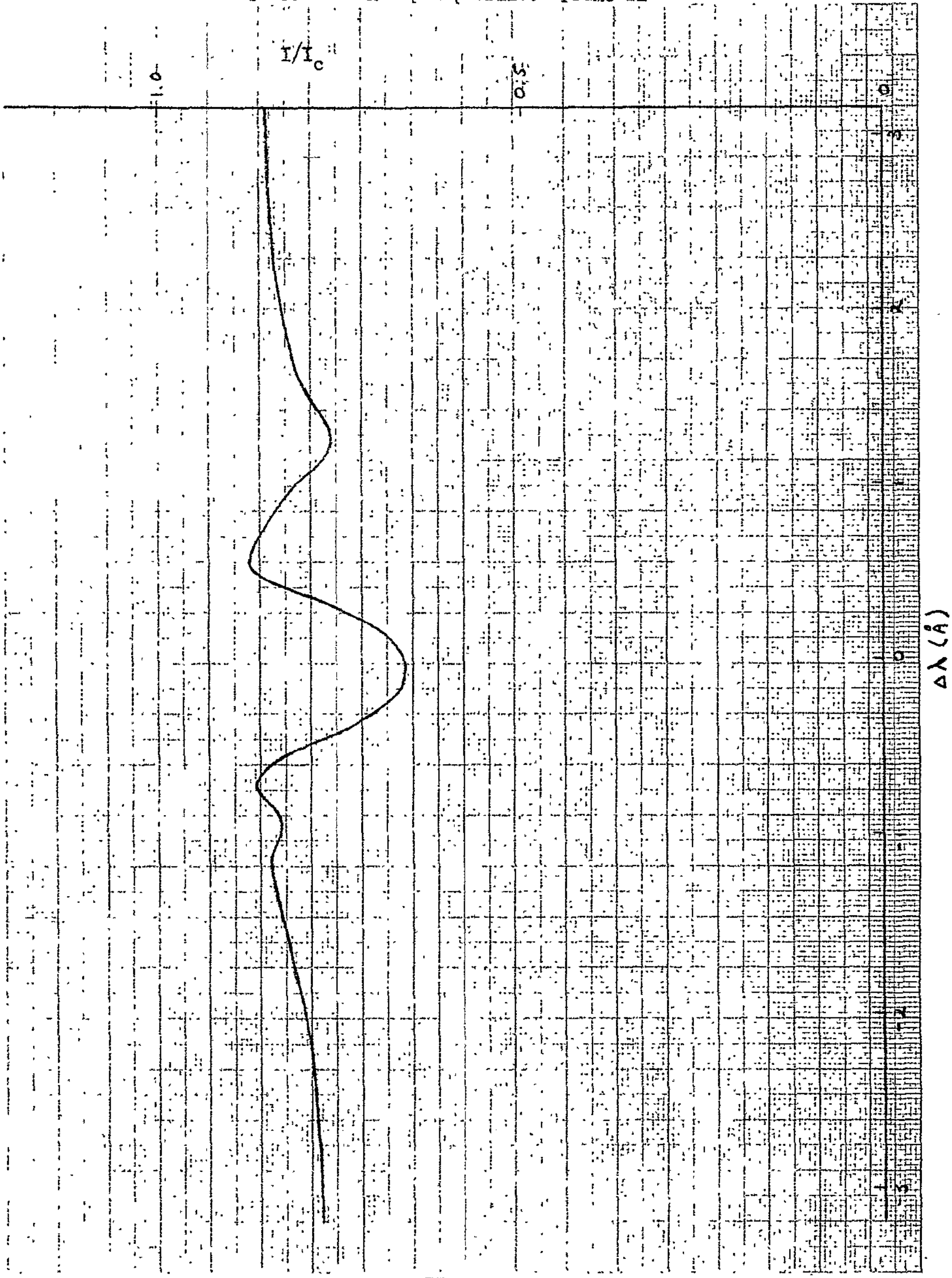

Fig. II-27. H-alpha profile. Frame 22

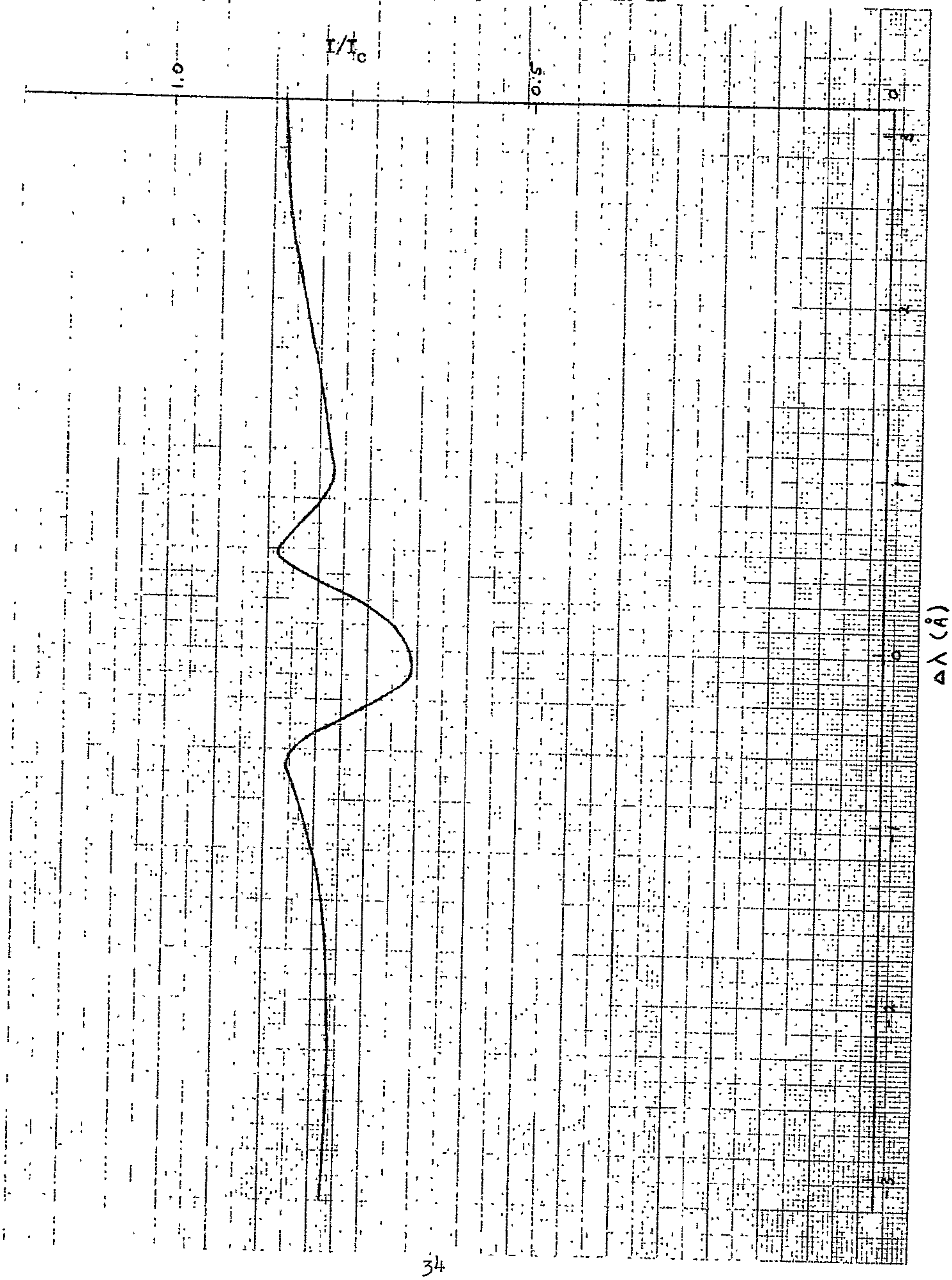

Fig. II-28. H-alpha profile. Frame 23

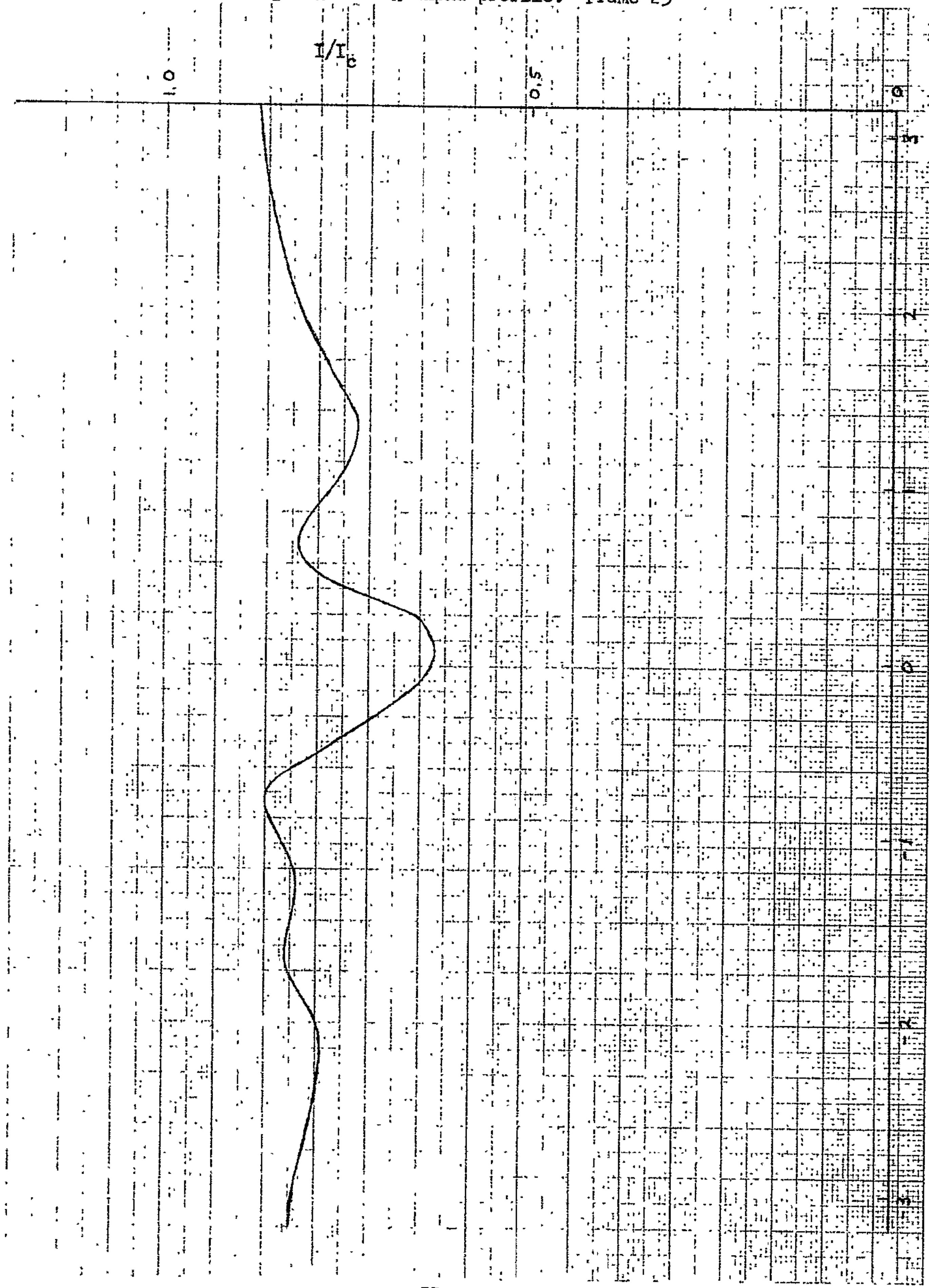

Fig. II-29. H-alpha profile. Frame 24

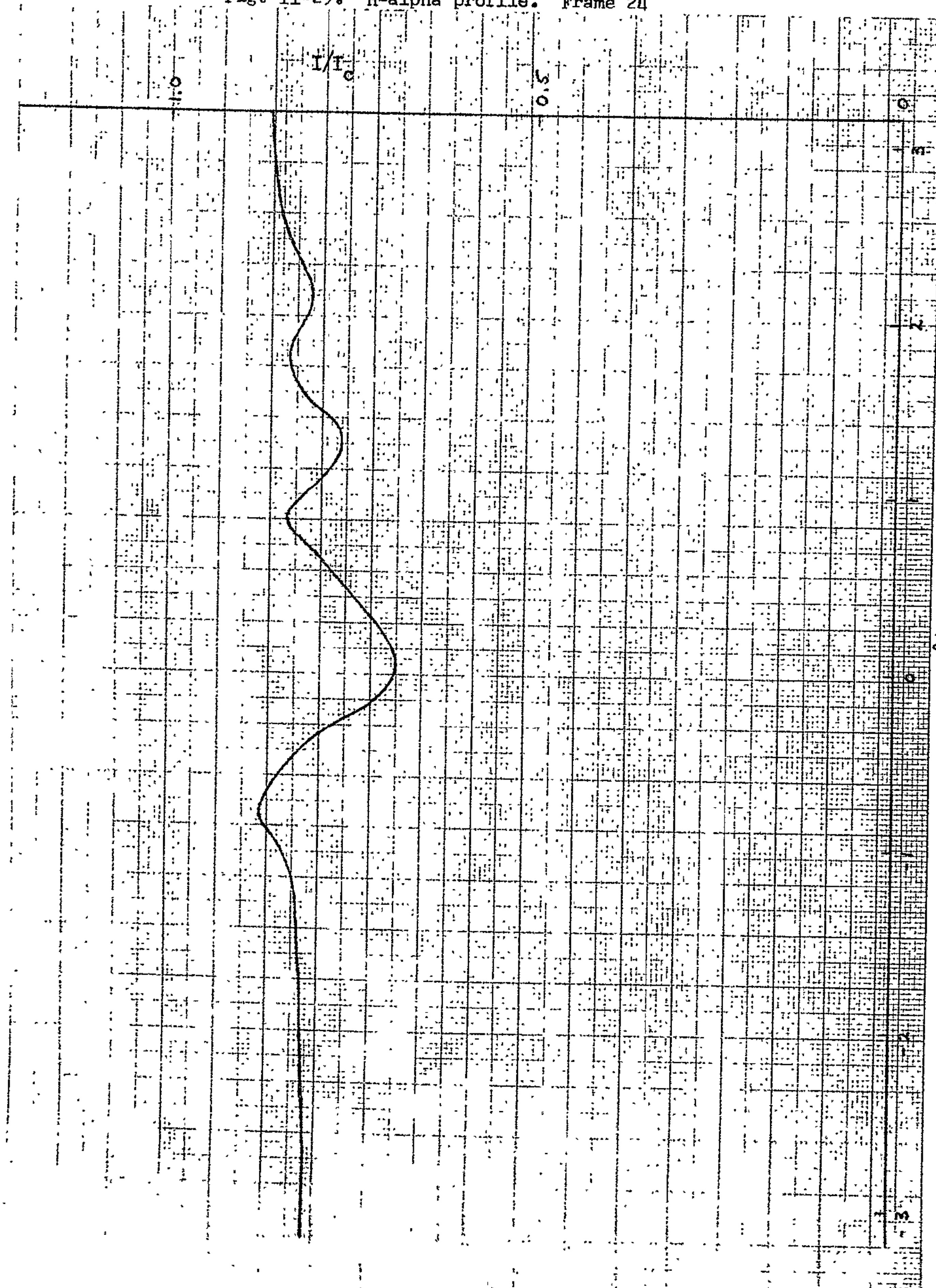

Fig. II-30. H-alpha profile. Frame 25

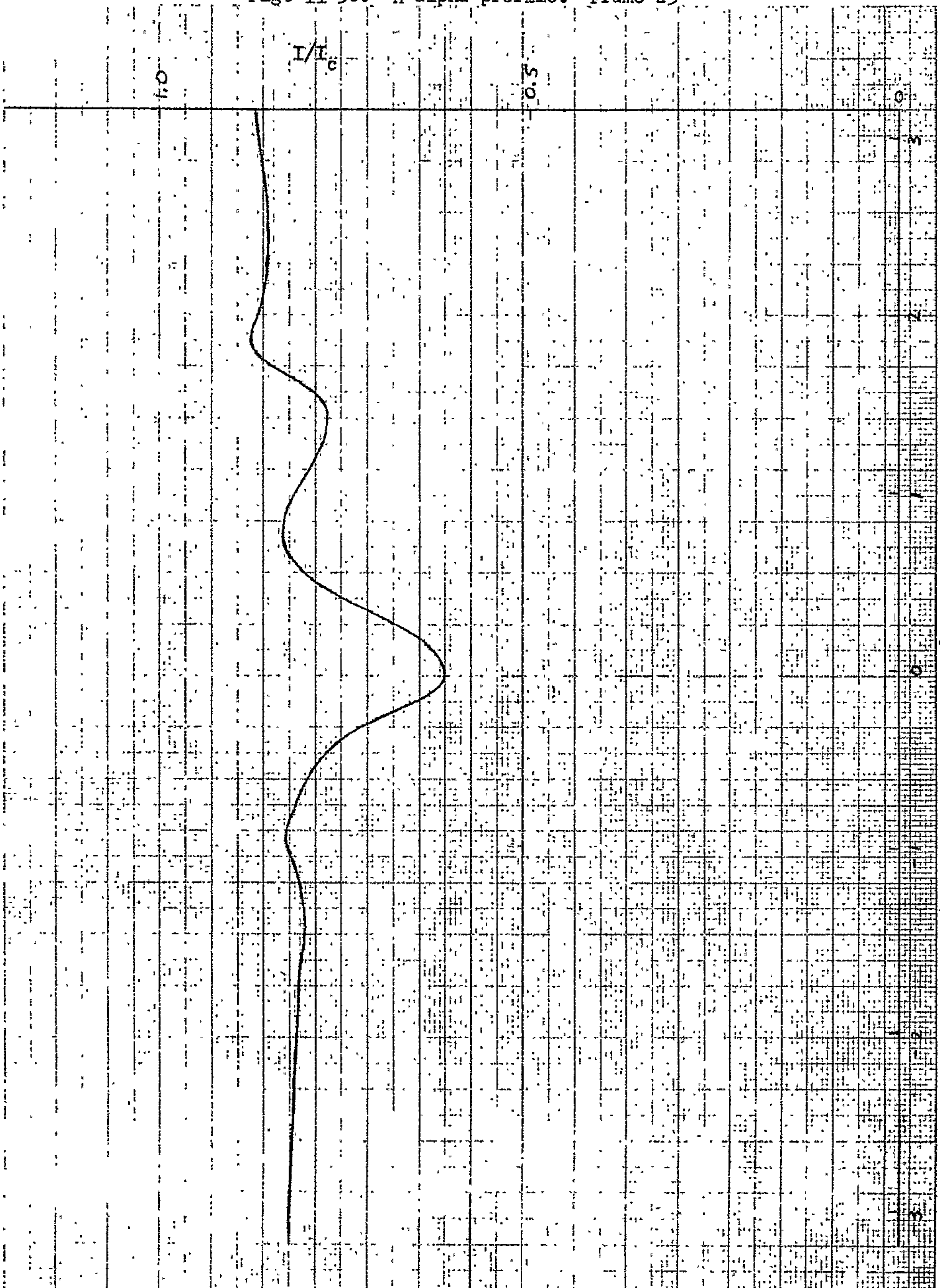

Fig. II-31. H-alpha profile. Frame 26

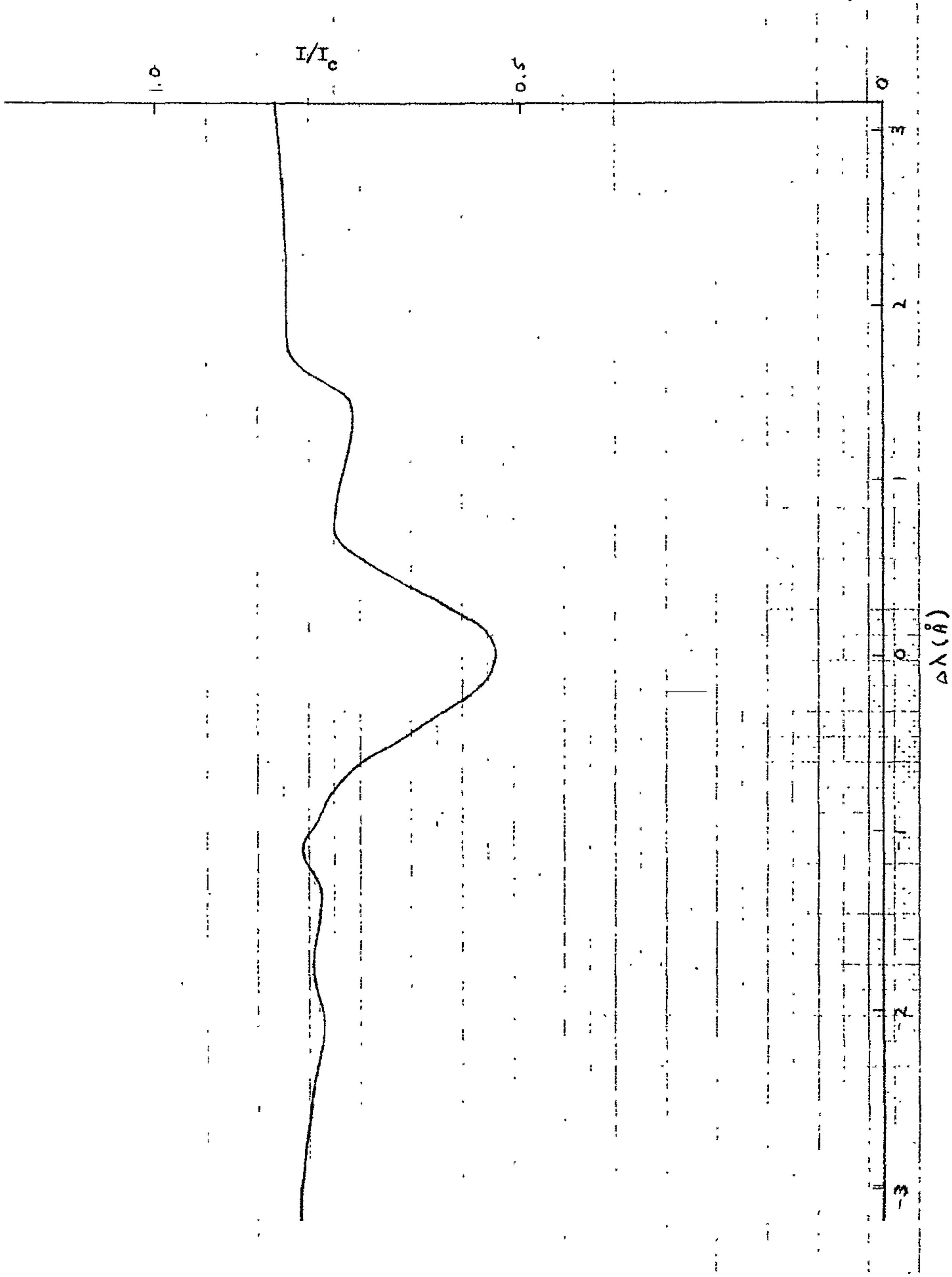

Fig. II-32. H-alpha profile. Frame 27

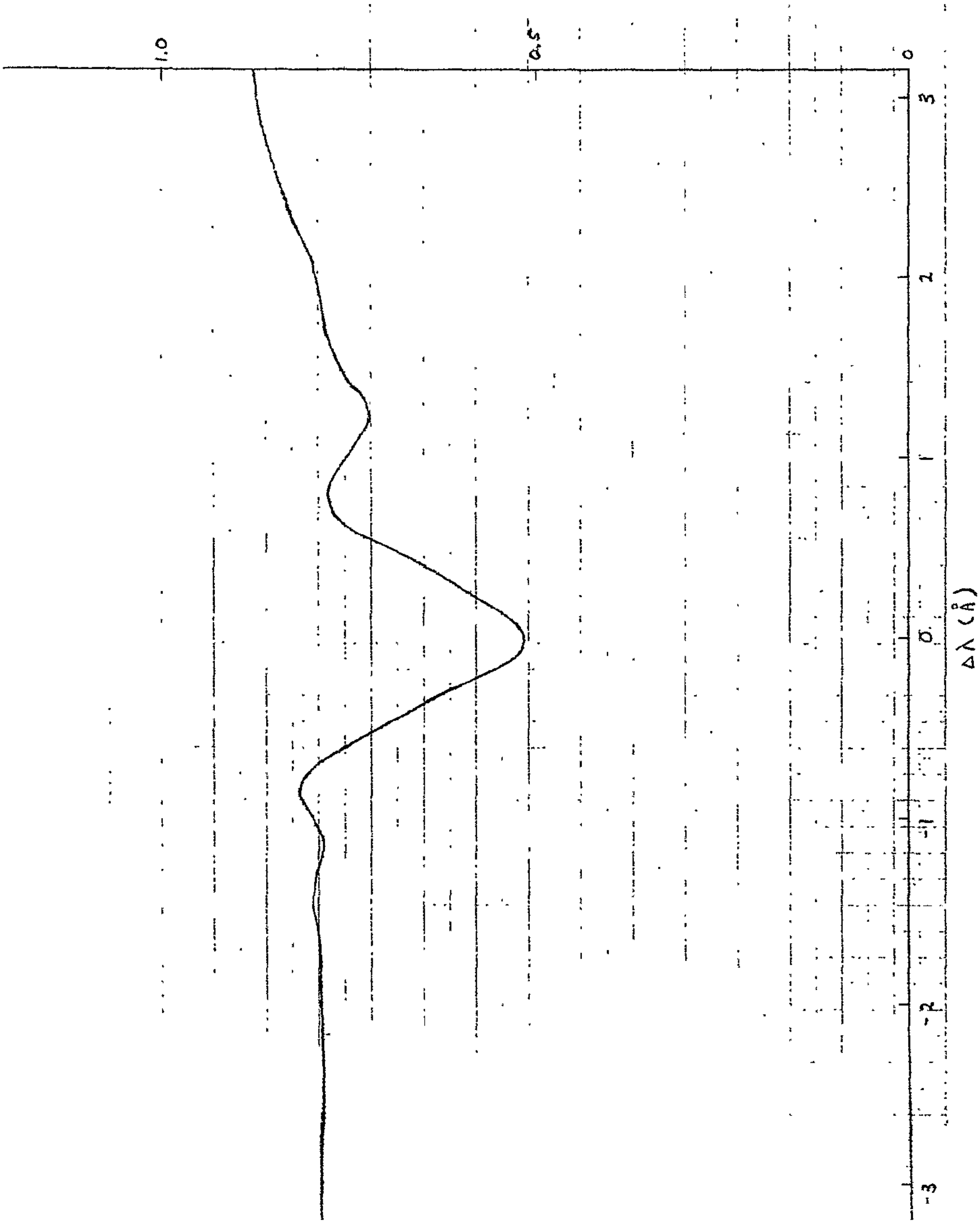

intensities are given in units of the nearby continuum. is the displacement in Å from the static line center.

Table II.2 lists the red to violet peak intensity ratio, the violet peak to center intensity ratio and the center, violet and red peak positions in Doppler width units assuming a Doppler width of 0.35 Å.

The line center and red and violet peak intensities are shown in Fig. II.33. Fig. II.34 shows the center and red and violet peak positions with respect to the static line center. A center shift to the red is indicated by a dashed line.

Details of the observations including the 5 Sept. 1973 flare are given by Martin, 1974.

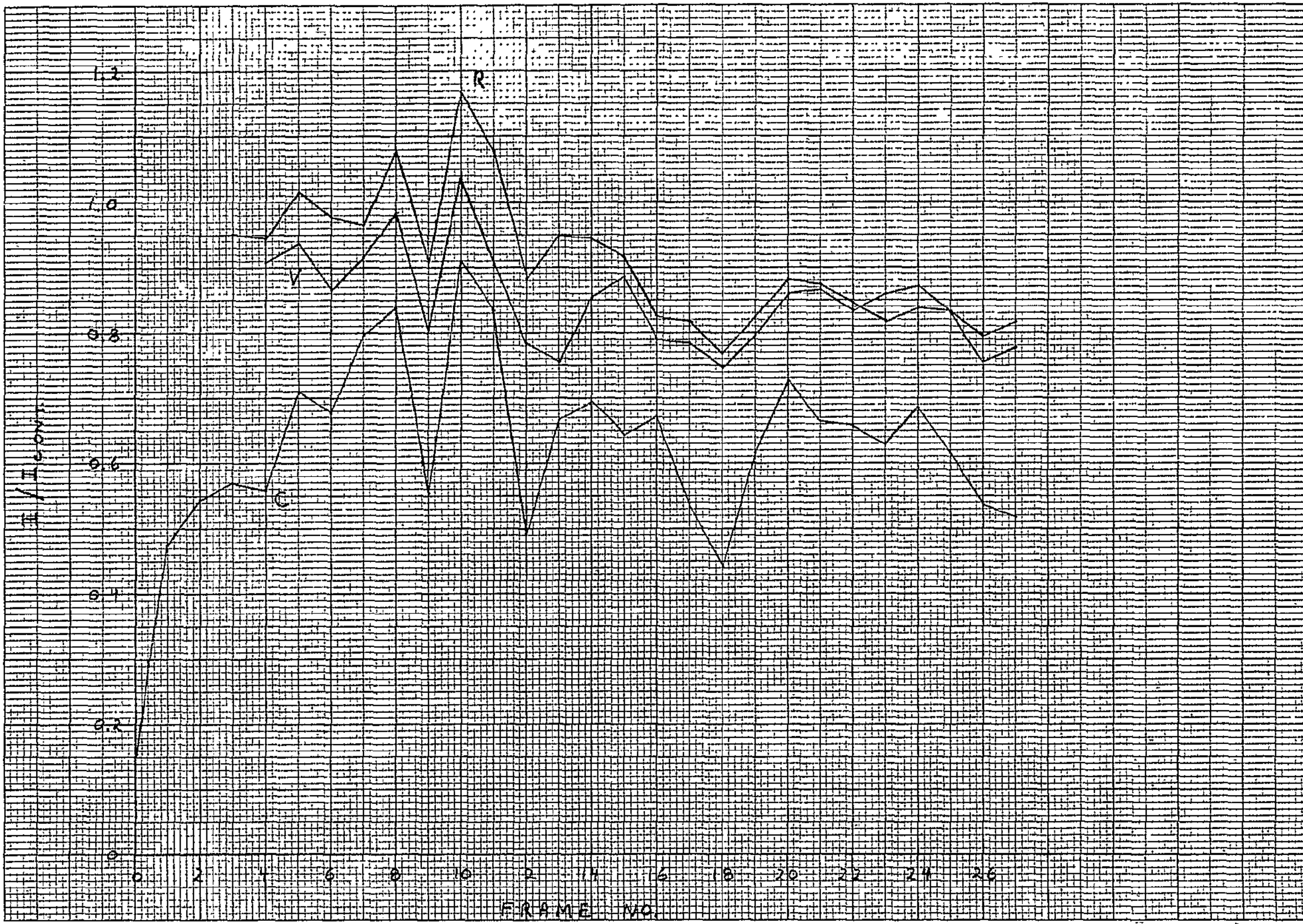

Fig. II.33. Center(C), Red(R)Peak and Violet(V) Peak H-alpha Intensities.

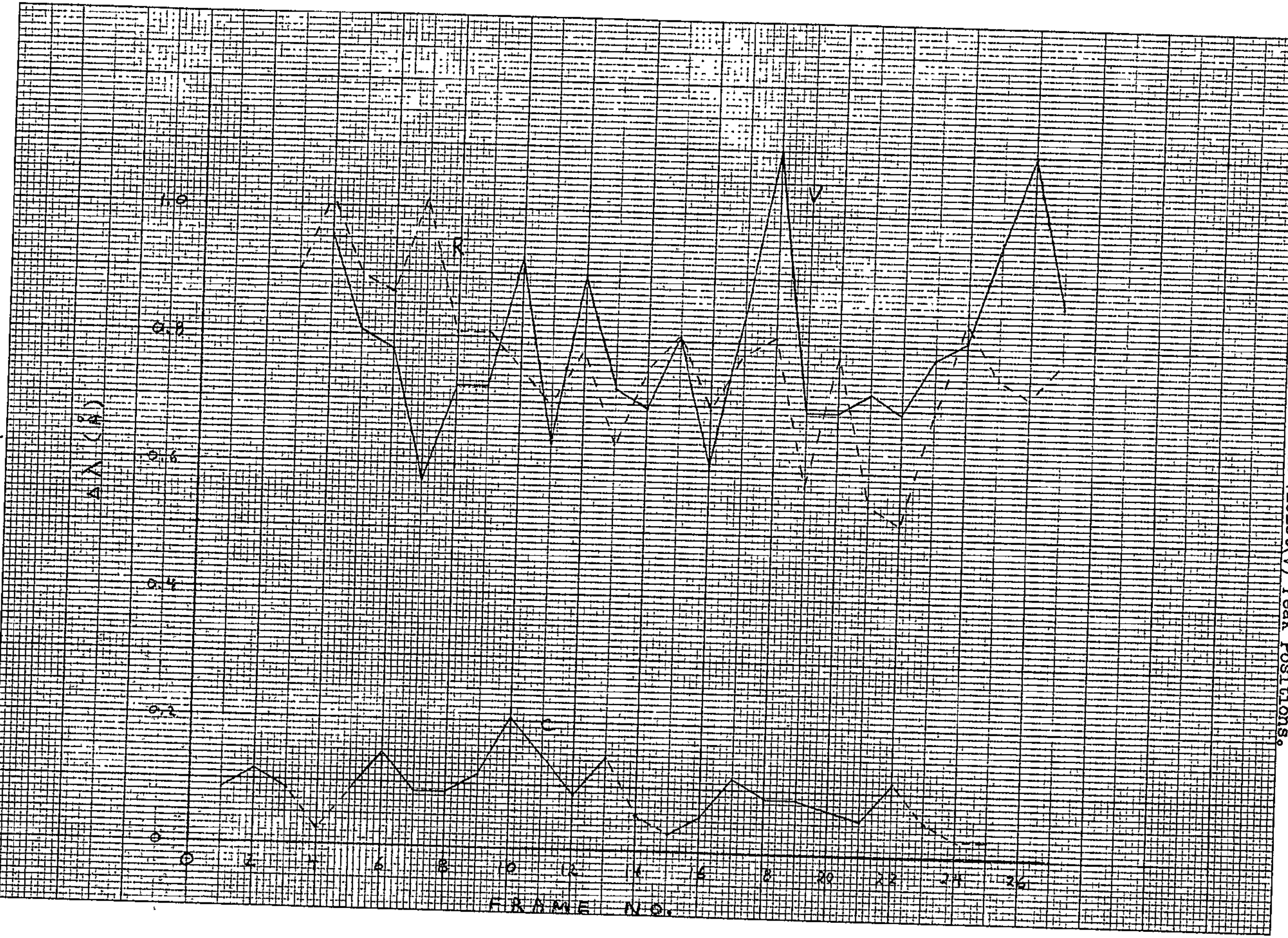

Fig. II.34. Center(C), Red(R) Peak and Violet(V) Peak Positions.

III. THEORETICAL CALCULATIONS

A. Source Function and Line Profile Equations

Source functions and line profiles for H-α have been generated by Canfield and Athay (1974) based on the kinematic flare shock model of Nakagawa, et al. (1973). The source function shows a maximum at line center optical depth ~ 20 and does not vary a great deal with the Mach number of the downward propagating shock wave. The source function for a shock of Mach 10 is shown in Figure III.A.1 by the dashed curve assuming a Planck function at 10^4 K.

To produce the self reversed profiles observed in most flare spectra the source function must have a maximum value at some optical depth. A manageable form which provides a maximum value and forms an asymmetry of the type exhibited by that shown in Figure III.A.1 is as follows:

$$\frac{S}{B} = \Delta + L\, e^{-kt} + L\, e^{-k(t_1 - t)} + F\, e^{-k(t_1 - t)} \qquad \text{III.1}$$

where Δ, L, k, t_1, F and B are constants.

This equation is the same as that for a finite layer of line center optical thickness t_1 in the one-point quadrature approximation to the frequency integration. t is the line center optical depth. The term F - - - represents irradiation of the finite layer from below. When F = 0 a symmetrical source function results. Δ represents a combination of source and sink terms for the line. Figure III.A.1 illustrates the source function given in Equation III.1 for $k = 10^{-2}$, F = 0, $\Delta = 1$, $L = -.9$, $t_1 = 300$, 1200; and $L = -.5$, $t_1 = 60$.

When the H-α line is basically a non-self reversed absorption line we shall consider the source function to have the form:

$$\frac{S}{B} = 1 - a\, e^{-kt} \qquad \text{III.2}$$

where a, k and B are constants. Following White (1961) for the quiet sun, a = .908, k = .07.

The line intensity at the surface of the layer at angle $\theta = \cos^{-1} \mu$ is given by:

Figure III.A.1

Source Functions vs. Line Center Optical Depth

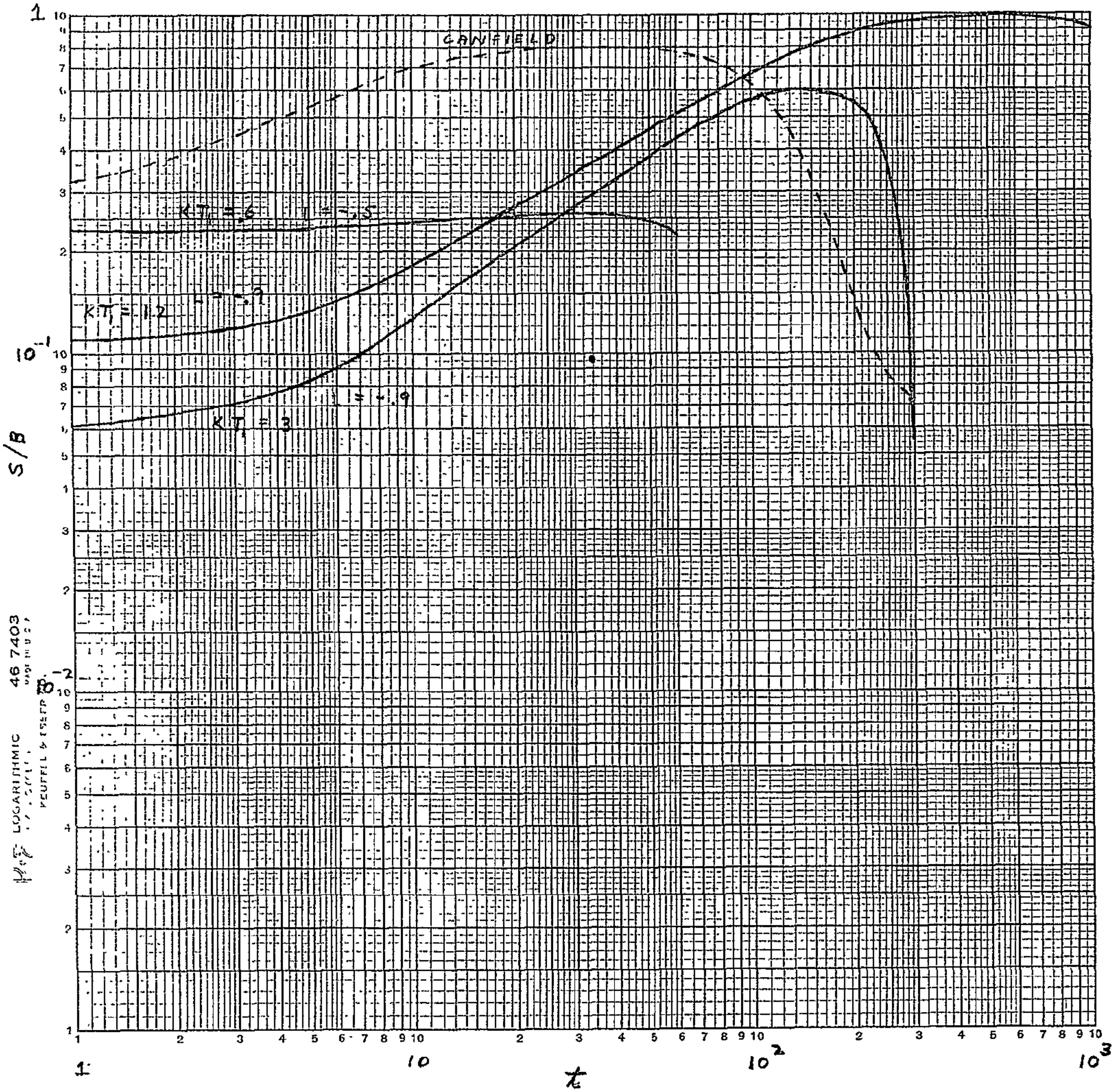

$$\frac{I_v\ (0,\mu)}{B\ (T_e)} = \int_0^{t_1} S_v\ e^{-\tau_v/\mu}\ d\ \tau_v/\mu + \frac{B\ (T_r)}{B\ (T_e)}\ e^{-\tau_{v1}/\mu} \qquad \text{III.3}$$

where $B(T_r)$ is the photospheric radiation (at T_r) incident upon the lower side of the layer and B is the Planck function within the layer (at T_e). $v = \Delta v/\Delta v_D$ where Δv_D is the Doppler half width.

$$S_v = \frac{S_L + r_v\ S_c}{1 + r_v} \qquad \text{and } d\ \tau_v = (\varphi_v + r_o)\ dt$$

where $r_v = K_c/K_L$, $r_o = K_c/K_{LO}$. K_c , K_L and K_{LO} are the continuum, line and line center absorption coefficients, respectively. φ_v is the line absorption coefficient. S_L and S_c are the line and continuum source functions. For a Doppler absorption coefficient

$$\varphi_v = \text{Exp} - [v + \mu V(t)]^2 \qquad \text{III.4}$$

where $V(t)$ is the gross velocity in Doppler half width units. The emergent line intensity can then be written

$$\frac{I_v\ (0,\mu)}{B\ (T_e)} = \int_0^{t_1} (\varphi_v\ S_L + r_o\ S_C)\ e^{-\int_0^{t} (\varphi_v + r_o) dt/\mu}\ dt/\mu$$
$$+ \frac{B\ (T_r)}{B\ (T_e)}\ e^{-\int_0^{t_1} (\varphi_v + r_o) dt/\mu} \qquad \text{III.5}$$

B. Absorption Profiles

Line profiles have been calculated for various values of V and t_1. The method we shall use of inferring the velocity for non-self reversed absorption profiles is that of measuring the bisector shift of the line. We have shown this to be a qualitatively valid method (Kulander and Jefferies, 1966). We illustrate in the next three figures some bisector shifts derived from synthetic profile calculations. Figure III.B.1 shows bisector shifts δv vs. mean line position Δv for layers with constant velocity $V/V_D = .072$ and thicknesses $t_1 = 1, 5, 25$ and 50. (V_D is the Doppler half width velocity). The quantity δv is the distance of the observed line center from the static line center. When t_1 is small the wing is hardly affected while for large t_1 the line as a whole is shifted by $\delta v = .072$.

Figure III.B.2 shows bisector shifts for $V = -.072/t^n$ with $t_1 = \infty$ and $n = 0, .1, .2, .5, 1.$ and 2. Figure III.B.3 shows bisector shifts for the velocity $V = .072\ (\alpha - \beta t^n)$ for various values of α, β, n and t_1.

Figure III.B.1

Bisector Shift δv vs. Mean Line Position Δv.

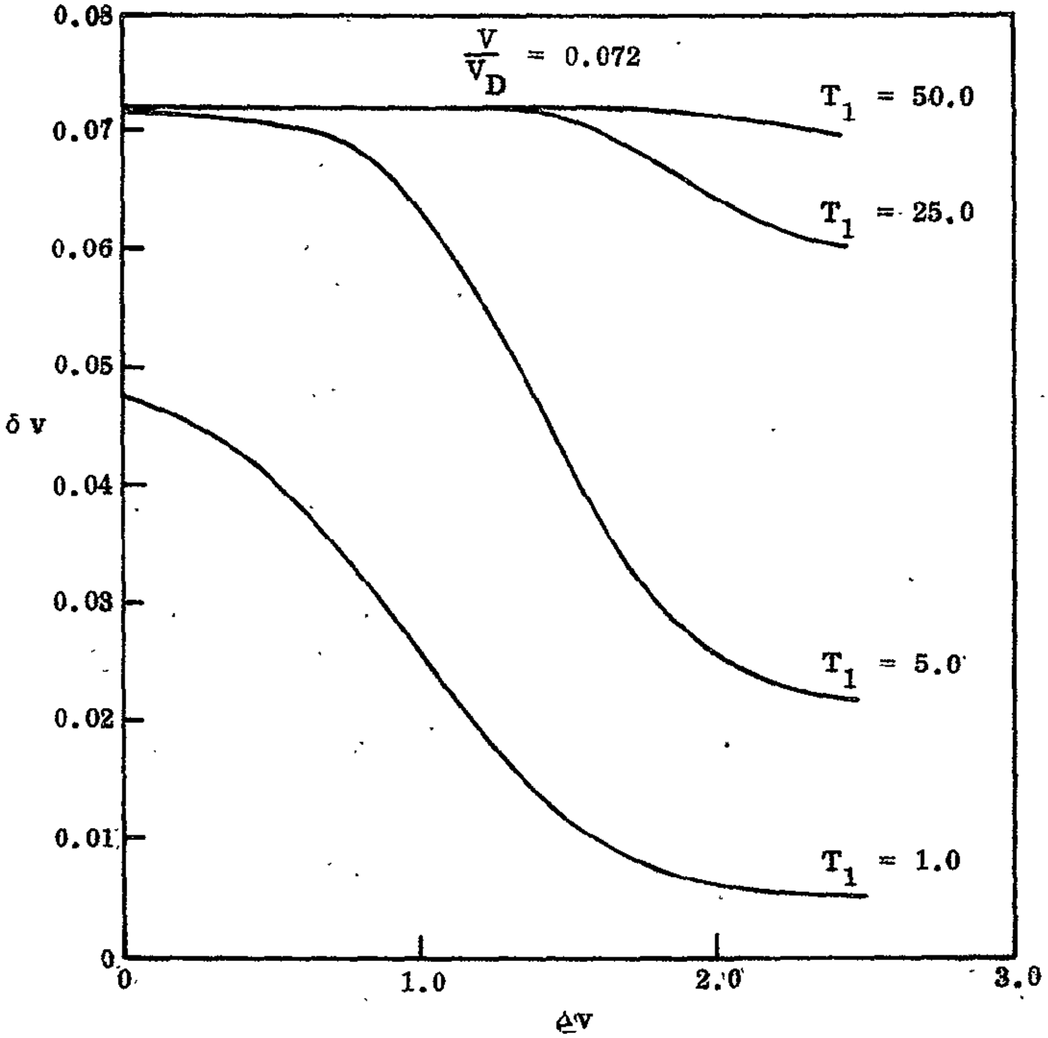

Figure III.B.2

Bisector Shift δ v vs. Mean Line Position Δ v.

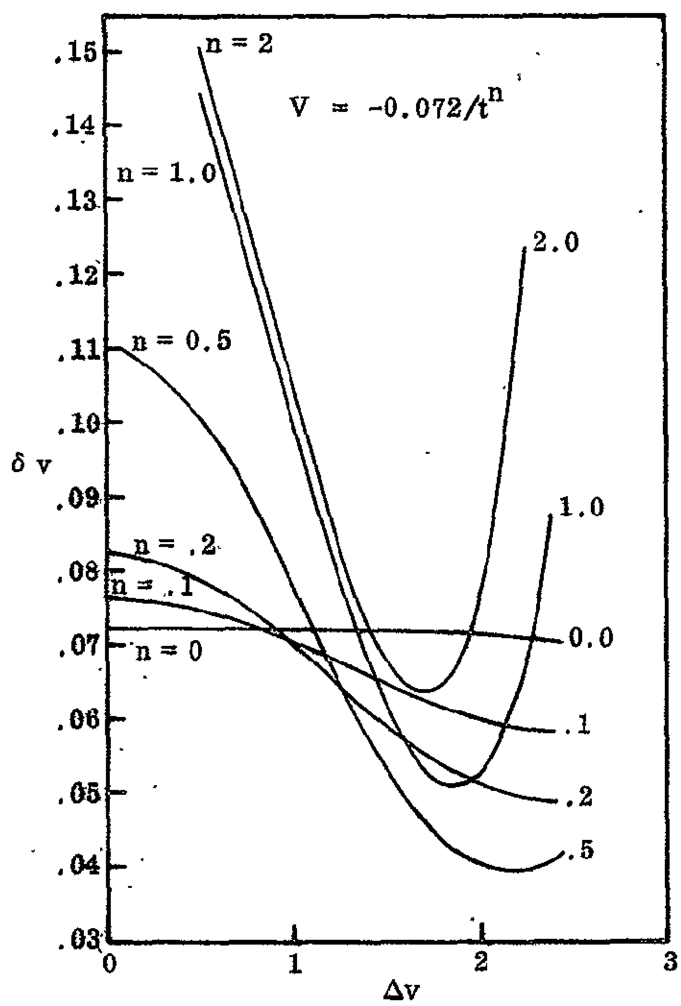

Figure III.B.3

Bisector Shift δv vs. Mean Line Position Δv.

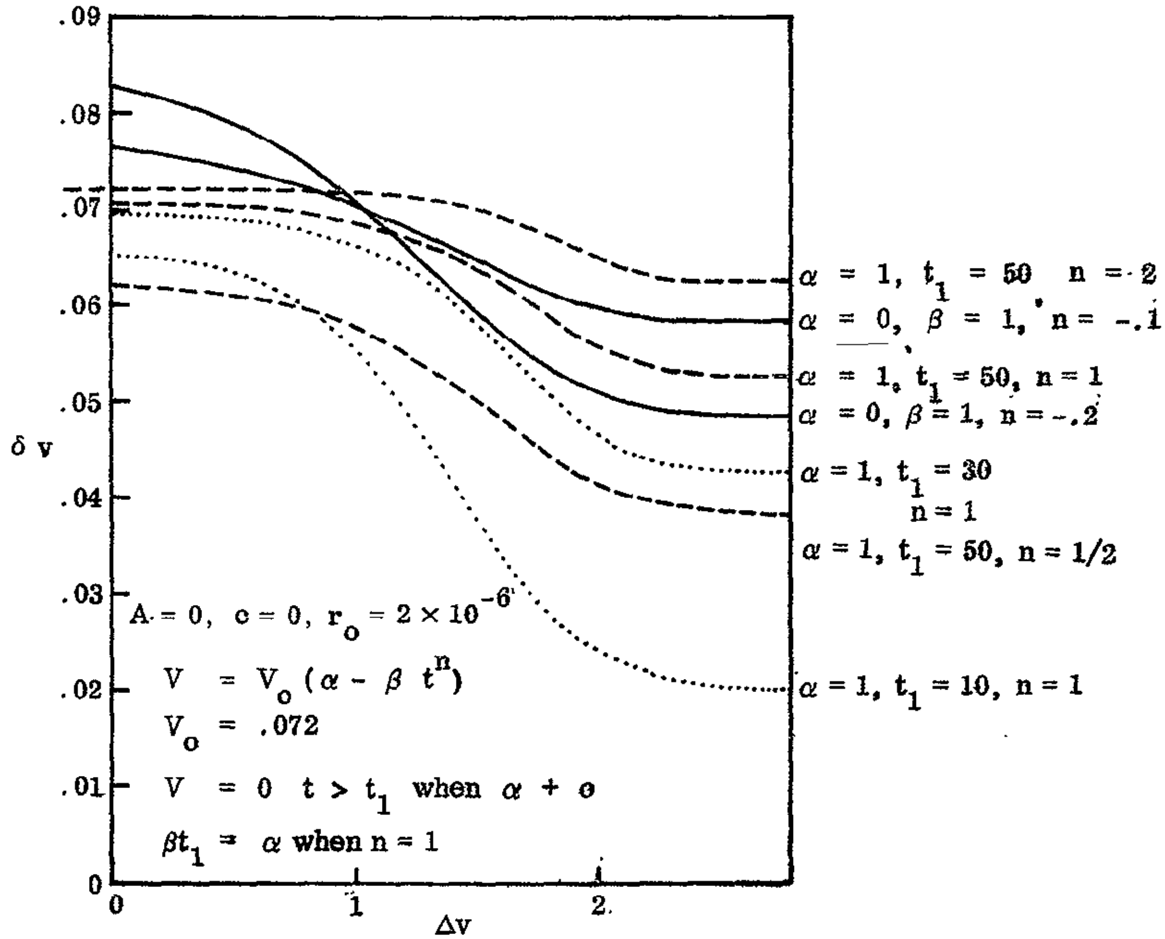

C. Self Reversed Profiles

Theoretical H-α profiles have been generated using the source function of Equation III.1 and the following assumed velocity in a finite layer of optical thickness t_1:

$$V = V_o/(1 + B_1 t)^{B_2}$$

where V_o, B_1 and B_2 are constants. When B_1 is positive the velocity decreases with increasing t. We will discuss in this section the effect of various values of the source function and velocity parameters on the line profiles.

Figures III.C.1 and III.C.2 illustrate static profiles for various layer thicknesses t_1. In Figure III.C.1, L = -.9 and in Figure III.C.2, L = -.5. The emission peaks move outward and become more intense as t_1 increases. Also the ratio of peak to center intensity increases as t_1 increases. Since the surface value of the source function does not change significantly as t_1 increases beyond a certain point the central intensities do not change. For all the profiles shown here we have assumed no photospheric radiation incident from below the flare layer.

Figure III.C. 3 shows profiles for a layer with optical thickness 600, $V_o = 1$, $B_1 = .1$ and $B_2 = 2$. (The assumed velocity is toward the observer). The upper curve represents L = -.5, the lower curve L = -.9. The corresponding static profiles in each case are shown by the dotted curves. The assumed velocity depresses the violet peak and enhances the red peak by increasing the overlying absorption on the violet side and decreasing it on the red side.

Figures III.C.4 and III.C.5 show results for $B_2 = 1$ and $B_2 = 2$ respectively for the case $t_1 = 300$, $k = 10^{-2}$, L = -.9. For $B_2 = 1$, $V_o = .5$ while for $B_2 = 2$, $V_o = 1$. The curves are labeled with the corresponding values of B_1. The static profile is labeled $B_1 = \infty$. The dotted curves represent a constant velocity in the layer equal to V_o. In this case the static profile is simply translated by the amount V_o. For velocity gradients 1, .1 and .01 to 0

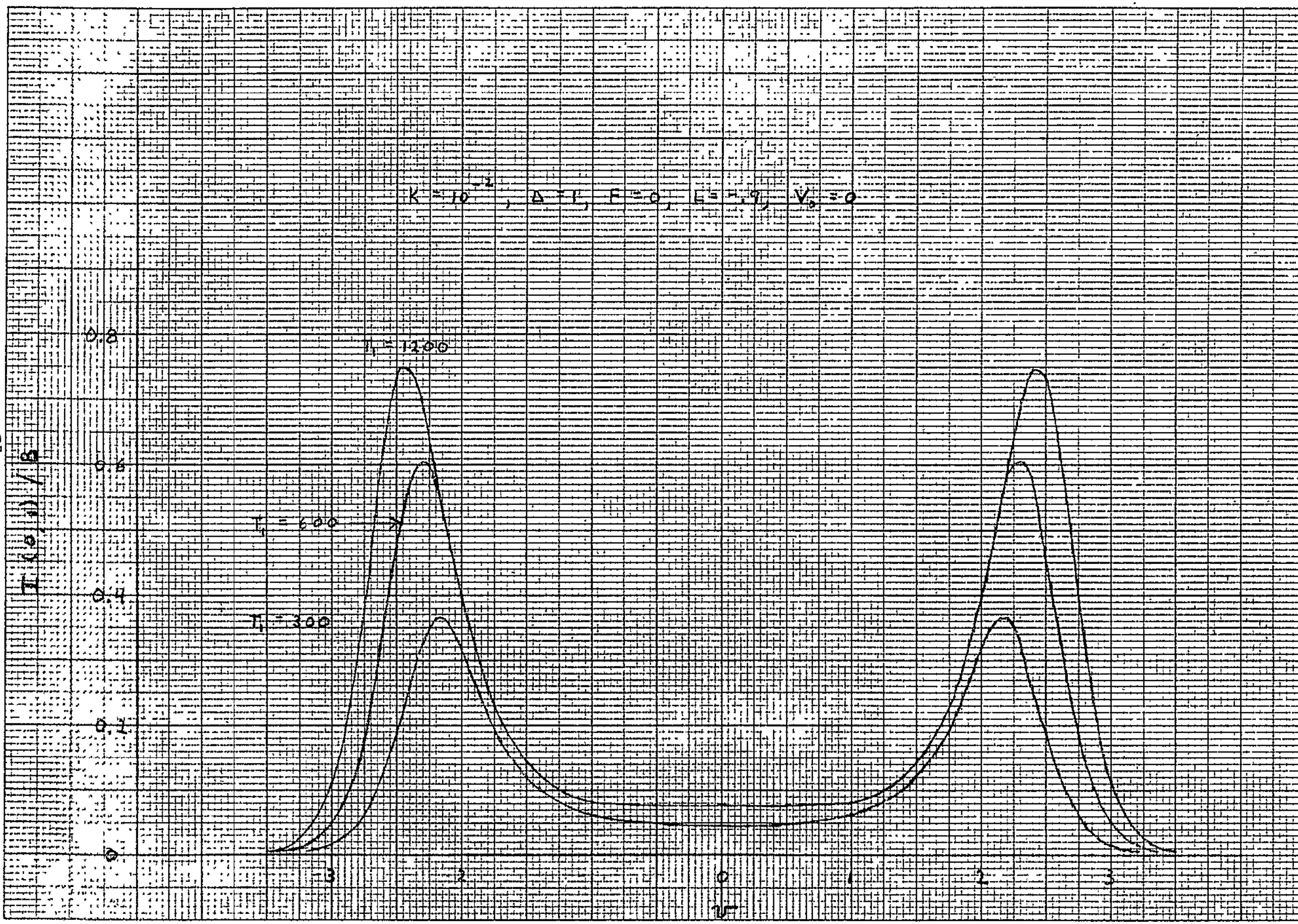

Fig. III.C.1. Static Synthetic H-alpha Profiles.

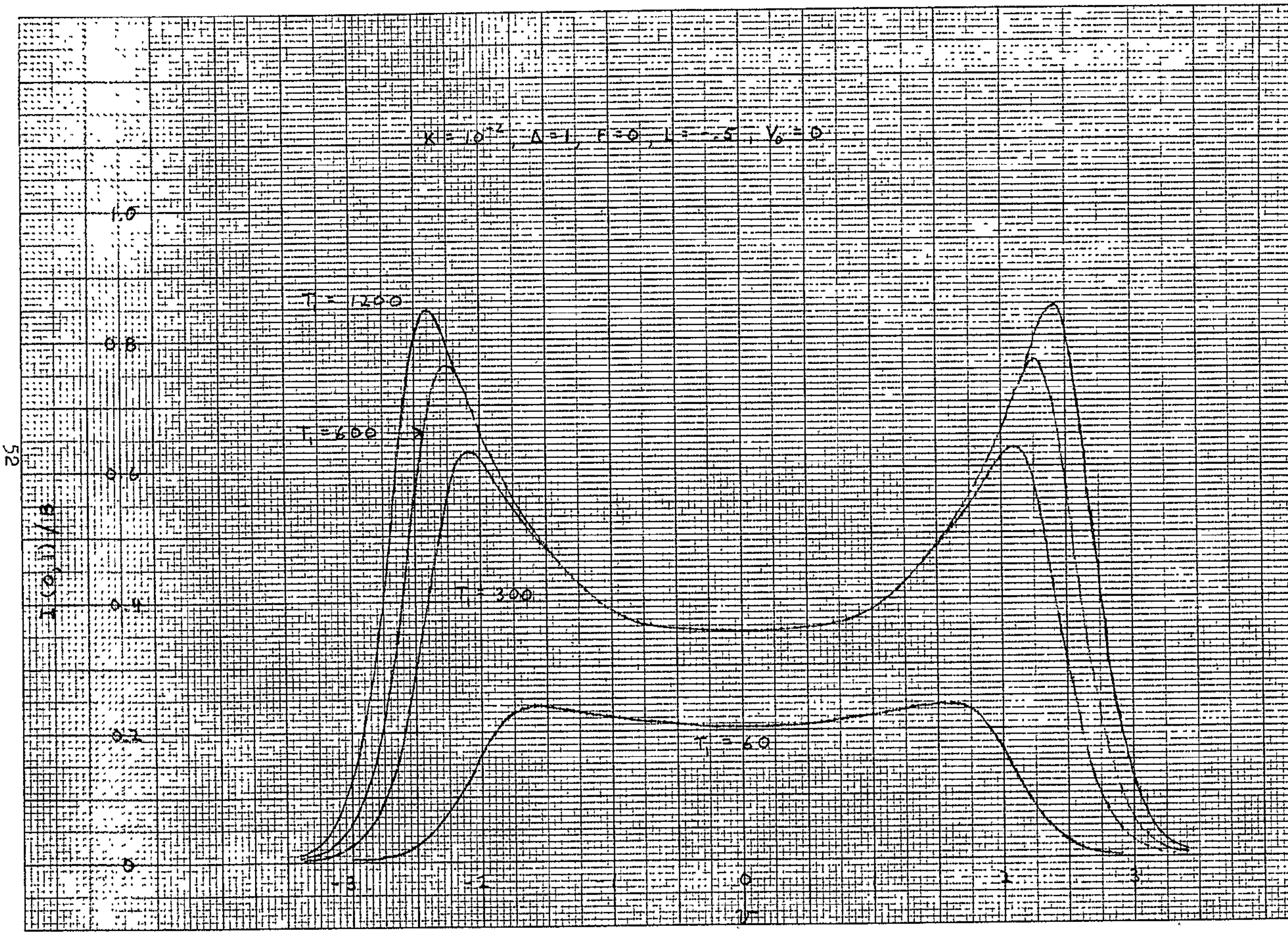

Fig. III.C.2. Static Synthetic H-alpha Profiles.

Fig. III.C.3. Synthetic H-alpha Profiles. Corresponding Static Profiles are Shown by Dotted Curves.

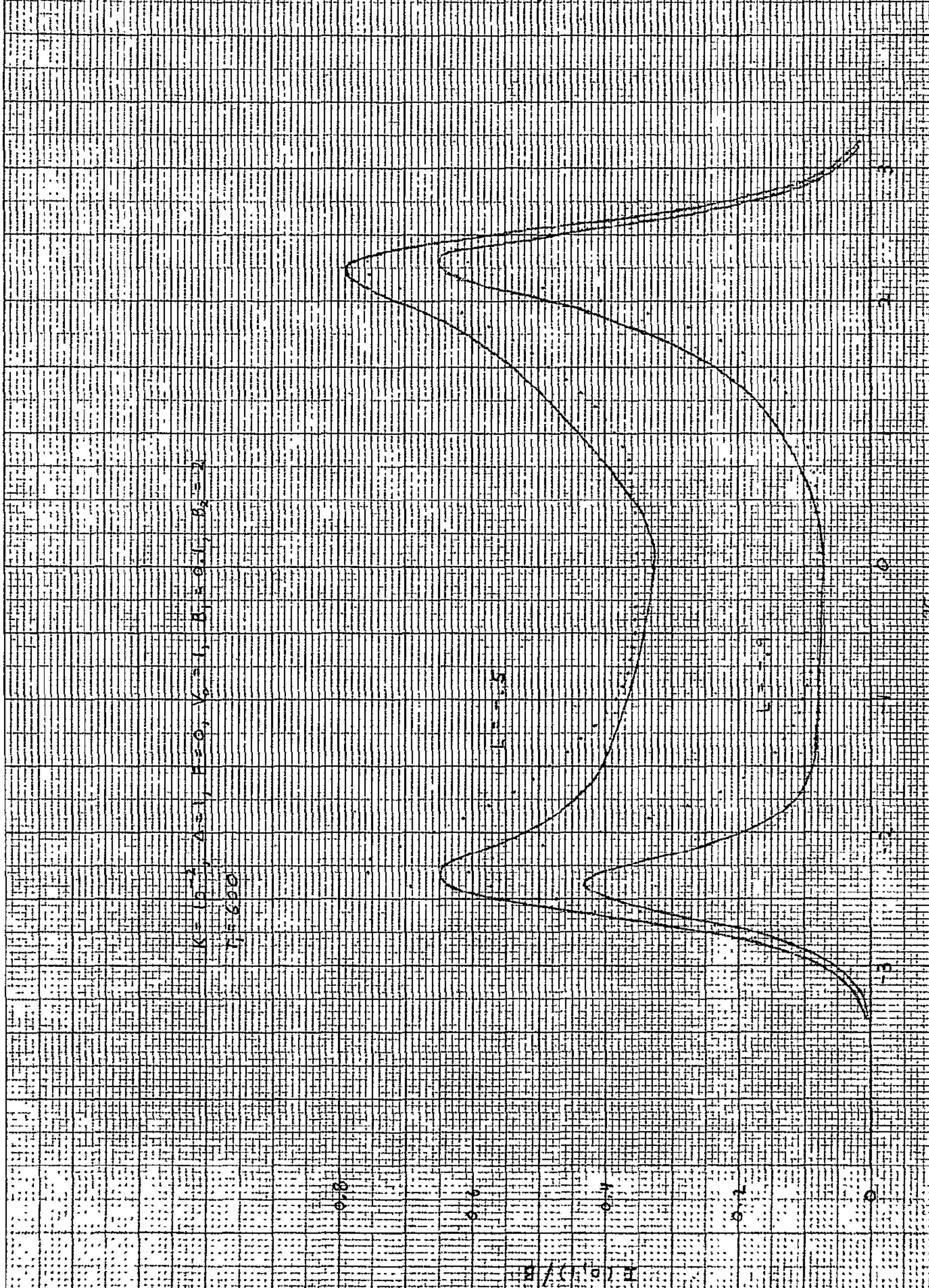

Fig. III.C.4. Synthetic H-alpha Profiles. Static Profile Labeled by •

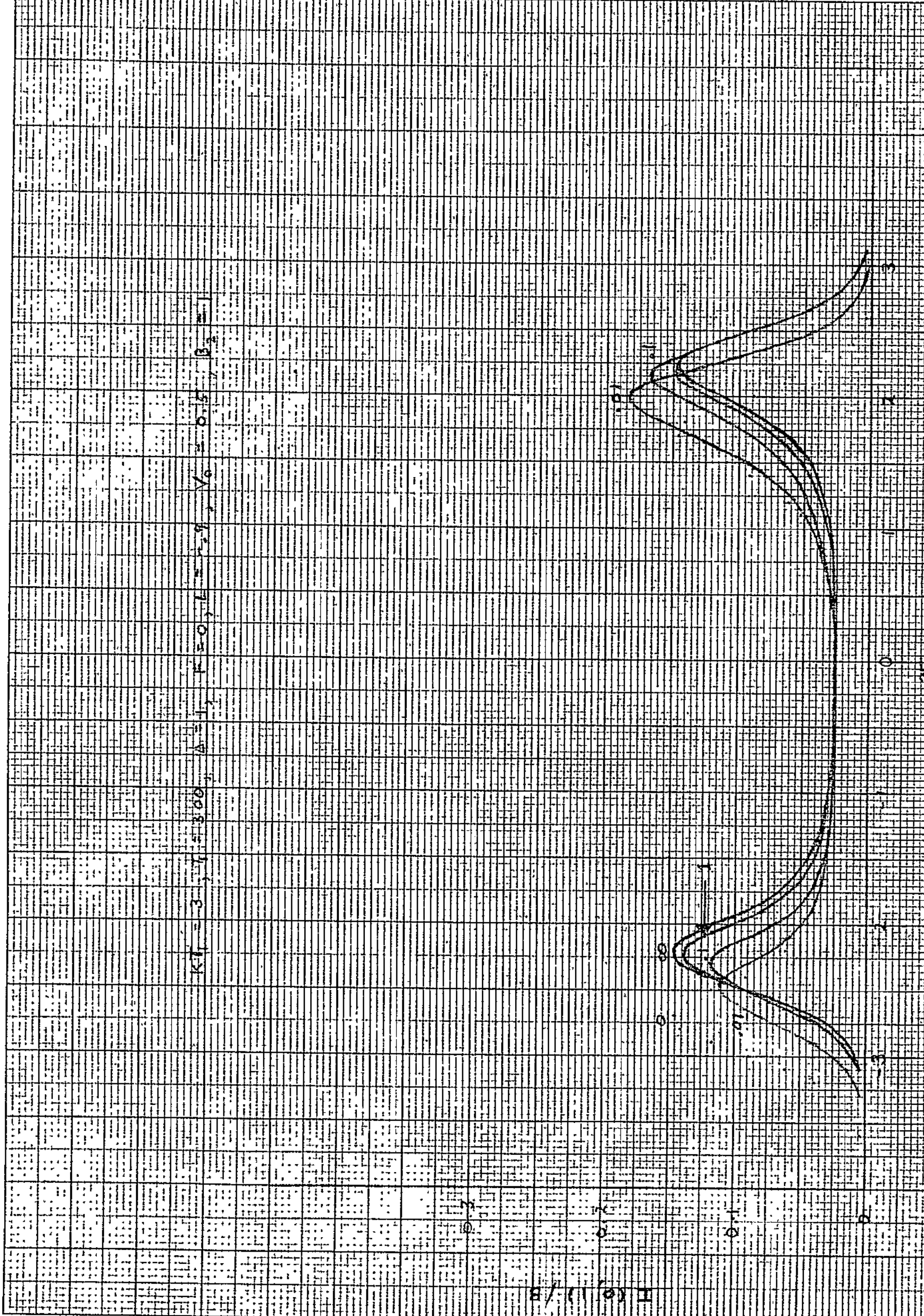

Fig. III.C.5. Synthetic H-alpha Profiles. Static Profile Labeled by .

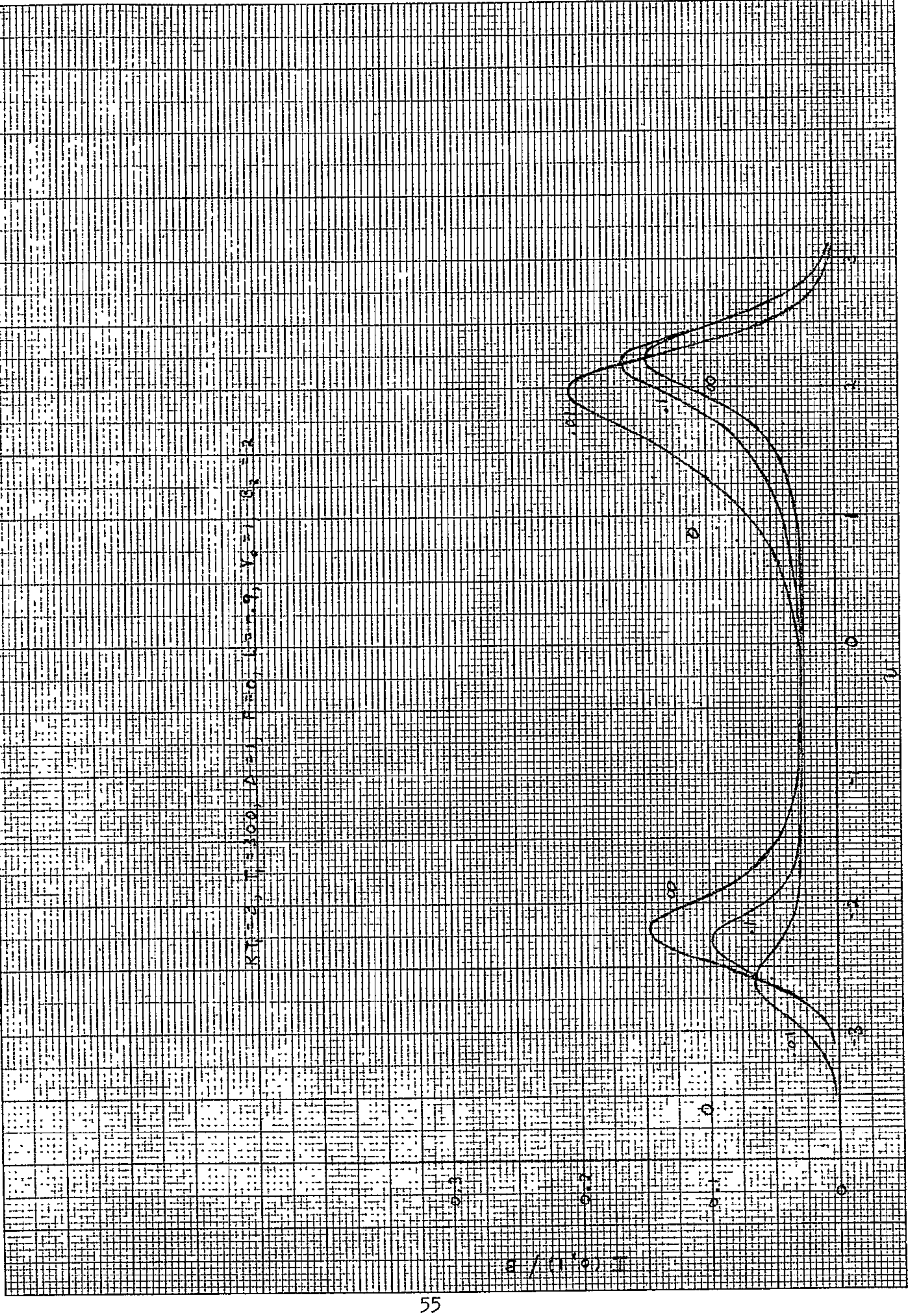

a smooth transition in profiles between the two limiting cases is made with one peak intensity rising to a maximum and falling back to its static value when $B_1 = 0$ and the other peak decreasing and then rising back to its static value. For some value of B_1 there is a maximum ratio of red to violet peak intensities. When $B_1 = 1$ only the layers very near the surface have any significant velocity and thus there is little change with respect to the static profile.

Figure III.C.6 illustrates profiles for a smaller value of t_1 - namely $t_1 = 60$ and $L = -.5$. Again the curves are labeled with values of B_1. Due to the small variation in source function in the layer there is little change in peak intensities as the velocity field changes. The emission peaks are also very small.

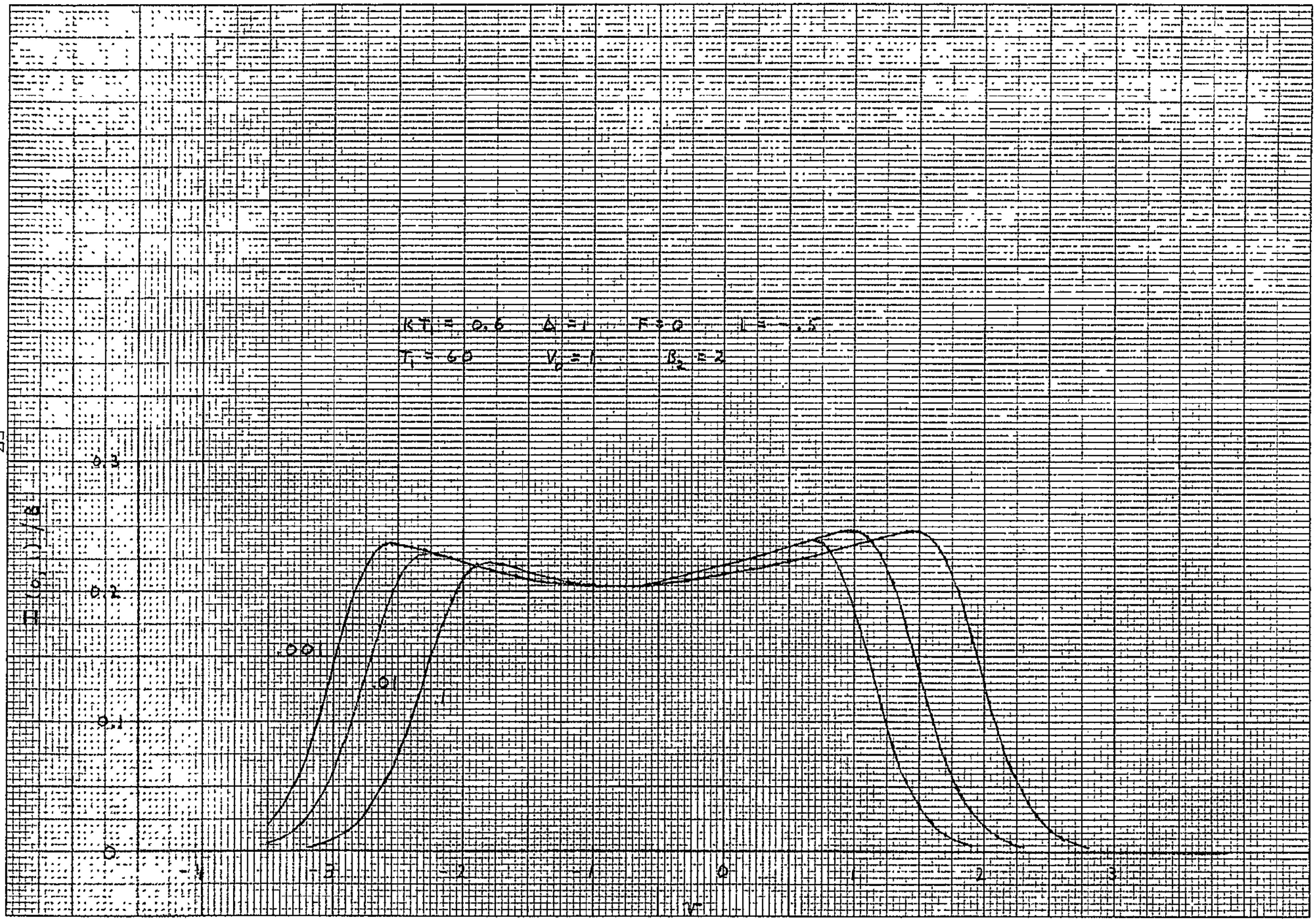

Fig. III.C.6. Synthetic H-alpha Profiles.

IV. COMPARISON OF OBSERVED AND THEORETICAL PROFILES

A. Qualitative Discussion

It is clear from the sequence of profiles that no large velocities are present. The central shifts as well as red to violet peak asymmetries are not large. Except for the last few frames the red peak is enhanced over the violet peak. This indicates an outward motion within the flare region and is in direct contradiction to the infall mechanisms of Nakagawa and Hyder (1971) and others. During the last one minute the velocity has definitely changed sign and indicates a downward motion within the flare. The surface velocity as indicated by the shift of the line center does change sign every 150 seconds showing a slight red shift every 150 seconds.

The central and peak intensities show a fairly sharp rise to a maximum at frame 10 followed by a slow decay. The profiles are not self reversed in the red and violet until frame 4. The central intensity reaches a maximum of .91 times the nearby continium while the red and violet peaks reach a maximum 1.17 and 1.04 times the intensity of the nearby continium.

The red to violet peak intensities are usually less than 1.1 reaching a maximum value of 1.19. As we shall see shortly, the largest ratios do not necessarily mean the largest magnitude of the velocity. The ratio of peak to central intensity is generally less than 1.4 reaching a maximum value of 1.70. This is one of the most striking conflicts with the various flare theory profiles which show much larger peak intensities (Canfield, 1974), (Canfield and Athay, 1974).

When the violet peak intensity is reduced the center should also be shifted to the violet which we observe generally to be the case. The center shift reflects the surface velocity while the peak shifts reflect the velocity of deeper layers. Thus if the center is shifted more than the peaks, which occurs frequently, the implication is a fairly large velocity gradient.

B. Theoretical Profiles

To facilitate determination of the velocities and source functions several hundred H-alpha profiles were generated from Eq. III.5 with $r_o = 0$, $\mu = 1$ and the incident intensity from below $B(T_r) = 0$. We let $B(T_r) = 0$ because it is relatively simple to add this contribution later for different values of T_r without having to perform the more time consuming integrations over again. Sample results of the profile calculations are given in Tables IV.B.1 - 7. Tables IV.B.1 - 5 show the center, violet peak and red peak positions V_C, V_V and V_R in Doppler half width units. Also shown are the violet and red peak intensities in units of the nearby continuum and the ratios I_R/I_V and I_V/I_C.

Each table corresponds to a particular value of t_1 with $V_o = 1$. The parameter values chosen are $B_2 = 1, 2$; $B_1 = .1, .01, .001$; $k = .01, .05, .1, .2$; $L = -.9, -.7, -.5$. Except for the case $B_1 = .1$ the center shift of the line is essentially equal to the surface velocity. The position of the peaks is relatively insensitive to L however the ratios I_R/I_V and I_V/I_C show a steady decrease as L increases. When $B_2 = 2$ the velocity decreases more rapidly with depth and the peak shifts are less than for $B_2 = 1$. The variation in peak intensity ratios with k is more complex depending also upon the value of t_1.

Table IV.B.6 gives line parameters for the static profiles with $\Delta = 1$, $V_o = 0$. The absolute values of V_V and I_V are of course the same as V_R and I_R. We note that the center and peak intensities increase as k or L increases. This Table also illustrates the effect of a non-zero F with F = .5. The F term contribution raises the value of S near the bottom of the layer and hence increases I_C and I_R. For larger layer thicknesses the effect of increasing S near the lower boundary is very small.

Table IV.B.7 illustrates results for $\Delta = 1$, $F = 0$, and $V_o = .5$ in contrast to the results of Tables IV.B.1-5 for $V_o = 1$. As would be expected considerably smaller values of I_R/I_V are indicated. Also shown are results for $L = -.3$.

Table IV.B.1

Characteristics of Synthetic H-alpha Profiles

$V_o = 1$, $t_1 = 30$,

	V_C	I_C	V_V	I_V	V_R	I_R	I_R/I_V	I_V/I_C
k=.05								
B_1=.1								
B_2=1								
L = −.7	−.95	.16	−2.00	.20	.97	.28	1.40	1.25
−.5	−.90	.38	−1.90	.42	.94	.48	1.14	1.11
B_2=2								
L = −.7	−.85	.16	−1.80	.19	1.19	.29	1.53	1.19
−.5	−.85	.38	−1.69	.41	1.15	.48	1.17	1.08
B_1=.01								
B_2=1								
L = −.7	−1.00	.16	−2.36	.23	.59	.26	1.13	1.44
−.5	−1.00	.38	−2.28	.44	.53	.46	1.05	1.16
B_2=2								
L = −.7	−1.00	.16	−2.28	.22	.68	.27	1.23	1.38
−.5	−1.00	.38	−2.19	.44	.63	.47	1.07	1.16
B_1=.001								
B_2=1								
L = −.7	−1.00	.16	−2.46	.24	.48	.25	1.04	1.50
−.5	−1.00	.38	−2.38	.45	.42	.45	1.00	1.18
B_2=2								
L = −.7	−1.00	.16	−2.49	.24	.50	.25	1.04	1.50
−.5	−1.00	.38	−2.37	.45	.43	.45	1.00	1.18
k = .1								
B_1 = .1								
B_2 = 1								
L = −.9	−.90	.12	−2.10	.25	1.00	.46	1.84	2.08
−.7	−.92	.30	−2.00	.40	.98	.57	1.43	1.33
−.5	−.92	.49	−1.95	.56	.95	.69	1.23	1.14
B_2 = 2								
L = −.9	−.85	.13	−1.90	.23	1.23	.47	2.04	1.77
−.5	−.85	.49	−1.75	.54	1.15	.69	1.28	1.10
B_1 = .01								
B_2 = 1								
L = −.9	−1.00	.12	−2.45	.33	.64	.39	1.18	2.75
−.7	−1.00	.31	−2.39	.47	.60	.52	1.11	1.52
−.5	−1.00	.49	−2.33	.61	.55	.65	1.07	1.24
B_2 = 2								
L = −.9	−1.00	.12	−2.35	.31	.73	.42	1.35	2.58
−.5	−1.00	.49	−2.24	.59	.65	.66	1.12	1.20

$V_o = 1,\ t_1 = 30$

k=.1, B_1=.001	V_C	I_C	V_V	I_V	V_R	I_R	I_R/I_V	I_V/I_C
B_2=1								
L = -.9	-1.00	.12	-2.52	.36	.55	.37	1.03	3.00
-.7	-1.00	.31	-2.46	.49	.50	.50	1.02	1.58
-.5	-1.00	.49	-2.42	.63	.45	.63	1.00	1.29
B_2=2								
L = -.9	-1.00	.12	-2.51	.36	.55	.37	1.03	3.00
-.7	-1.00	.49	-2.41	.62	.46	.63	1.02	1.27
k = .2								
B_1 = .1								
B_2 = 1								
L = -.9	-.90	.23	-2.08	.44	1.00	.74	1.68	1.91
-.7	-.92	.39	-2.04	.55	.97	.79	1.44	1.41
-.5	-.95	.55	-1.97	.66	.95	.84	1.27	1.20
B_2 = 2								
L = -.9	-.85	.24	-1.87	.39	1.20	.76	1.95	1.63
-.7	-.85	.39	-1.84	.51	1.18	.81	1.59	1.31
-.5	-.84	.55	-1.78	.63	1.16	.85	1.35	1.15
B_1 = .01								
B_2 = 1								
L = -.9	-1.00	.23	-2.42	.56	.62	.65	1.16	2.43
-.7	-1.00	.39	-2.38	.64	.60	.72	1.13	1.64
-.5	-1.00	.55	-2.35	.73	.56	.79	1.08	1.33
B_2 = 2								
L = -.9	-1.00	.23	-2.34	.52	.71	.68	1.31	2.26
-.7	-1.00	.39	-2.30	.62	.69	.75	1.21	1.59
-.5	-1.00	.55	-2.26	.71	.66	.81	1.14	1.29
B_1 = .001								
B_2 = 1								
L = -.9	-1.00	.23	-2.52	.60	.53	.61	1.02	2.61
-.7	-1.00	.39	-2.48	.68	.50	.69	1.01	1.74
-.5	-1.00	.55	-2.45	.76	.46	.76	1.00	1.38
B_2 = 2								
L = -.9	-1.00	.23	-2.50	.59	.54	.61	1.03	2.56
-.7	-1.00	.39	-2.47	.67	.51	.69	1.03	1.72
-.5	-1.00	.55	-2.44	.75	.48	.77	1.03	1.36

Table IV.B.2

Characteristics of Synthetic H-alpha Profiles

$V_o = 1, \quad t_1 = 60$

k = .01	V_C	I_C	V_V	I_V	V_R	I_R	I_R/I_V	I_V/I_C
B_1 = .1								
B_2 = 1								
L = -.5	-.90	.20	-1.98	.22	1.25	.25	1.14	1.10
B_2 = 2								
L = -.5	-.80	.20	-1.79	.22	1.45	.25	1.14	1.10
B_1 = .01								
B_2 = 1								
L = -.5	-1.00	.20	-2.38	.23	.80	.24	1.04	1.15
B_2 = 2								
L = -.5	-1.00	.20	-2.26	.23	.95	.25	1.09	1.15
B_1 = .001								
B_2 = 1								
L = -.5	-1.00	.20	-2.55	.24	.60	.24	1.00	1.20
B_2 = 2								
L = -.5	-1.00	.20	-2.54	.24	.64	.24	1.00	1.20
k = .05								
B_1 = .1								
B_2 = 1								
L = -.9	-.90	.086	-2.20	.22	1.36	.47	2.14	2.56
-.7	-.90	.27	-2.12	.38	1.34	.58	1.53	1.41
-.5	-.90	.45	-2.05	.54	1.32	.70	1.30	1.20
B_2 = 2								
L = -.9	-.84	.086	-2.01	.20	1.55	.46	2.30	2.33
-.7	-.81	.27	-1.94	.36	1.52	.58	1.61	1.33
-.5	-.80	.45	-1.86	.53	1.49	.69	1.30	1.18
B_1 = .01								
B_2 = 1								
L = -.9	-1.00	.086	-2.58	.31	.92	.42	1.35	3.60
-.7	-1.00	.27	-2.52	.44	.89	.54	1.23	1.63
-.5	-1.00	.45	-2.46	.59	.85	.66	1.12	1.31
B_2 = 2								
L = -.9	-1.00	.086	-2.49	.27	1.05	.45	1.67	3.14
-.7	-1.00	.27	-2.40	.41	1.04	.57	1.39	1.52
-.5	-1.00	.45	-2.35	.56	1.03	.69	1.23	1.24
B_1 = .001								
B_2 = 1								
L = -.9	-1.00	.086	-2.72	.36	.77	.37	1.03	4.18
-.7	-1.00	.27	-2.68	.49	.74	.50	1.02	1.81
-.5	-1.00	.45	-2.64	.62	.69	.63	1.02	1.38

$V_o = 1,\ t_1 = 60$

	V_C	I_C	V_V	I_V	V_R	I_R	I_R/I_V	I_V/I_C
k = .05								
B_1 = .001								
B_2 = 2								
L = -.9	-1.00	.085	-2.70	.35	.79	.38	1.09	4.12
-.7	-1.00	.27	-2.65	.48	.75	.50	1.04	1.78
-.5	-1.00	.45	-2.60	.62	.71	.64	1.03	1.38
k = .1								
B_1 = .1								
B_2 = 1								
L = -.9	-.90	.16	-2.17	.38	1.35	.75	1.97	2.38
-.7	-.90	.32	-2.14	.50	1.34	.80	1.60	1.56
-.5	-.90	.49	-2.08	.63	1.30	.86	1.37	1.29
B_2 = 2								
L = -.9	-.85	.16	-2.00	.35	1.54	.74	2.11	2.19
-.7	-.83	.33	-1.95	.47	1.52	.80	1.70	1.42
-.5	-.81	.49	-1.90	.61	1.49	.85	1.39	1.24
B_1 = .01								
B_2 = 1								
L = -.9	-1.00	.16	-2.58	.52	.92	.69	1.33	3.25
-.7	-1.00	.32	-2.54	.61	.88	.75	1.23	1.91
-.5	-1.00	.49	-2.48	.71	.86	.81	1.14	1.45
B_2 = 2								
L = -.9	-.98	.16	-2.45	.46	1.05	.73	1.59	2.88
-.7	-.98	.32	-2.43	.56	1.04	.79	1.41	1.75
-.5	-.98	.49	-2.36	.67	1.03	.84	1.25	1.37
B_1 = .001								
B_2 = 1								
L = -.9	-1.00	.16	-2.71	.59	.76	.61	1.03	3.69
-.7	-1.00	.32	-2.68	.67	.74	.69	1.03	2.09
-.5	-1.00	.49	-2.65	.75	.69	.77	1.03	1.53
B_2 = 2								
L = -.9	-1.00	.16	-2.68	.58	.78	.63	1.09	3.63
-.7	-1.00	.32	-2.66	.66	.75	.70	1.06	2.06
-.5	-1.00	.49	-2.63	.75	.73	.77	1.03	1.53

Table IV.B.3

Characteristics of Synthetic H-alpha Profiles

$V_o = 1, \quad t_1 = 300$

	V_C	I_C	V_V	I_V	V_R	I_R	I_R/I_V	I_V/I_C
$k = .01$								
$B_1 = .1$								
$B_2 = 1$								
$L = -.9$	-.80	.045	-2.40	.19	2.00	.45	2.30	4.31
-.7	-.75	.20	-2.35	.35	1.97	.56	1.60	1.75
-.5	-.70	.35	-2.30	.51	1.95	.68	1.33	1.46
$B_2 = 2$								
$L = -.9$	-.65	.045	-2.27	.23	2.10	.41	1.78	5.11
-.5	-.47	.34	-2.17	.54	2.05	.66	1.22	1.59
$B_1 = .01$								
$B_2 = 1$								
$L = -.9$	-1.00	.045	-2.78	.21	1.64	.48	2.29	4.67
-.7	-1.00	.20	-2.70	.36	1.62	.60	1.67	1.80
-.5	-1.00	.35	-2.65	.53	1.60	.71	1.34	1.51
$B_2 = 2$								
$L = -.9$	-.95	.045	-2.62	.17	1.85	.49	2.88	3.78
-.5	-.93	.35	-2.46	.50	1.82	.71	1.42	1.43
$B_1 = .001$								
$B_2 = 1$								
$L = -.9$	-1.00	.045	-3.08	.32	1.25	.40	1.25	7.11
-.7	-1.00	.20	-3.02	.46	1.21	.53	1.15	2.30
-.5	-1.00	.35	-2.97	.60	1.18	.66	1.10	1.71
$B_2 = 2$								
$L = -.9$	-1.00	.045	-3.00	.29	1.35	.43	1.48	6.44
-.5	-1.00	.35	-2.88	.58	1.30	.68	1.17	1.66
$k = .05$								
$B_1 = .1$								
$B_2 = 1$								
$L = -.9$	-.85	.098	-2.38	.46	1.95	.90	1.96	4.69
-.7	-.75	.24	-2.35	.55	1.95	.92	1.67	2.29
-.5	-.75	.38	-2.30	.66	1.95	.94	1.42	1.74
$B_2 = 2$								
$L = -.9$	-.72	.098	-2.28	.50	2.05	.86	1.72	5.10
-.7	-.60	.24	-2.23	.59	2.04	.89	1.51	2.46
-.5	-.55	.37	-2.19	.69	2.03	.92	1.33	1.86

$V_o = 1, \quad t_1 = 300$

k = .05

	V_C	I_C	V_V	I_V	V_R	I_R	I_R/I_V	I_V/I_C
B_1 = .01								
B_2 = 1								
L = -.9	-1.00	.098	-2.71	.53	1.60	.93	1.75	5.41
-.7	-1.00	.24	-2.70	.62	1.59	.95	1.53	2.58
-.5	-1.00	.38	-2.68	.71	1.58	.96	1.35	1.87
B_2 = 2								
L = -.9	-1.00	.098	-2.58	.44	1.80	.95	2.16	4.48
-.7	-.95	.24	-2.55	.54	1.80	.96	1.78	2.25
-.5	-.90	.38	-2.51	.65	1.79	.96	1.48	1.71
B_1 = .001								
B_2 = 1								
L = -.9	-1.00	.098	-3.01	.72	1.21	.84	1.17	7.35
-.7	-1.00	.24	-3.00	.78	1.20	.87	1.11	3.25
-.5	-1.00	.38	-2.99	.83	1.19	.90	1.08	2.18
B_2 = 2								
L = -.9	-1.00	.098	-2.96	.67	1.33	.88	1.31	6.83
-.7	-1.00	.24	-2.94	.73	1.31	.90	1.23	3.04
-.5	-1.00	.38	-2.91	.80	1.28	.93	1.16	2.11

Table IV.B.4

Characteristics of Synthetic H-alpha Profiles

$V_o = 1,\ t_1 = 600$

$k = .01$

	V_C	I_C	V_V	I_V	V_R	I_R	I_R/I_V	I_V/I_C
$B_1 = .1$								
$B_2 = 1$								
L = -.9	-.90	.076	-2.50	.35	2.20	.70	2.00	4.60
-.7	-.85	.21	-2.45	.47	2.20	.76	1.62	2.24
-.5	-.85	.34	-2.40	.60	2.15	.82	1.37	1.76
$B_2 = 2$								
L = -.9	-.90	.070	-2.38	.43	2.27	.65	1.51	6.14
-.7	-.85	.20	-2.36	.53	2.25	.71	1.34	2.65
-.5	-.85	.33	-2.33	.65	2.22	.79	1.22	1.97
$B_1 = .01$								
$B_2 = 1$								
L = -.9	-1.00	.076	-2.80	.31	1.90	.78	2.52	4.07
-.7	-1.00	.22	-2.75	.43	1.90	.83	1.93	1.95
-.5	-1.00	.36	-2.70	.57	1.90	.87	1.53	1.58
$B_2 = 2$								
L = -.9	-1.00	.076	-2.65	.26	2.12	.77	2.96	3.42
-.7	-1.00	.22	-2.58	.40	2.10	.82	2.05	1.82
-.5	-1.00	.36	-2.55	.54	2.08	.86	1.59	1.50
$B_1 = .001$								
$B_2 = 1$								
L = -.9	-1.00	.076	-3.15	.48	1.50	.71	1.48	6.31
-.7	-1.00	.22	-3.12	.59	1.47	.77	1.31	2.68
-.5	-1.00	.36	-3.10	.69	1.45	.82	1.19	1.92

$k = .05$

$B_1 = .1$								
$B_2 = 1$								
L = -.9	-.90	.095	-2.45	.54	2.11	.95	1.76	5.68
-.7	-.85	.23	-2.42	.62	2.11	.96	1.55	2.72
-.5	-.85	.36	-2.40	.71	2.10	.97	1.37	1.97
$B_2 = 2$								
L = -.9	-.90	.093	-2.37	.62	2.18	.92	1.48	6.66
-.7	-.85	.22	-2.33	.68	2.18	.94	1.38	3.09
-.5	-.85	.34	-2.31	.76	2.17	.95	1.25	2.24

$V_o = 1, \quad t_1 = 600$

$k = .05$

$B_1 = .01$	V_C	I_C	V_V	I_V	V_R	I_R	I_R/I_V	I_V/I_C
$B_2 = 1$								
$L = -.9$	-.95	.096	-2.78	.56	1.86	.97	1.73	5.83
-.7	-1.00	.24	-2.75	.63	1.85	.98	1.56	2.63
-.5	-1.00	.38	-2.72	.72	1.85	.98	1.36	1.89
$B_2 = 2$								
$L = -.9$	-.95	.096	-2.61	.48	2.05	.97	2.02	5.00
-.7	-1.00	.24	-2.59	.56	2.04	.98	1.75	2.35
-.5	-1.00	.37	-2.58	.66	2.04	.98	1.48	1.78
$B_1 = .001$								
$B_2 = 1$								
$L = -.9$	-1.00	.096	-3.09	.78	1.41	.93	1.19	8.12
-.7	-1.00	.24	-3.08	.80	1.41	.94	1.18	3.33
-.5	-1.00	.38	-3.07	.84	1.40	.96	1.14	2.24
$B_2 = 2$								
$L = -.9$	-1.00	.096	-3.00	.71	1.57	.96	1.35	7.39
-.7	-1.00	.24	-2.98	.76	1.57	.97	1.28	3.17
-.5	-1.00	.38	-2.96	.81	1.57	.97	1.20	2.13

Table IV.B.5

Characteristics of Synthetic H-alpha Profiles

$V_o = 1, \quad t_1 = 1200$

$k = .01$

$B_1 = .1$	V_C	I_C	V_V	I_V	V_R	I_R	I_R/I_V	I_V/I_C
$B_2 = 1$								
$L = -.9$	-1.00	.073	-2.58	.48	2.37	.83	1.73	6.58
$-.7$	-1.00	.19	-2.53	.57	2.35	.86	1.51	3.00
$-.5$	-1.00	.32	-2.50	.67	2.34	.89	1.33	2.09
$B_2 = 2$								
$L = -.9$	-.95	.068	-2.50	.59	2.42	.79	1.34	8.68
$-.5$	-1.00	.29	-2.45	.74	2.38	.87	1.18	2.55
$B_1 = .01$								
$B_2 = 1$								
$L = -.9$	-1.00	.082	-2.85	.35	2.16	.91	2.60	4.27
$-.7$	-1.00	.22	-2.81	.47	2.15	.93	1.98	2.14
$-.5$	-1.00	.36	-2.78	.59	2.15	.94	1.59	1.64
$B_2 = 2$								
$L = -.9$	-1.00	.080	-2.70	.33	2.32	.89	2.70	4.12
$-.5$	-1.00	.35	-2.62	.57	2.28	.93	1.63	1.63
$B_1 = .001$								
$B_2 = 1$								
$L = -.9$	-1.00	.083	-3.20	.56	1.71	.89	1.59	6.75
$-.7$	-1.00	.23	-3.18	.64	1.71	.91	1.42	2.78
$-.5$	-1.00	.37	-3.15	.72	1.70	.94	1.31	1.95
$B_2 = 2$								
$L = -.9$	-1.00	.083	-3.08	.46	1.93	.93	2.02	5.54
$-.5$	-1.00	.37	-3.02	.66	1.90	.96	1.45	1.78

$k = .02$

$B_1 = .1$								
$B_2 = 1$								
$L = -.9$	-1.00	.082	-2.56	.55	2.32	.92	1.67	6.70
$-.7$	-1.00	.20	-2.52	.63	2.32	.93	1.48	3.15
$-.5$	-1.00	.32	-2.50	.72	2.30	.95	1.32	2.25
$B_2 = 2$								
$L = -.9$	-1.00	.077	-2.48	.66	2.38	.88	1.33	8.57
$-.7$	-.95	.19	-2.47	.72	2.36	.90	1.25	3.79
$-.5$	-.92	.30	-2.44	.78	2.35	.92	1.18	2.60

$V_o = 1, \quad t_1 = 1200$

	V_C	I_C	V_V	I_V	V_R	I_R	I_R/I_V	I_V/I_C
$k = .02$								
$B_1 = .01$								
$B_2 = 1$								
$L = -.9$	-1.00	.090	-2.84	.45	2.14	.97	2.16	5.00
$-.7$	-1.00	.22	-2.80	.55	2.12	.97	1.76	2.50
$-.5$	-1.00	.45	-2.78	.65	2.11	.98	1.51	1.44
$B_2 = 2$								
$L = -.9$	-1.00	.089	-2.70	.41	2.28	.96	2.34	4.60
$-.7$	-1.00	.23	-2.66	.50	2.27	.96	1.92	2.17
$-.5$	-1.00	.36	-2.64	.61	2.26	.97	1.59	1.69
$B_1 = .001$								
$B_2 = 1$								
$L = -.9$	-1.00	.091	-3.18	.68	1.71	.95	1.40	7.47
$-.7$	-1.00	.23	-3.15	.73	1.70	.96	1.32	3.17
$-.5$	-1.00	.37	-3.13	.79	1.68	.97	1.23	2.14
$B_2 = 2$								
$L = -.9$	-1.00	.091	-3.06	.57	1.90	.97	1.70	6.26
$-.7$	-1.00	.23	-3.04	.65	1.89	.97	1.49	2.83
$-.5$	-1.00	.37	-3.01	.73	1.88	.98	1.34	1.97
$k = .05$								
$B_1 = .1$								
$B_2 = 1$								
$L = -.9$	-1.00	.11	-2.54	.63	2.26	.97	1.54	5.73
$-.7$	-1.00	.29	-2.52	.70	2.26	.97	1.39	2.41
$-.5$	-1.00	.46	-2.48	.77	2.26	.98	1.27	1.67
$B_2 = 2$								
$L = -.9$	-.80	.10	-2.48	.72	2.34	.95	1.32	7.20
$-.7$	-.95	.21	-2.45	.76	2.32	.96	1.26	3.62
$-.5$	-.95	.31	-2.42	.82	2.31	.97	1.18	2.65
$B_1 = .01$								
$B_2 = 1$								
$L = -.9$	-1.00	.11	-2.80	.59	2.06	.98	1.66	5.36
$-.7$	-1.00	.29	-2.78	.66	2.06	.99	1.50	2.28
$-.5$	-1.00	.38	-2.75	.73	2.05	.99	1.36	1.92
$B_2 = 2$								
$L = -.9$	-1.00	.11	-2.68	.52	2.23	.98	1.88	4.73
$-.7$	-1.00	.25	-2.65	.60	2.22	.98	1.63	2.40
$-.5$	-1.00	.38	-2.62	.68	2.22	.98	1.44	1.79
$B_1 = .001$								
$B_2 = 1$								
$L = -.9$	-1.00	.11	-3.15	.80	1.68	.97	1.21	7.27
$-.7$	-1.00	.25	-3.12	.83	1.66	.98	1.18	3.32
$-.5$	-1.00	.39	-3.10	.87	1.65	.98	1.13	2.23
$B_2 = 2$								
$L = -.9$	-1.00	.11	-3.02	.72	1.86	.98	1.36	6.55
$-.7$	-1.00	.25	-3.00	.77	1.85	.99	1.29	3.08
$-.5$	-1.00	.39	-2.98	.82	1.85	.99	1.21	2.10

Table IV.B.6

Characteristics of Static Synthetic H-alpha Profiles

($V_o = 0$, $= 1$)

$t_1 = 30$

	F = 0			F = .5		
	I_c	V_R	I_R	I_c	V_R	I_R
k = .05						
L = −.9	--	--	--	.046	1.62	.22
−.7	--	--	--	.27	1.55	.42
−.5	.38	1.39	.45	.49	1.48	.62
k = .1						
L = −.9	.12	1.54	.36	.15	1.58	.44
−.5	.49	1.44	.63	.52	1.48	.70
k = .2						
L = −.9	.23	1.52	.60	.23	1.54	.62
−.7				.39	1.52	.70
−.5	.55	1.45	.76	.55	1.48	.78

$t_1 = 60$

	F = 0			F = .5		
k = .01						
L = −.5	.20	1.58	.24	.45	1.65	.54
k = .05						
L = −.9	.085	1.75	.36	.11	1.77	.44
−.5	.45	1.66	.63	.47	1.71	.70
k = .1						
L = −.9	.16	1.74	.60	.16	1.76	.62
−.5	.49	1.66	.76	.49	1.69	.78

$t_1 = 300$

	F = 0			F = .5		
k = .01						
L = −.9	.045	2.16	.36	.064	2.18	.44
−.5	.35	2.09	.63	.37	2.12	.69
k = .05						
L = −.9	.098	2.12	.78	.098	2.12	.79
−.5	.38	2.07	.87	.38	2.08	.87

$t_1 = 600$

$k = .01$	F = 0 I_c	V_R	I_R	F = .5 I_c	V_R	I_R
L = -.9	.077	2.30	.60	.077	2.31	.63
-.5	.36	2.27	.76	.36	2.28	.78
$k = .05$						
L = -.9	.096	2.25	.86	.096	2.25	.86
-.5	.38	2.21	.91	.38	2.21	.91

$t_1 = 1200$

$k = .01$						
L = -.9	.083	2.42	.75	.083	2.43	.75
-.5	.37	2.39	.85	.37	2.40	.85
$k = .02$						
L = -.9	.092	2.40	.84	.092	2.41	.85
-.5	.37	2.37	.90	.37	2.38	.90
$k = .05$						
L = -.9	.11	2.37	.92	.11	2.37	.92
-.5	.39	2.35	.94	.39	2.35	.94

Table IV.B.7

Characteristics of Synthetic H-alpha Profiles

$= 1$, $F = 0$, $V_o = .5$

$t_1 = 60$, $L = -.7$

	V_C	I_C	V_V	I_V	V_R	I_R	I_R/I_V	I_V/I_C
$k = .05$								
$B_2 = 1.$								
$B_1 = .1$	-.45	.27	-1.90	.43	1.51	.55	1.27	1.59
.01	-.50	.27	-2.12	.47	1.29	.52	1.11	1.74
$B_2 = 2$								
$B_1 = .1$	-.42	.27	-1.81	.43	1.60	.54	1.25	1.59
.01	-.50	.27	-2.05	.45	1.36	.53	1.18	1.67
$k = .1$								
$B_2 = 1$								
$B_1 = .1$	-.45	.32	-1.90	.59	1.51	.75	1.27	1.84
$B_2 = 2$								
$B_1 = .1$	-.45	.32	-1.82	.58	1.60	.75	1.30	1.81

$t_1 = 300$, $L = -.3$

	V_C	I_C	V_V	I_V	V_R	I_R	I_R/I_V	I_V/I_C
$k = .01$								
$B_2 = 1$								
$B_1 = .1$	-.35	.50	-2.13	.73	1.97	.79	1.08	1.46
.001	-.50	.50	-2.47	.76	1.60	.78	1.03	1.52
$B_2 = 2$								
$B_1 = .1$	-.40	.50	-2.06	.74	2.04	.78	1.05	1.48
.001	-.50	.50	-2.45	.75	1.66	.78	1.04	1.50
$k = .005$								
$B_2 = 1$								
$B_1 = .1$	-.35	.46	-2.10	.64	1.95	.67	1.05	1.39
.001	-.50	.46	-2.46	.66	1.55	.67	1.02	1.43
$B_2 = 2$								
$B_1 = .1$	-.20	.46	-2.05	.65	1.97	.67	1.02	1.41
.001	-.50	.46	-2.41	.65	1.64	.67	1.02	1.41
$k = .01$								
$B_2 = 1$								
$B_1 = .1$								
$L = -.9$	-.40	.045	-2.27	.29	2.07	.41	1.41	6.44
-.7	-.35	.20	-2.22	.43	2.05	.53	1.23	2.15
-.5	-.35	.35	-2.17	.58	2.02	.66	1.14	1.66
-.3	-.35	.50	-2.13	.73	1.97	.79	1.08	1.46

C. Velocity and Source Function Determination

Each of the observed profiles has been individually fitted to a synthetic profile with the most similar characteristics. For the first few frames the bisector shifts were compared with calculated bisector shifts to obtain the velocity field. The following discussion deals with the self reversed profiles. We find that the smaller velocity gradients are unacceptable as they produce too large a shift of the peaks and too little peak asymmetry. Too large a velocity gradient produces too little peak shift and asymmetry. As can be seen from Tables IV.B.1-5 the larger negative L values produce peak to center intensities larger than those observed.

The distance of the self reversed peaks from the line center is essentially determined by the value of $\Delta\lambda_D$ and t_1. We have established the values of L, k, V_o, t_1, B_1 and B_2 as those that best represent I_C, I_V, I_R, V_C, V_V and V_R. In most cases we have not had sufficient time to compare profiles in enough detail to distinguish between B_2 values. The small observed peak to center intensities generally restrict L to about -.3 while the center and peak shifts reflect V_o values in the range .3 to .7 V_D (V_D is the Doppler velocity) until the velocity changes direction in frame 23. The red to violet peak intensity ratio essentially establishes B_1 which is found to usually be between .1 and .01.

Fig. IV.C.1 shows the observed profile of frame 13 (dashed curve) along with several synthetic profiles. $\Delta\lambda_D$ has been set equal to .35 Å for all of the profiles. The profiles labeled 2 and 3 are for $t_1 = 60$, $L = -.5$, $B_1 = .1$, $B_2=1$, and $V_o = 1$ with $k = .05$ and .01 resp. The profile labeled 1 represents the parameters $t_1 = 300$, $L = -.3$, $B_1 = .1$, $B_2 = 1$, $V_o = .5$ and $k = .01$. The value of $B(T_B)$ for each profile has been adjusted so that the center intensities are all equal. The $t_1 = 300$ profiles show peak to center intensities which are too large. The effect of changing k is very evident from the difference between curves 2 and 3. Comparison with profiles for other parameters finally results in a best fit for $t_1 = 120$.

The source function and velocity parameters which best describe the observed profiles are given in Table IV.C. 1. The optical thickness of the flare region remains essentially between 60 and 300. The variation of the source function with depth is not large as indicated by the small peak to center intensities observed. A number of the source functions represented in Table IV.C.1 are shown in Fig. IV.C..2. Also shown is the H-alpha source function calculated by Canfield and Athay (1974) for a Mach 5 shock model of the flare. (assuming a Planck function temperature of 10000 ^{o}K).

The surface velocities are outward and of the order

Table IV.C. 1

CALCULATED LINE PROFILE PARAMETERS

$\Delta = 1, F = 0$

Frame	t_1	k	L	V_o	B_1	B_2	T_D (^oK)
1				.2	.05	1	
2				.2	.05	1	
3				.2	.1	1	
4	300	.01	-.35	.2	.3	1	28000
5	300	.01	-.3	.7	.1	1	22000
6	60	.03	-.5	.5	.05	1	32000
7	60	.01	-.5	.5	.1	1	31000
8	60	.05	-.3	.5	.1	1	28000
9	300	.01	-.3	.5	.1	1	17000
10	1200	.02	-.1	.6	.01	1	16000
11	60	.05	-.3	.5	.1	1	22000
12	300	.01	-.5	.4	.1	1	20000
13	120	.05	-.5	.6	.05	1	17000
14	60	.05	-.5	.3	.1	1	24000
15	300	.005	-.3	.5	.1	2	20000
16	60	.01	-.5	.3	.1	1	21000
17	300	.01	-.3	.5	.1	1	19000
18	300	.01	-.3	.3	.1	1	27000
19	60	.05	-.3	.4	.03	1	19000
20	60	.05	-.3	.3	.3	1	26000
21	60	.03	-.5	.2	1.	1	19000
22	30	.03	-.5	.3	.01	1	24000
23	60	.05	-.5	-.3	.1	1	25000
24	60	.01	-.5	-.3	.1	1	33000
25	60	.04	-.5	0	-	-	33000
26	300	.005	-.3	-.5	.1	1	24000
27	300	.01	-.3	-.5	.1	2	20000

Fig. IV.C.2. H-alpha Source Functions Best Reproducing Observed Profiles.

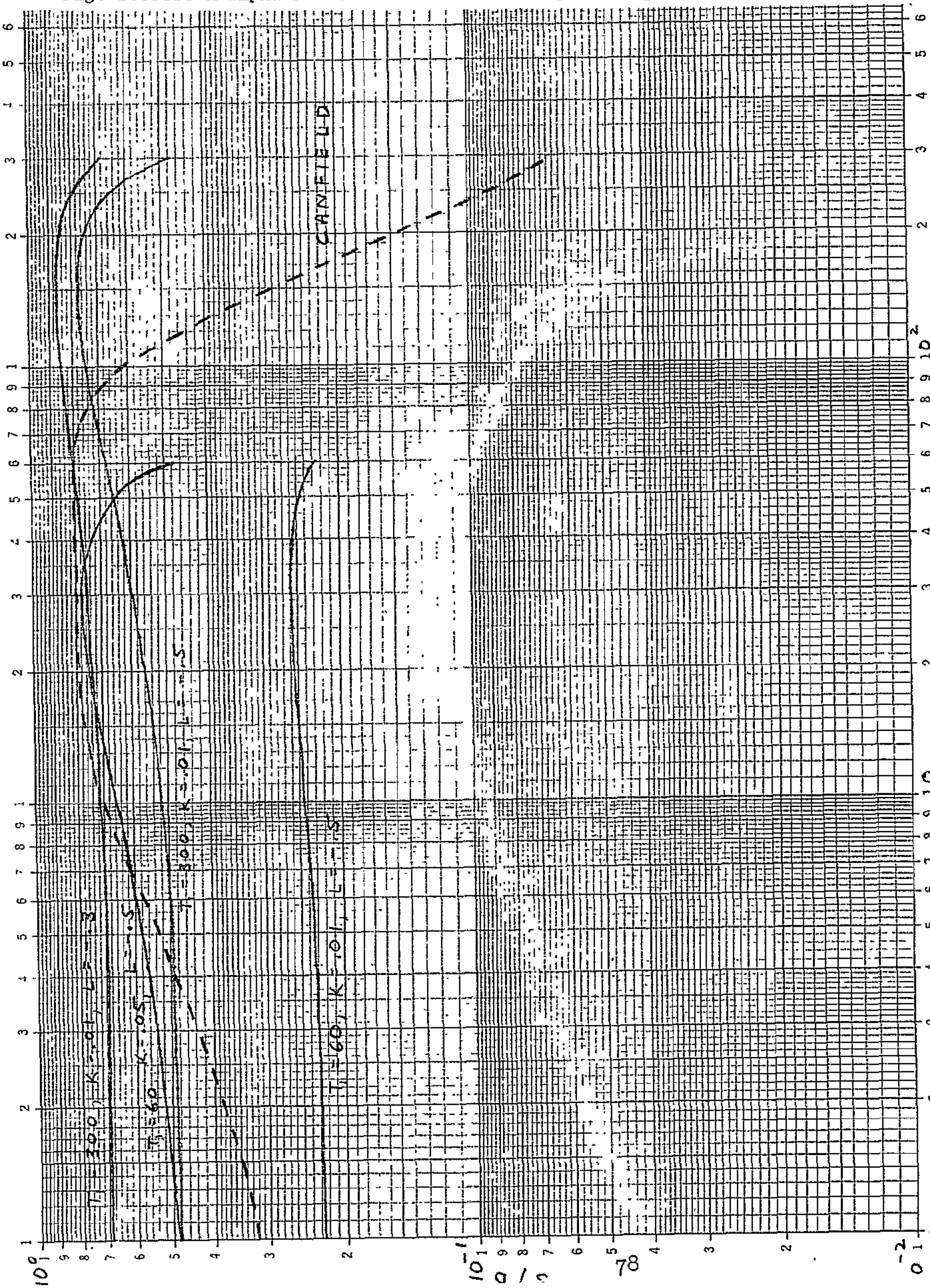

of .5 V_D showing a gradual decay with time. After about five minutes the velocity shifts to an inward velocity with a similar magnitude. The velocity gradients are quite constant at about 0.1. Using the Canfield and Athay model the surface velocity decreases by 2 in about 200 km. The derived velocity as a function of optical depth is shown in Fig. IV.C.3 for various times about 75 seconds apart. The curves are labeled with the frame number. The depth variation can only be considered qualitative as we did not have time to make the detailed comparisons necessary for each time frame. The dashed line shows the velocity predicted for a Mach 5 shock by Canfield and Athay (1974). The location we have chosen in the flare shows smaller velocities and velocities generally outward.

In fitting the observed profiles it was generally not possible to find a value of t_1 giving both the correct intensities and peak positions. Table IV.C.1 was prepared by considering intensities, center and peak shifts but not absolute peak positions. The correct peak to peak separation was obtained by varying the Doppler half width $\Delta\lambda_D$. Fig. IV.C.4 shows the Doppler half width variation with time showing an initial increase and decay and a later increase when the velocity changes sign. The Doppler half width varies between .36 and .52 Å. The Figure also shows the surface velocity V_O/V_D and illustrates the initial rise followed by a steady decline and then a change

Fig. IV.C.3. Observed Flare Velocities vs. Line Center Optical Depth. Curves Labeled with Frame No.

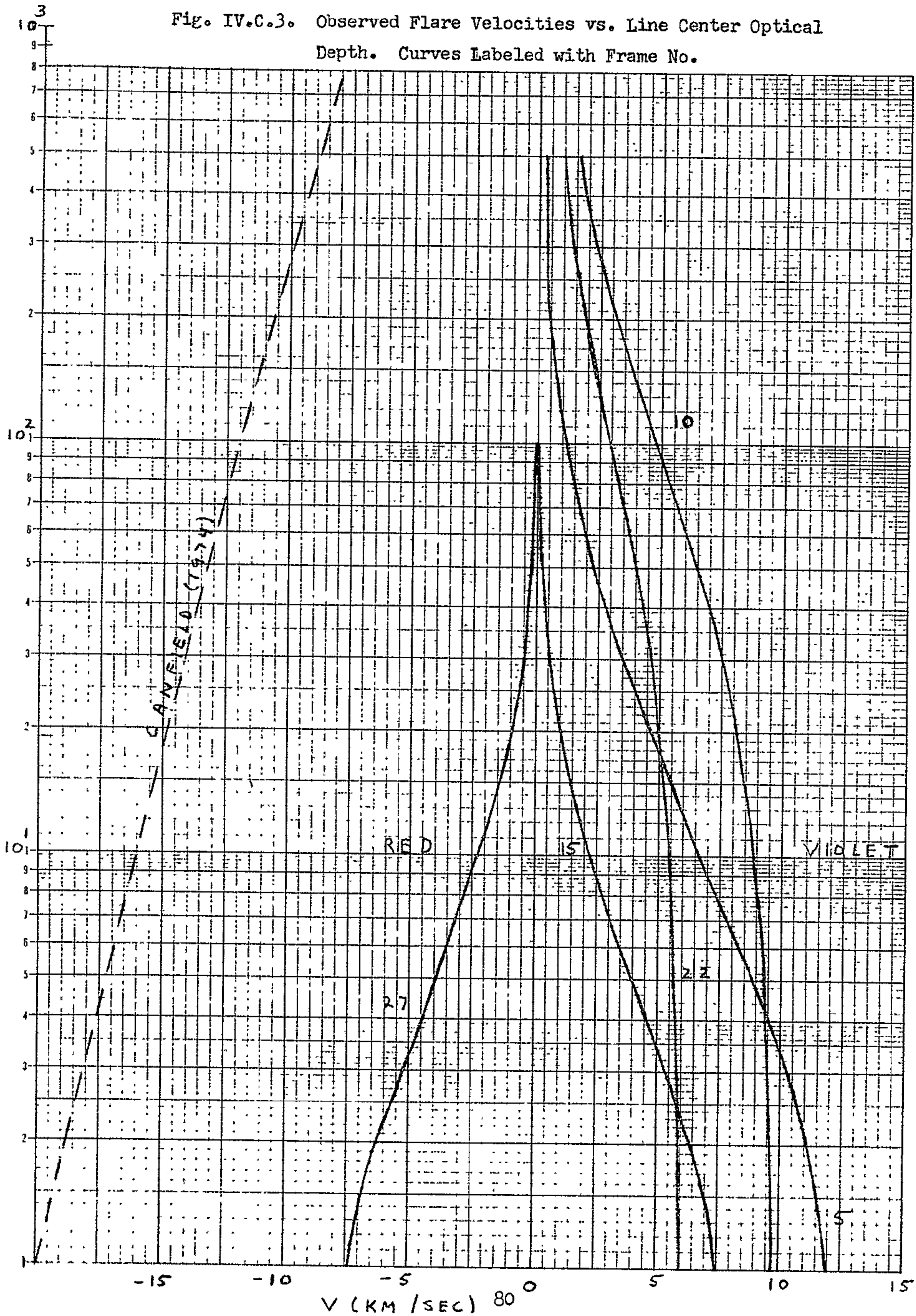

Fig. IV.C.4. Time Variation of Doppler Width, Surface Velocity, and Planck Function Temperature.

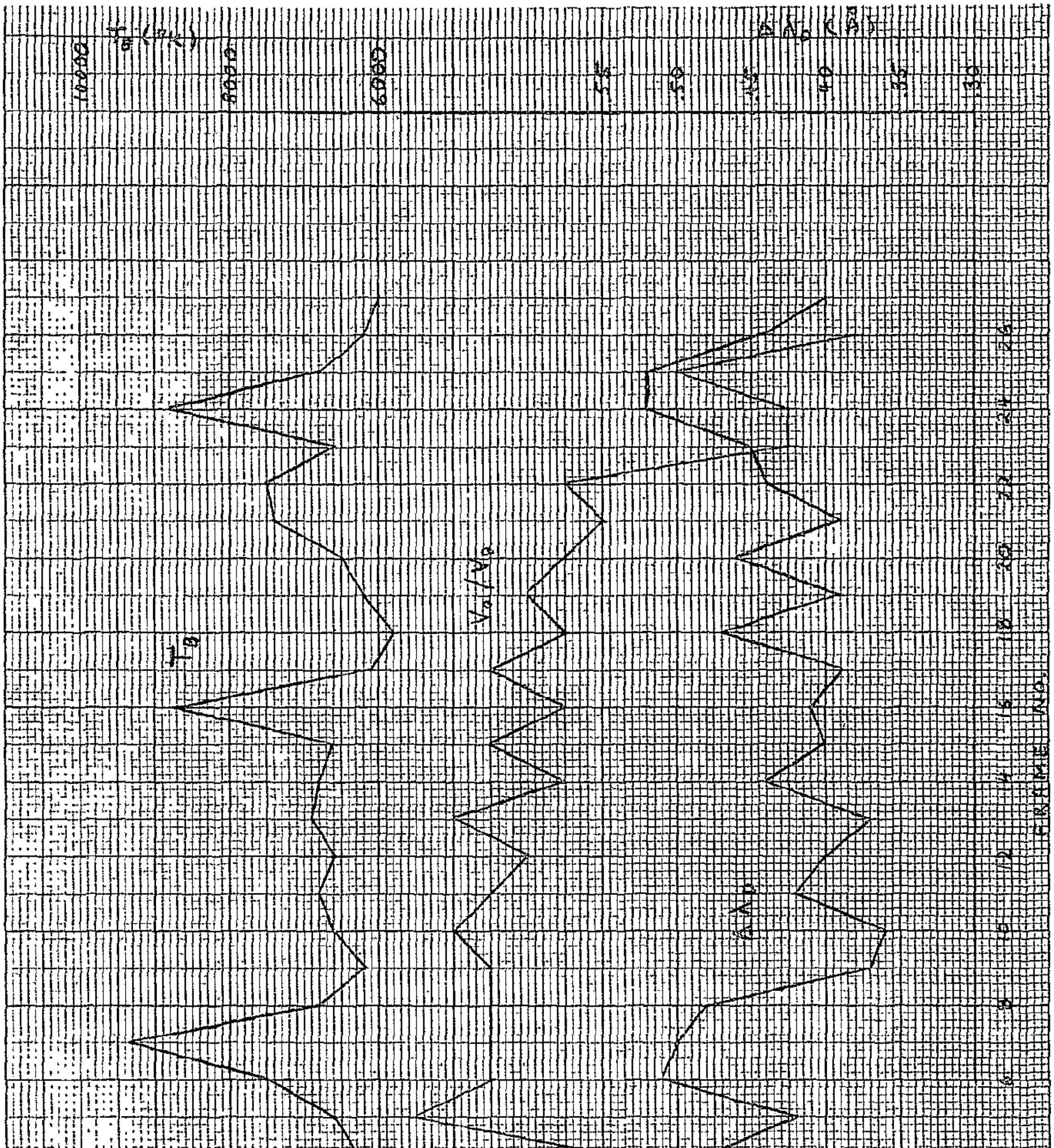

in direction.

The line profiles require a particular value of B to give the correct central intensity with respect to the observed continuum. The corresponding temperatures which we call T_B are shown in Fig. IV.C.4. The temperatures derived from the Doppler half widths which we call T_D are given in Table IV.C.1. We note that these temperatures vary between 15000 and 33000 $^{\circ}$K. When T_B is large T_D is usually also large. The Doppler half width may also include a contribution due to turbulence. If we interpret the turbulent velocity as that corresponding to the difference between T_B and T_D the turbulent velocities obtained are between 12 and 22 km/sec. These turbulent velocities are not nearly as large as would be required to decrease the large self reversals predicted by Canfield and Athay (1974).

In future work we would like to consider more carefully the effect of a variable Doppler width and other line absorption mechanisms in fitting the wing intensities. We would also like to consider other velocity fields, in particular one which changes direction at some depth as this is what seems to be necessary to fit the peak positions with respect to the line center. Of course the velocity field at nearby locations and in other types of flares would be most informative.

V. ACKNOWLEDGEMENTS

We would like to acknowledge the help of Steve Schoolman in obtaining the enlarged H-alpha profiles from the flare spectra and to Sara Martin for helpful discussions.

VI. REFERENCES

Brown, J. C., Solar Physics, 31, 143, 1973.

Canfield, R. C., Solar Physics, 34, 339, 1974.

Canfield, R. C., and R. G. Athay, Solar Physics, 34, 193, 1974.

Hyder, C. L., Mass Motions in Solar Flares, Nobel Symp. 9, 57, 1968.

Kostyak, N. D., Sov. Astron., 19, 458, 1976.

Martin, S. F., Final Report, Contract NAS8-29608, July, 1974.

Nakagawa, Y., et al., Solar Physics, 30, 111, 1973.

Nakagawa, Y., and C. L. Hyder, Environmental Research Papers, No. 320, AFCRL-70-0273.

Piddington, J. H., Solar Physics, 31, 229, 1973.

White, O. R., Ph.D. Thesis, University of Colorado, 1962.

White, O. R., Ap. J., 139, 1340, 1964.